(2)

[redacted]

HANDBOOK FOR NUCLEAR WEAPONS EFFECTS UNDER ARCTIC CONDITIONS [redacted]

K-80-143(R)-SAN

30 April 1980

This work sponsored by the Defense Nuclear Agency under: Subtask Code I25AAXHX633 and Work Unit 39 and by the Office of Naval Research Task NR089-145

[redacted]

KAMAN SCIENCES CORPORATION
1500 Garden of the Gods Road
Colorado Springs, Colorado 80907

A KAMAN COMPANY

[redacted]

Classified by DC Form 254 for N00014-79-C-0532 dated 4 May 1979. [redacted]

[redacted]

[redacted]

[redacted]

[redacted] TABLE 1-7

DENSITY OF FROZEN MATERIALS (g/cm^3)

[redacted]

Percent Water	Sand	Till	Ice
0	1.65	1.86	-
20	1.72	-	-
50	1.84	2.05	-
100	1.96	2.21	.917

[redacted] TABLE 1-8

ACOUSTIC PARAMETERS

[redacted]

	Temperature °C T	Density g/cm^3 ρ_o	Velocity m/sec C	Impedance mks rayl $\rho_o C$
Ice	-	.92	300	2.95×10^6
Water/fresh	20	.998	1481	1.48×10^6
Water/sea	13	1.026	1500	1.54×10^6
Air	0	1.293×10^{-3}	331.6	428
Air	20	1.21×10^{-3}	343	415

[redacted]

[redacted]

SECTION 2
AIR BLAST

[redacted] Traditionally, the air blast parameter which has attracted the most interest is the maximum static overpressure. For the typical static overpressure vs time profile as measured by a pressure sensor, the maximum pressure occurs at the shock front, or almost coincident with the arrival of the wave at the sensor location. If one is concerned about damage or injury from air blast, one must, in addition to maximum static overpressure, be interested in the static overpressure impulse, the maximum dynamic overpressure, the dynamic overpressure impulse, and the time of arrival of the air blast shock front as a function of distance from the explosion.

2.1 [redacted] Arctic Environmental Differences

[redacted] The basic parameters of interest in determining the free field air blast values are the pressure and the sound velocity, which depends on the temperature and wind velocity. As shown in Section 1, the standard pressure for the Arctic is essentially the same as the midlatitude value. The temperature, however, is markedly colder during the winter months. The January standard 75° sea level temperature is given as -24°C and inspection of Figure 1-4 shows that the mean temperature is below this value for much of the Arctic. The extreme that can reasonably be expected is about -57°C. The effect of these decreased temperatures will be noted in Section 2.2.

[redacted] Temperature inversions are more probable, stronger, and more extensive in Arctic than in temperate climates. This can enhance the propagation of low overpressure values to long

[redacted]

distances. Wind also affects the transmission of the low overpressure shock wave and causes an enhancement to low overpressure damage in the downwind direction.

A major environmental difference in the Arctic is the high probability of snow or ice cover and frozen ground. Air blast over snow can be strongly affected as will be discussed in Section 2.3. The attenuation of the shock in snow can affect the coupling of the blast energy to the ground or structures. The presence of the ice layer over the sea can influence the air blast [illegible] from underwater bursts. Surface effects will be discussed in Section 2.4.

2.2 Free Air Blast Prediction

Free air blast predictions for nonstandard atmospheric conditions are generated as described in EM-1 (DNA, 1978) from the standard 1 kt curves by using Sachs scaling relationships. The effects of Arctic meteorological phenomena on predictions will be discussed.

2.2.1 Sachs Scaling Techniques

Two basic assumptions are inherent in the Sachs relations. First, it is assumed that the air blast wave propagates in a homogeneous atmosphere with the ambient conditions at the altitude of the observation point. Second, the total energy available for air blast is independent of altitude; that is, the energy partition is unchanged.

The maximum static, maximum dynamic and total pressures are related by the expressions

$$P_2 = \left(\frac{P_{02}}{P_{01}}\right) P_1, \qquad (2.1)$$

where the ranges are given by

$$R_2 = \left(\frac{P_{01}}{P_{02}}\right)^{1/3} \left(\frac{W_2}{W_1}\right)^{1/3} R_1, \qquad (2.2)$$

[redacted]

[redacted]

and the variables are defined as:

P is the appropriate maximum pressure,
P_a is the ambient atmospheric pressure,
R is the distance from the explosion, and
W is the yield of nuclear explosion.

The subscripts 1 and 2 refer to conditions for the "reference" explosion (usually considered as 1-kt yield at standard sea level conditions) and the "problem" explosion, respectively.

[redacted] The time of arrival of shock front and the positive phase duration are given by

$$t_2 = \left(\frac{W_2}{W_1}\right)^{1/3} \left(\frac{P_{01}}{P_{02}}\right)^{1/3} \left(\frac{C_{01}}{C_{02}}\right) t_1, \qquad (2.3)$$

where C_0 is the speed of sound in ambient atmosphere and the ranges are related by Equation 2.2.

[redacted] The total positive phase overpressure impulse and the dynamic pressure impulse are given by the expression

$$i_2 = \left(\frac{W_2}{W_1}\right)^{1/3} \left(\frac{P_{02}}{P_{01}}\right)^{2/3} \left(\frac{C_{01}}{C_{02}}\right) I_1, \qquad (2.4)$$

where the variables are as previously defined and the ranges are related by Equation 2.2.

[redacted] In our application, the subscript 1 refers to the mid-latitude standard values and subscript 2 refers to the Arctic values of interest. The yield will be taken as 1 kt so we are interested in the changes that will occur when the 1 kt mid-latitude standard curves are scaled to 1 kt Arctic conditions.

[redacted]

[redacted]

[redacted]

The pressures in the Arctic at sea level are virtually identical to those found in the midlatitudes. The variations from the standard values caused by meteorological perturbations is of the same order as for temperate climates. Thus, the pressure ratio P_{02}/P_{01} is essentially unity, and no differences are expected in the pressure radius curves in the Arctic.

[redacted] Note that the time and the impulse scaling relations also involve the ratio of the sound speed which is related to the temperature by the expression

$$\frac{C_{01}}{C_{02}} = \left(\frac{T_{01}}{T_{02}}\right)^{1/2}, \tag{2.5}$$

where the temperatures must be degrees Kelvin. For the mean January Arctic temperature at sea level this ratio is 1.075, implying a 7.5% increase in the time and impulse values in the Arctic. For the extreme temperature case (-60°C) the increase is 15.5%.

[redacted] In Figure 2-1 the change in the shock front arrival time is noted for the extreme case. In Figure 2-2 the change in the impulse values for the extreme case is shown. Even these changes for the extreme case are of marginal interest since a 15% increase in the impulse would not in general cause any practical systems effects, and it would occur with only a small probability. The mean 7.5% increase which can be expected in the coldest months is within the basic uncertainties in the impulse predictions and the resulting damage effects.

[redacted]

[redacted]

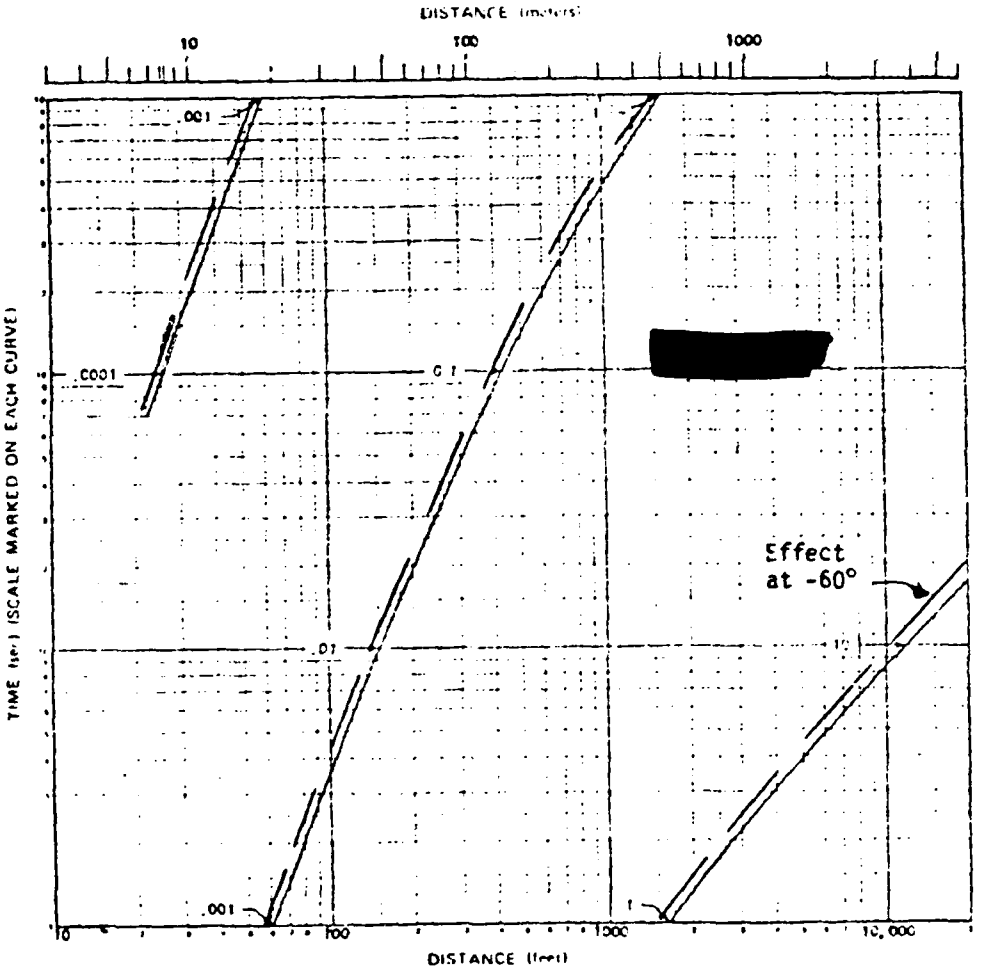

[redacted] Figure 2-1 Time of Arrival of the Shock Front from a 1 kt Free Air Burst in a Standard Sea Level Atmosphere [redacted]

[redacted]

[redacted]

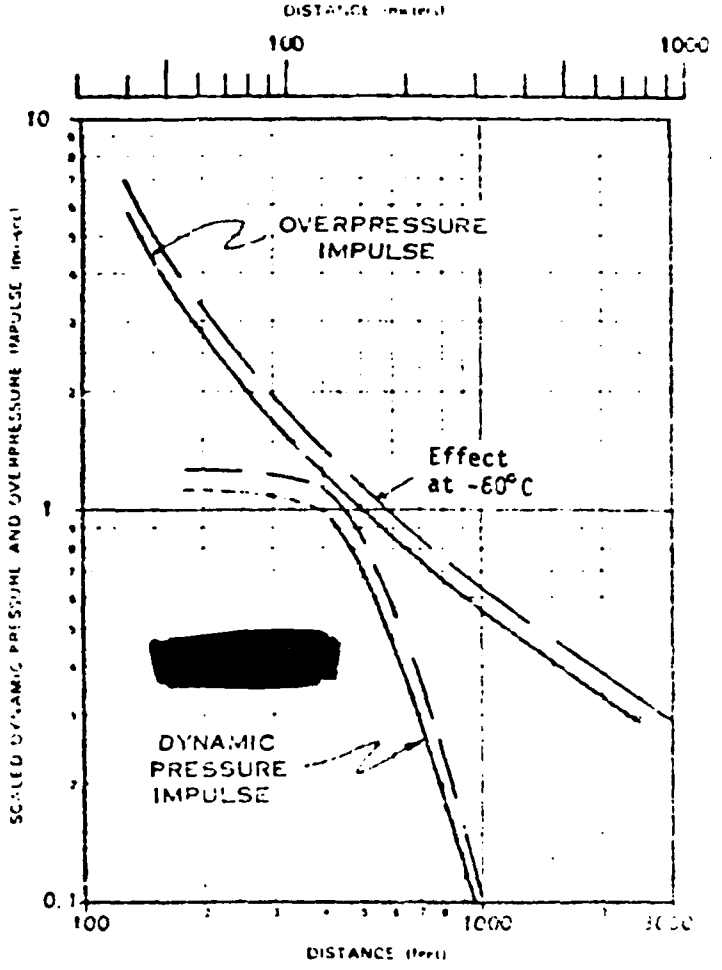

[redacted] Figure 2-2 Overpressure and Dynamic Pressure Impulse from a 1 kt Free Air Burst in a Standard Sea Level Atmosphere [redacted]

[redacted]

[redacted]

[redacted] Inspection of Table 1-1 shows a small deviation of the Arctic pressures from the midlatitude values as a function of altitude. From equations 2.1 and 2.2 the coaltitude ranges to various overpressure values were calculated as a function of burst altitude for the Arctic and midlatitude pressure - altitude profiles. For all overpressure values considered between 1 and 1000 psi there were insignificant differences (<5%) in the Arctic and midlatitude coaltitude ranges.

[redacted] The conclusion is that no significant differences will be found in the free air blast values under Arctic conditions. Sachs scaling can be used to provide the free air values if precise time and impulse values are required.

[redacted] The reliability of Sachs scaling under Arctic conditions may be questionable. The Sachs relations can be derived rigorously from theoretical considerations. However, the 1 kt free air curve is based on a combination of theory, calculations and experimental data. For the low overpressure values there has always been some uncertainty. Scaling this curve to conditions far removed from the experimental data on which it is based must be treated cautiously.

[redacted] There is some evidence that Sachs scaling at depressed temperatures is valid. The technique has been used to correlate data in all of the high explosive (HE) tests that have been performed over snow and ice. In the Distant Plain events to be described in the next section, Sachs scaling was used to correlate summer and winter results and no inconsistencies were found.

[redacted] Modified Sachs scaling between altitudes using the atmospheric parameters at the target location has been used to correlate and predict blast values in inhomogeneous air with a high degree of success. Comparisons of computer code calculations in non-uniform air (Wells, 1971) with Sachs scaled blast parameters

[redacted]

[redacted]

indicate that the technique can be used reliably for these cases. This would imply that modified Sachs scaling can be used for predicting the blast environment if a temperature inversion is present if the pressures are nigh enough to ignore refraction effects.

2.2.2 [redacted] The Effect of Temperature Inversion

[redacted] A temperature inversion causes a sound speed gradient to exist at low altitudes resulting in refractive effects and can, therefore, amplify the overpressure at the ground from a burst occurring below an inversion. Conversely, surface overpressures are reduced if the detonation is above the inversion. These refractive effects are important only for very low overpressures (<1 psi). The effects are serious enough in consideration of safety from HE tests, to restrict shots when inversions exist to inhibit long range damage to windows etc. This may be of interest militarily since in the very severe arctic winter losing building integrity due to window breakage is much more important than in temperate climates.

[redacted] The lapse rates of Arctic inversions are more severe than is typical of temperate areas, as described in Section 1. It is therefore likely that inversions will exert a more significant influence on blast phenomena in the Arctic than elsewhere. The increased incidence of inversions in Arctic areas will increase the probability of seeing these effects.

[redacted] Although corrections for inversions are small, the enhancement of low static overpressure at long ranges may somewhat increase the possibility of damage to blast-sensitive targets for bursts below the inversion. Later this year a report (Reed, 1980) of an extensive experimental study will be published detailing the effect of inversions and wind velocity on air blast. This study will supersede anything available at this time. Quantitative predictions should be delayed until the report is available.

[redacted]

[redacted]

2.2.3 [redacted] The Effect of Wind

[redacted] In addition to the temperature, the wind velocity causes a change in the relative sound speed and, therefore, on the blast parameters at very low overpressures. No direct effects would be expected at higher pressures. The effects of wind will be considered in a report to be published during 1980 (Reed, 1980).

[redacted] The dry snow of cold regions is easily lifted by turbulent winds to create a dense cloud that obscures vision and can become integrated with an air blast wave. Any wind of velocity over 15 miles per hour causes blowing snow if the temperature is well below the freezing point. As examples, periods during which blowing snow has reduced visibility to less than 1000 yards extend from 75 hours in one area to as long as 260 consecutive hours in another area. In sub-Arctic forests, such as grow in eastern Siberia, surface winds are impeded by the trees and blowing snow is less prevalent.

[redacted] The reduced visibility would have the most direct effect on the amount of thermal radiation from a nuclear weapon burst reaching the ground. This, in turn, would have an indirect effect upon the air blast phenomena; that is, the possibility of the formation of a precursor under these conditions would be very remote.

[redacted] A more significant aspect of the presence of dry snow is the fact that a blast wave could carry many snow particles as it propagates along the surface of the ground (or ice/water surfaces). This might lead to enhanced damage, which will be discussed in Section 2.5.

2.2.4 [redacted] The Effects of Precipitation, Fog and Clouds

[redacted] The effects of atmospheric moisture on blast propagation are not well known; however, theoretical studies agree qualitatively with the small amount of experimental data. As a strong blast wave propagates through air containing water droplets it

[redacted]

[redacted]

[redacted]

vaporizes some or all of the water. Vaporization of the water absorbs energy that otherwise would be available for the blast wave to propagate through the air. As a result, the blast wave is attenuated more rapidly in air that contains water droplets than in air that does not.

[redacted] The effect of water droplets on peak overpressure may be calculated in terms of effective yield. This procedure is used to obtain lower calculated overpressures at some distance from the burst. Rain or fog has a negligible effect on the amount of available energy close to the nuclear source. The energy density within the fireball is orders of magnitude higher than the energy required to vaporize whatever water may be present, and the amount by which the suspended liquid increases effective air density, even under the extreme conditions within clouds producing severe thunderstorms, is not likely to exceed 2 percent.

[redacted] Figure 2-3 shows the effective yield for three yields and two conditions of moisture content. The water densities used in the calculations correspond roughly to precipitation rates of 0.1 (light rain) and 0.5 (heavy rain) inches per hour.

[redacted] The curves shown in Figure 2-3 are based on the assumption of uniform water content between the source and the target. In an actual rainstorm, this assumption is artificial, but without such an assumption the analysis of rain's effect would be unduly complex. Typically, water content is several times as high within a rain cloud as it is below the cloud. Actual water distribution patterns are complex, different for different rainstorms, and generally unpredictable.

[redacted]

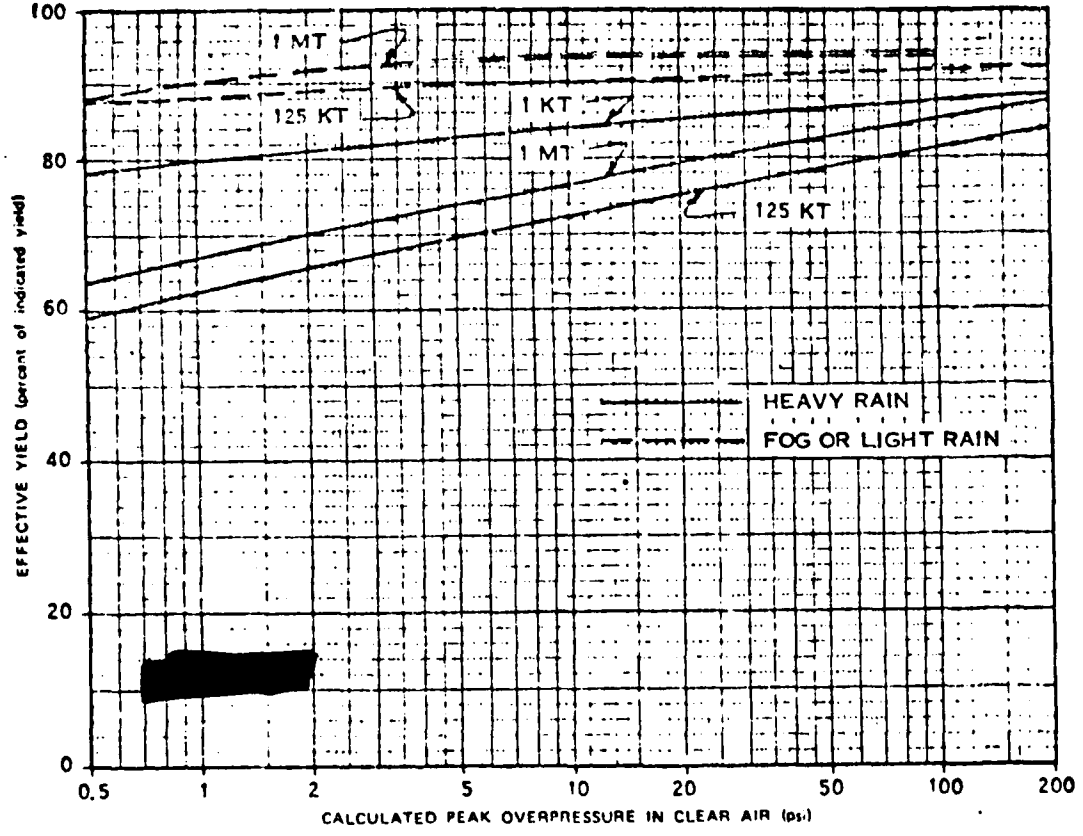

FIGURE 2-3 REDUCTION OF PEAK OVERPRESSURE AT THE SURFACE BY RAIN OR FOG - NEAR-IDEAL SURFACE

[redacted]

[redacted] As stated in EM-1, rain or fog effects should be evaluated only when the optimization of blast against soft targets is important, and then only if the rain or fog extends throughout a volume that includes both the target and the burst. HOB curves for thermally near-ideal surface conditions should be used with Figure 2-3 since thermal energy is attenuated by rain or fog and precursor effects would not be expected above a wet surface.

[redacted] The effects of atmospheric moisture on other blast parameters, such as time of arrival, positive-phase duration, and dynamic pressure are not well known; however, theoretical considerations indicate that arrival times will remain essentially unchanged, positive-phase durations will be slightly reduced, and dynamic pressures will be slightly increased. Calculations of these other air blast parameters should be made in the normal manner, without applying any effective yield factors. Enhanced effects on dynamic overpressures are discussed in Section 2.3.6. Referring to Figure 2-3, and recalling that $(Y_{eff})^{1/3} = R_o/R_1$, one can derive some conclusions related to the applications to Arctic environments:

(1) For light rain or fog, the 125 KT and 1 MT curves indicate effective yields of 90% or above for the peak overpressures of interest. Since $(0.90)^{1/3} = 0.97$, it is evident that light rain or fog is not going to cause a significant perturbation to the ordinary air blast effects.

(2) For heavy rain and for peak overpressures in the 5-20 psi range, effective yields can be in the 70-80% range for the larger yields. Since $(0.7)^{1/3} = 0.89$, it is unlikely that, even for this extreme case, the deviations in blast effects from normal would be considered significant.

[redacted]

[redacted]

[redacted] No test data from nuclear bursts in snow are available to the U.S. A possible estimation of the general effect of snow can be made by an extension of the reasoning of the preceding paragraphs if we assume that the amount of water in heavy and light snows is similar to the amount of water in heavy and light rains. The snow particles would have to be first melted and then heated to evaporation with the resultant transfer of more of the blast energy. This could result in an increase in attenuation over that noted in Figure 2-3 since an additional energy of about 100 calories per gram of water would be required to melt the snow and evaporate it. The interaction may involve breakup of the snow flakes and water droplets for more efficient energy transfer. The force required to shatter the crystaline structure is probably larger, but the effect of this on the energy transfer is unknown. There is, however, no positive evidence that this reduction should be greatly different than that occasioned by temperate forms of precipitation at militarily significant ranges. It should be emphasized here that no valid numerical evaluation of this aspect of Arctic environment can be made without further experimentation.

[redacted] Since low dense clouds are very prevalent over the polar ice during the summer, the effect might be worth studying in more detail. A recent review and analytical consideration of this effect (Friedberg, 1976) points out that the attenuation in fogs and clouds is more severe because of the smaller water drops and more efficient transfer of energy to the water and subsequently larger attenuation of blast energy. No work in this area was referenced after the 1950s in the above report.

[redacted]

[redacted]

2.3 [redacted] Air Blast Over Frozen Surfaces

2.3.1 [redacted] Reflection Characteristics of Snow Layers

(U) When a shock front enters a layer of snow it is attenuated strongly. Drag forces on the snow crystals dissipate energy contained in the wind behind the shock front. The energy transmitted to the snow crystals is then consumed in compacting the snow layer.

[redacted] Reflection occurs at the top surface of a deep snow layer just as it does at a ground surface. Momentum is conserved in the interaction. A blast wave striking the earth transmits only a small fraction of its energy as ground shock; consequently, the earth's surface approximates an ideal reflector. A blast wave striking a snow surface is analogous to a ball bouncing from a heavy rug. The reflecting surface has a cushioning effect that makes it a poorer reflector.

[redacted] In the case of a thin layer of snow, the cushioning effect ceases when the pressure wave penetrates the snow layer, reflects from the ground surface, and propagates back to the snow surface. At this time, the snow layer is supported by an internal pressure as high as the pressure produced by the blast wave reflecting from the surface; the reflecting qualities of the snow layer then approach the near-ideal reflecting qualities of the underlying surface.

[redacted] Neither theoretical nor experimental data are available on the effects of thin snow layers on a blast wave, however, a rough calculation is enlightening. If a shock front in snow moves with a speed comparable to that of sound in air, a layer of snow one foot thick, struck by a normally incident blast wave, will absorb energy from the blast wave for about 2 milliseconds and will have the properties of a near-ideal reflecting surface after that time. This 2-millisecond interval is appreciably long only

[redacted]

[redacted]

[redacted]

when compared with relatively short duration blast waves. For example, it might alter a 750 psi blast wave from a 1 kt source. The overpressure pulses of this blast wave have an effective triangular duration of about 20 milliseconds. At lower overpressures, the pulse becomes broader, and the snow layer would have less effect. For a given overpressure, larger yields than 1 kt also produce broader pulses. It should also be noted that, for a 1000-lb HE detonation, the triangular duration of about 20 msec occurs at a maximum overpressure of only 20 psi. For HE detonations of smaller charges, these durations would correspond to even lower peak overpressures. This discussion indicates the following:

- If a blast wave with a very short-duration pressure pulse strikes a thin layer of snow, the snow may alter the leading edge of the pressure pulse enough to reduce peak reflected overpressure. The short pressure vs time pulse corresponds to high overpressures from relatively low yield nuclear detonations and/or virtually all overpressures from small-charge HE detonations.

- For a situation where interest is in lower overpressures and yields greater than 1 kt a thin snow cover affects such a small portion of the overpressure pulse that peak reflected overpressure is essentially the same as for a near-ideal surface.

[redacted] Measurements of the properties of snow under dynamic loading have been made (Napadenskv, 1964) which indicate that relatively small amounts of energy will be absorbed by a snow layer because the snow is compacted to densities equivalent to ice by pressures in the 20 - 40 bar region. As one might expect,

[redacted]

[redacted]

[redacted]

a very large variation in snow properties was found for different types of snow in different stages of compaction. The experiments were not taken to large pressure values so the integral of PdV cannot be obtained with any degree of accuracy. If the approximation 1/2 PΔV is used, which will overestimate the integral, then the energy loss due to this mechanism could be significant in reducing the effective blast yield for a 1 kt burst detonated over 1 m of snow, which is a reasonable upper limit for Arctic winter conditions.

[redacted] The U.S. has never detonated a nuclear weapon in the atmosphere in an Arctic environment. Therefore, all predictions related to the effects of an Arctic environment upon air blast parameters from nuclear explosions must be deduced either from theoretical calculations or from the results of experiments using HE sources. For many years, we have been interested in predicting the behavior of air blast phenomena from nuclear bursts in temperate environments; during that time, these deductive methods have proven effective, except for cases where thermal/air blast interactions are important, e.g. precursor wave formation and propagation. Experience and advancing developments in instrumentation techniques have revealed the utility of and the limitations on the data obtained from the small and large charge HE tests.

[redacted] Other than the inability of the HE charge tests to properly simulate the nuclear bursts' thermal/air blast interaction, the most important "sin of omission" in HE tests is insufficient band width of the instrumentation system used. Sometimes this is referred to as "inadequate frequency response of the transducer circuitry". In effect, this limited frequency response has a similar effect on the pressure vs time measure-

[redacted]

[redacted]

ment as was described above for the snow layer case. That is, the gage electronic system would "chop off" the true peak overpressure and the recorded result would be in error. The magnitude of the error depends on the bandwidth of the circuit and the magnitude of the peak pressure.

[redacted] Recent HE experimental programs have emphasized these band width aspects; in particular the TRW 3-lb 9404 experiments (Carpenter and Brode, 1974) and the BRL (Dipole West) 1000-lb TNT tests (Reisler et al, 1975 and 1976) employed instrumentation band widths which were compatible with the sizes of the explosive charge. Unfortunately, the same was not the case for many HE experiments performed during the 1950's and 1960's.

[redacted] To explain this concept further, Table 2-1 is presented. The Table lists the instrumentation band widths normalized to Carpenter's experiment, which are required to be compatible with each size of explosive charge used for an HE test. It is obvious that as the charge sizes increase the band width requirement relaxes.

2.3.2 [redacted] Air Blast Over Shallow Snow

[redacted] An interesting pair of HE events was conducted as part of the DISTANT PLAIN test series (Reisler et al, 1967). These events were 20 ton TNT surface bursts with the same conditions except that Event 3 was a summer shot and Event 5 was a winter shot. The temperature for the summer shot was 110°F and for the winter shot was 33°F. The winter shot had a snow cover of about 4 inches over soil frozen to a depth of about 9".

[redacted]

[redacted]

TABLE 2-1

"REQUIRED" BANDWIDTH VS. TNT CHARGE SIZE

	CHARGE SIZE (TNT)	REQUIRED BANDWIDTH *(NORMALIZED TO CARPENTER'S)
	1 lb.	800 kHz
Carpenter	8 lb.	400 kHz
	32 lb.	252 kHz
	256 lb.	126 kHz
Dipole West	1000 lb.	80 kHz
Suffield, etc	20 tons	23.4 kHz
	100 tons	13.7 kHz
	500 tons	8 kHz

[redacted]

*i.e., These are the bandwidths required so that the data system would be equivalent to Carpenter's system used for the 8-lb. experiments.

[redacted]

[redacted]

[redacted] The comparison of the overpressures obtained on the two shots is shown in Figure 2-4. Note that the data points agree closely except at the high overpressure values where the experimenters drew the pressure curve for the winter event below the curve for the summer event. There is obviously some scatter in the data points, and there are only four gage positions in the high pressure region. The interesting fact is that the pressure-time records for these high pressure positions indicate a very narrow pulse of the order of shock traversal time through the shallow snow while the time width for the shock at the lower pressures is significantly longer than the snow shock transit time. This may be only an interesting coincidence. Additional experiments or calculations could resolve the question.

[redacted] The dynamic pressure and impulse measurements indicated good agreement between the two events. In this case there was no increase in dynamic pressure due to entrainment of snow by the blast wave.

2.3.3 [redacted] Air Blast Over Deep Snow

[redacted] Denver Research Institute (DRI) (Wisotski, 1966) and U.S. Army Waterways Experiment Station (WES) (Ingram, 1960 and 1962, Joachim, 1964 and 1967) performed HE tests which are most applicable to our Arctic environment situation. The DRI tests employed 1-lb and 8-lb size charges, while WES used 32-lb and 256-lb charges, primarily. In both cases, the band width of the instrumentation was in the region of 0-20 kHz, too limited with respect to the size of the sources used. Fortunately, most of these measurements were confined to the lower overpressures (less than 20 psi) where the limited band width would have less effect on the accuracy of the measurements. However, because it is difficult to determine the magnitude of the errors due to the

[redacted]

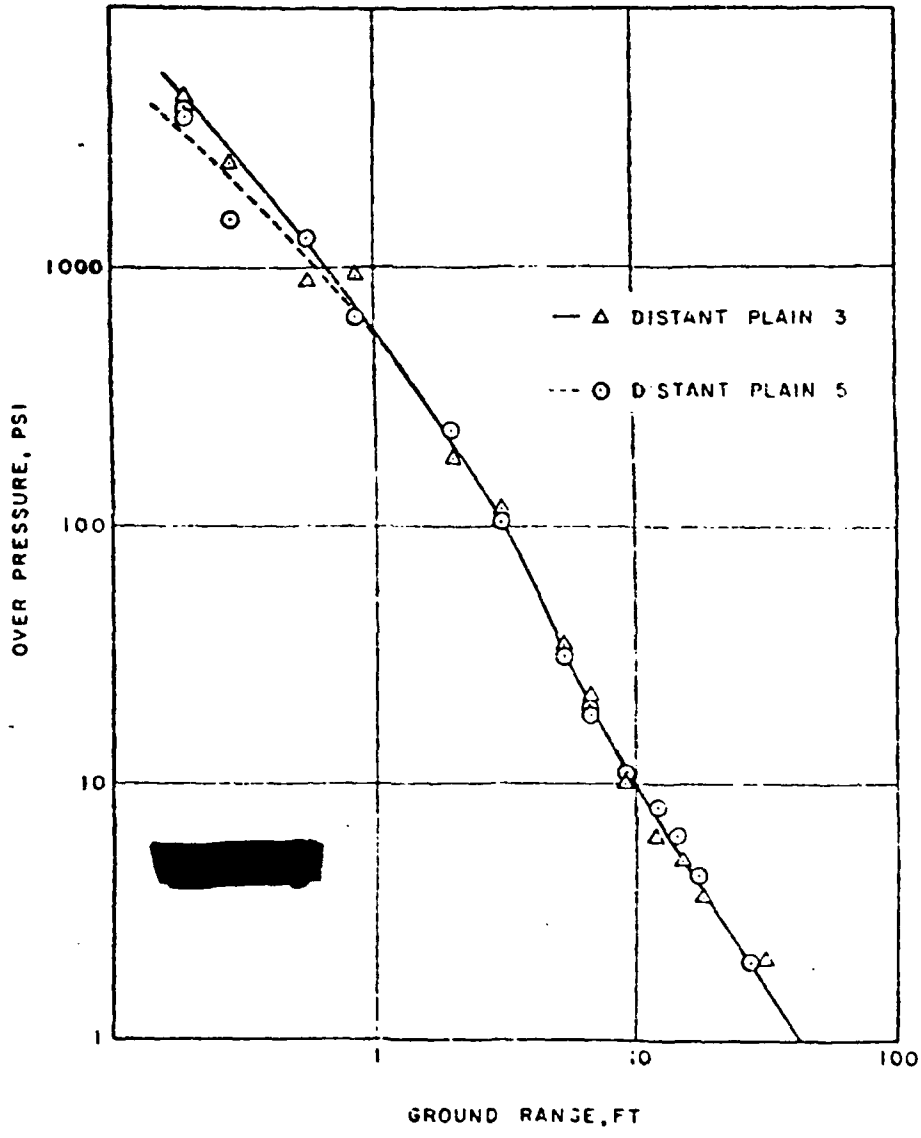

FIGURE 2-4. Measured overpressure for Events 3 and 5 (Reisler, et al, 1967)

[redacted]

[redacted] limited band width, one must be very cautious when attempts are made to compare data collected by one agency with similar data collected by another group using different instrumentation. Thus, the most valid conclusions come from the DRI bare ground vs snow-covered ground air blast data; more tentative conclusions are derived from the WES data taken in the Arctic compared with data taken over bare ground by BRL at Suffield, Canada.

[redacted] Of course, we must not forget that all of these conclusions are based upon HE test data; therefore, the implied assumption is that the thermal radiation from the nuclear burst fireball affects the air blast parameters similarly in both temperate and Arctic environments--an assumption which requires much more thorough investigation.

[redacted] DRI performed a series of small-charge HE tests over bare ground and over snow-covered ground using the same gage arrays and electronic instrumentation on each test. These data comprise the most complete set of results available on the effects of a deep snow layer on air blast parameters. Although the charges used were only 1-lb and 8-lbs, since the same instrumentation was used for all tests, the lack of sufficient band width is probably not serious as far as the overall comparisons are concerned.

[redacted] The effect of snow and bare ground surfaces on Mach-region peak static overpressures is summarized in Figures 2-5 through 2-8. Note that the plotted data are "as read" and they correspond to an average ambient atmospheric pressure of 510 mm Hg (9.86 psi). The results shown in Figure 2-5 are typical; the data indicate that the peak static overpressures for the snow-covered surface are depressed from those measured over bare ground. For the Hc = 1/2 ft case, the two curves are very close to parallel,

[redacted]

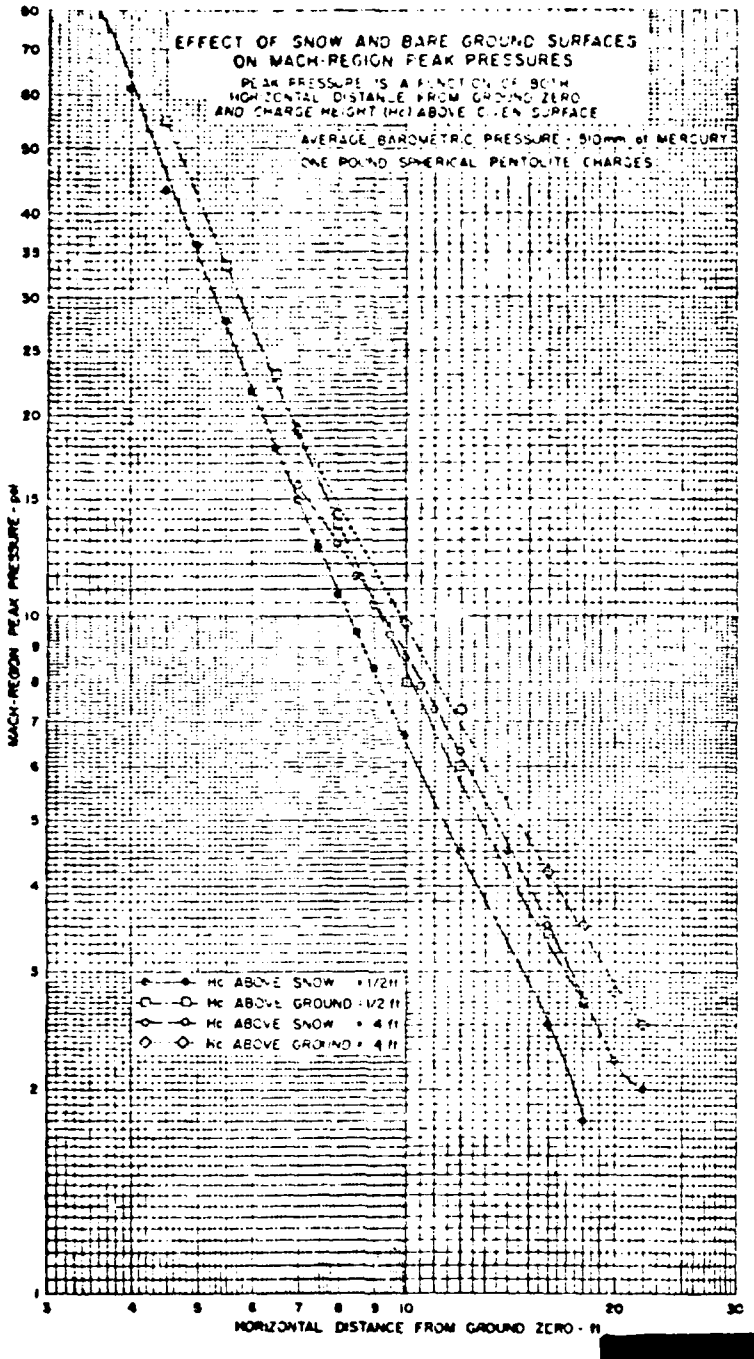

FIGURE 2-5. (Wisotski and Snyer, 1966)

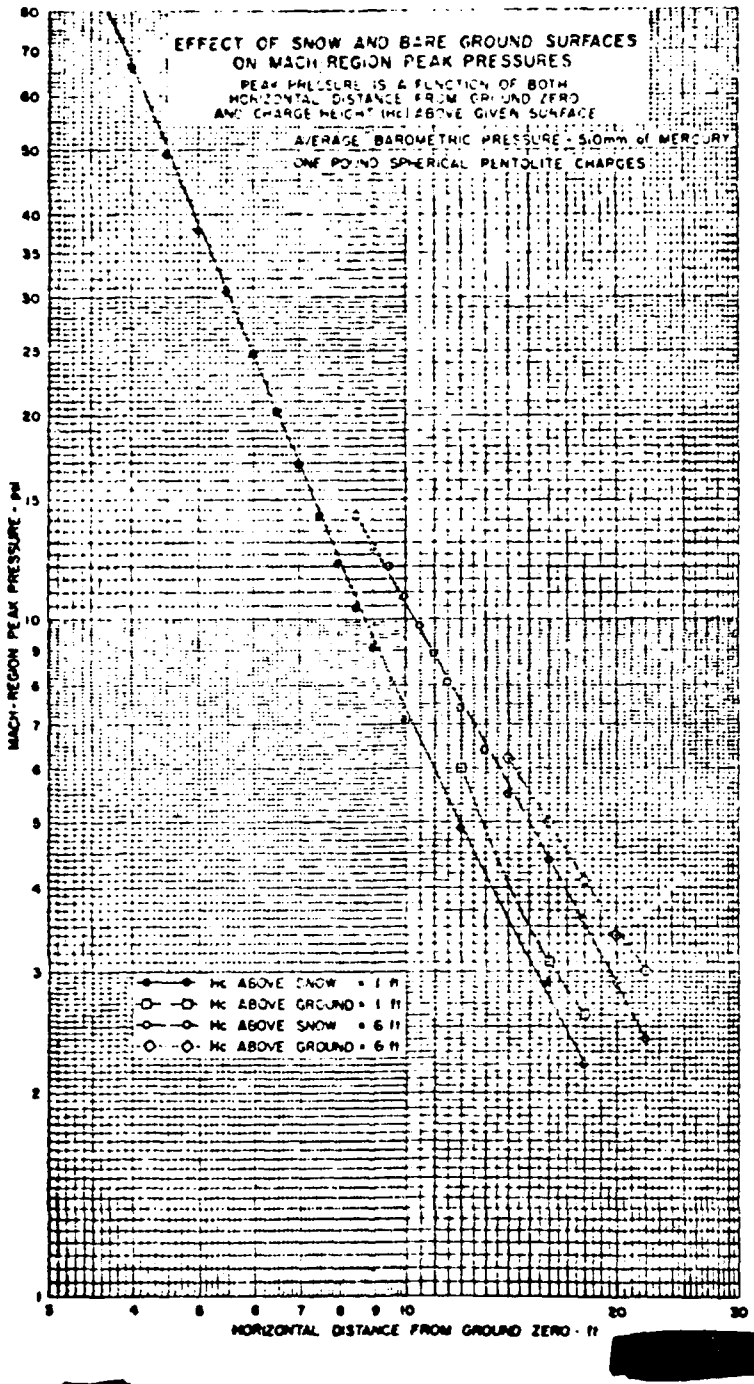

FIGURE 2-6. (Wisotski and Snyer, 1966)

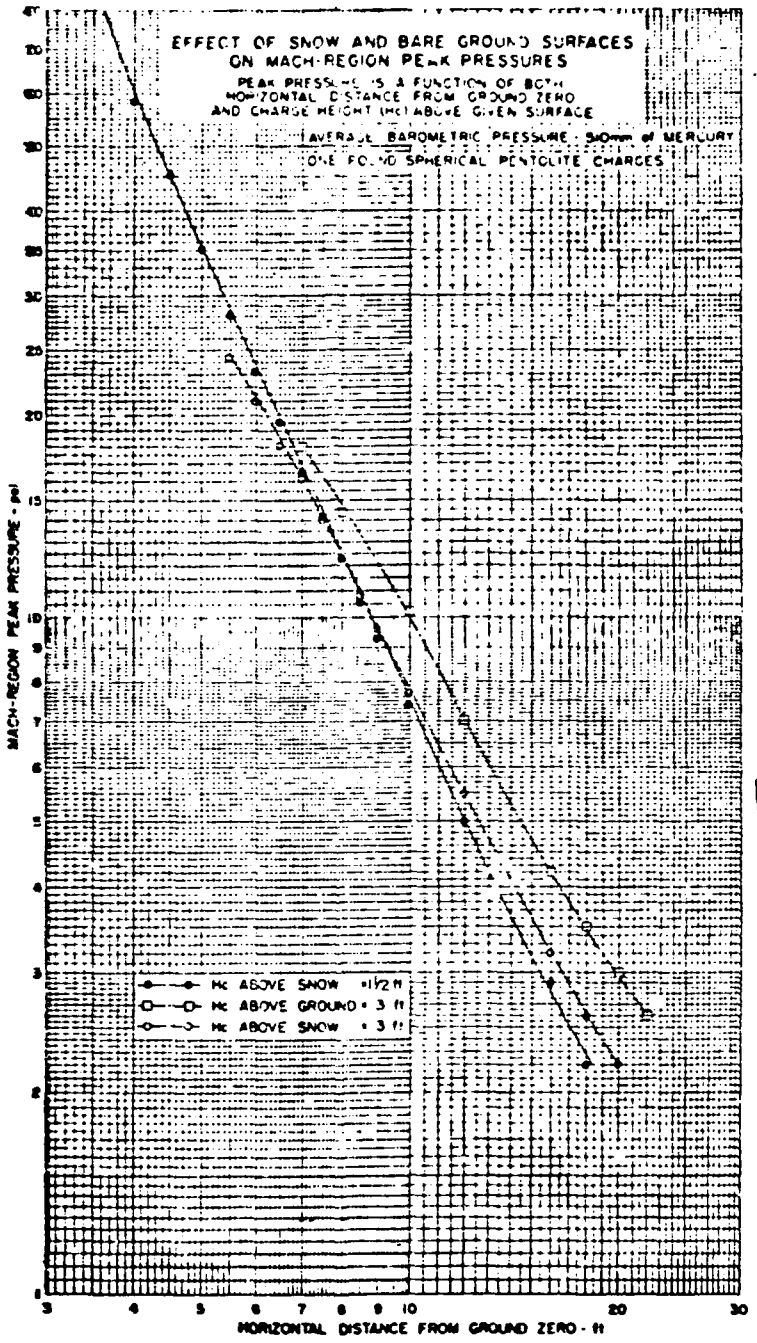

FIGURE 2-7. (Wisotski and Snyer, 1966)

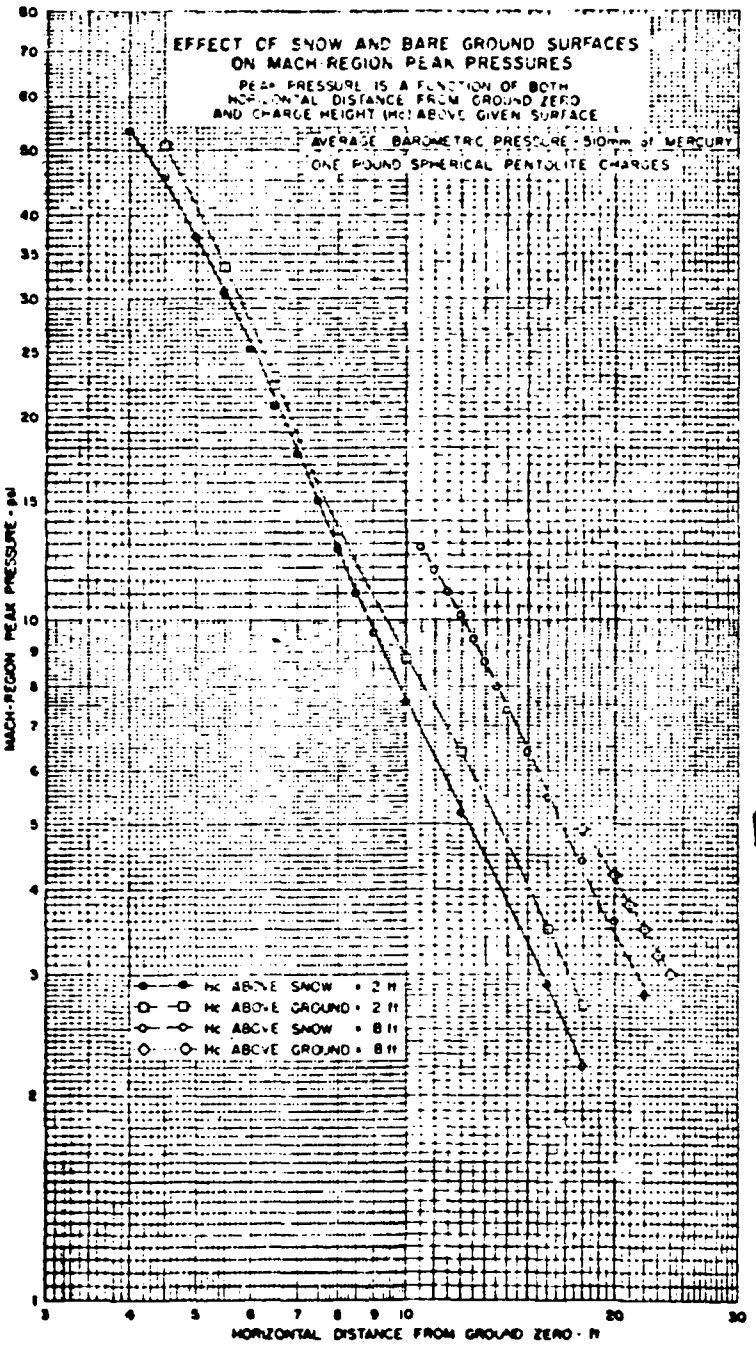

FIGURE 2-8. (Wisotski and Snyer, 1966)

[redacted]

so the decrease in pressure over snow is independent of pressure magnitude. For Hc = 4 ft, there is some variation with pressure level indicated; particularly at the higher overpressures where the above-snow curve appears to "turn over" slightly. This latter behavior is noted also on Figures 2-7 and 2-8 at the higher overpressures. Also, the figures indicate that the peak overpressures for the low burst height (Hc = 1/2 ft) are depressed the most by the snow cover.

[redacted] The effect of snow-covered and bare ground on static overpressure impulse is shown on Figures 2-9 through 2-12 for the various burst heights. In general, the comparisons indicate that the snow layer tends to suppress the total impulse; however, the scatter in the data is quite severe, and it is difficult to detect a consistent amount of suppression due to the different surfaces. Looking at Figure 2-12, it is evident that the variations between the snow-covered and bare ground values are reduced as the burst height is increased.

[redacted] The reflection coefficients from snow, bare ground and concrete are plotted vs scaled charge height in Figure 2-13. Qualitatively, the results are as expected; one would expect that the least amount of energy of the explosive would be transferred to the concrete surface and that the most would be absorbed by the snow. Because we are comparing data (concrete) taken on another test, using instrumentation with an unknown bandwidth, we must be cautious in using the values shown for prediction purposes.

[redacted] The effect of snow-covered and bare ground on the path of the Mach triple point is shown in Figure 2-14. In general, the triple point rises faster over bare ground than over the snow cover. Data from tests having burst heights higher than

[redacted]

[redacted]

EFFECT OF SNOW AND BARE GROUND SURFACES
ON IMPULSE VALUES

IMPULSE AS A FUNCTION OF BOTH
HORIZONTAL DISTANCE FROM GROUND ZERO
AND CHARGE HEIGHT (Hc) ABOVE GIVEN SURFACE

AVERAGE BAROMETRIC PRESSURE - 510mm of MERCURY
ONE POUND SPHERICAL PENTOLITE CHARGES

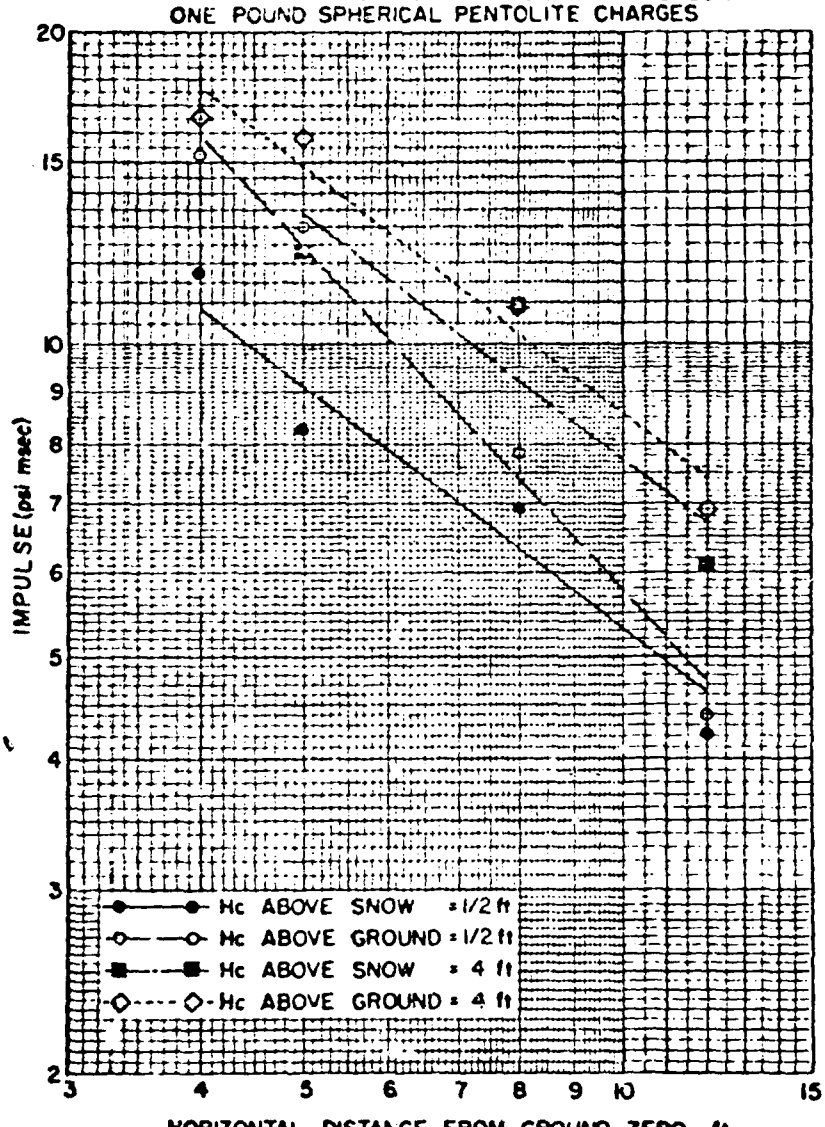

[redacted]

FIGURE 2-9. (Wisotski and Snyer, 1966)

[redacted]

EFFECT OF SNOW AND BARE GROUND SURFACES
ON IMPULSE VALUES

IMPULSE AS A FUNCTION OF BOTH
HORIZONTAL DISTANCE FROM GROUND ZERO
AND CHARGE HEIGHT (Hc) ABOVE GIVEN SURFACE

AVERAGE BAROMETRIC PRESSURE - 510mm of MERCURY
ONE POUND SPHERICAL PENTOLITE CHARGES

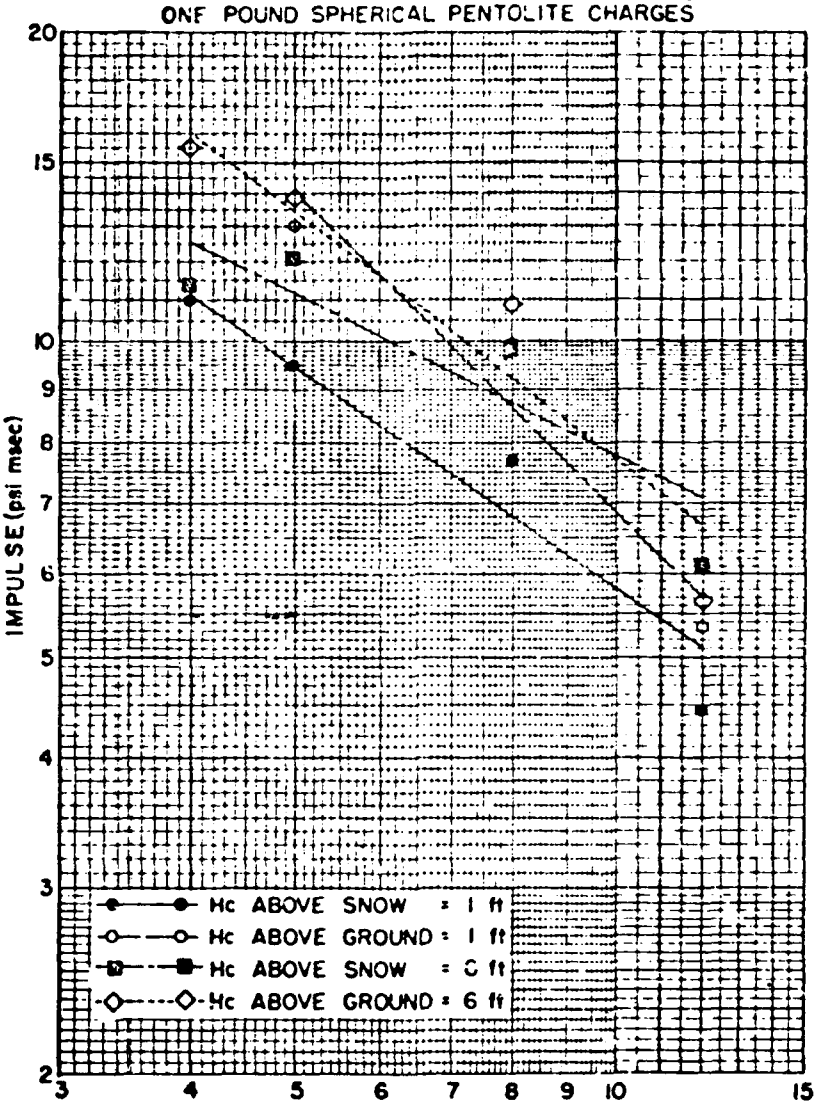

FIGURE 2-10. (Wisotski and Snyer, 1966)

[redacted]

EFFECT OF SNOW AND BARE GROUND SURFACES
ON IMPULSE VALUES

IMPULSE AS A FUNCTION OF BOTH
HORIZONTAL DISTANCE FROM GROUND ZERO
AND CHARGE HEIGHT (Hc) ABOVE GIVEN SURFACE

AVERAGE BAROMETRIC PRESSURE - 510mm of MERCURY
ONE POUND SPHERICAL PENTOLITE CHARGES

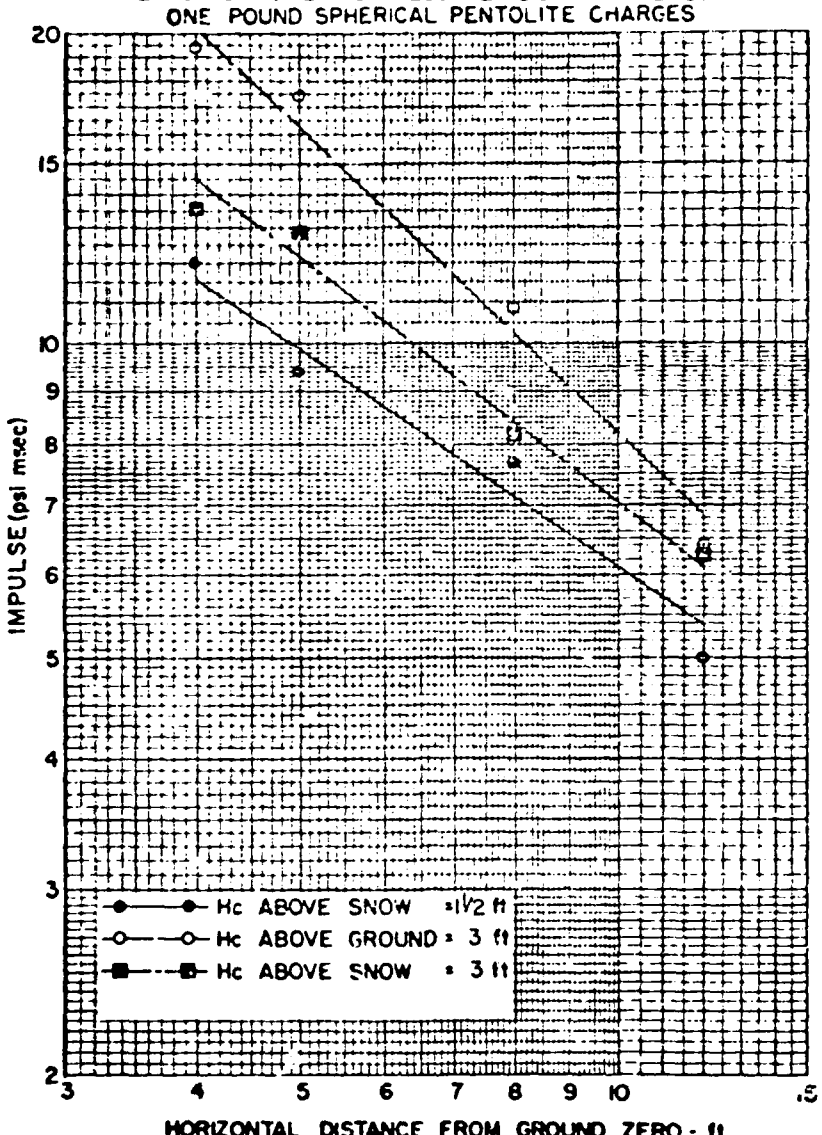

[redacted]

FIGURE 2-11. (Wisotski and Snyer, 1966)

[redacted]

EFFECT OF SNOW AND BARE GROUND SURFACES ON IMPULSE VALUES

IMPULSE AS A FUNCTION OF BOTH HORIZONTAL DISTANCE FROM GROUND ZERO AND CHARGE HEIGHT (Hc) ABOVE GIVEN SURFACE

AVERAGE BAROMETRIC PRESSURE - 510mm of MERCURY
ONE POUND SPHERICAL PENTOLITE CHARGES

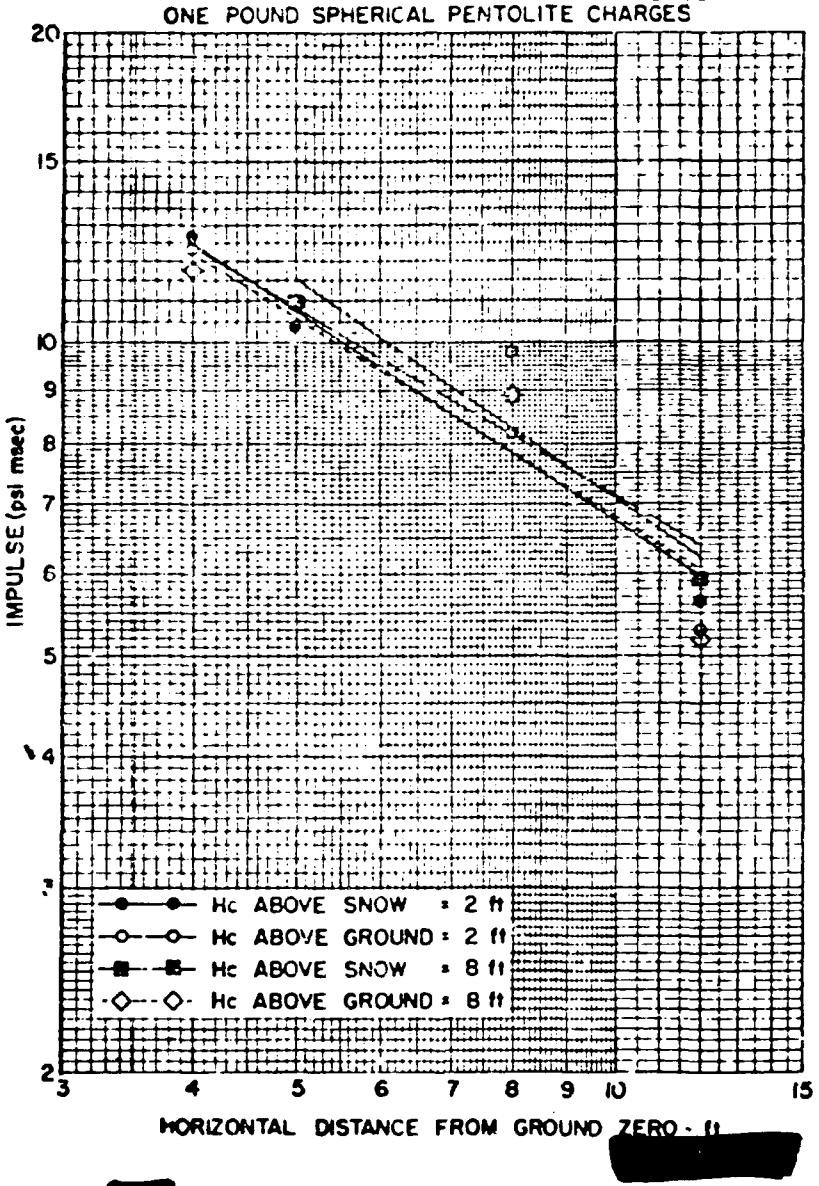

FIGURE 2-12. (Wisotski and Snyer, 1966)

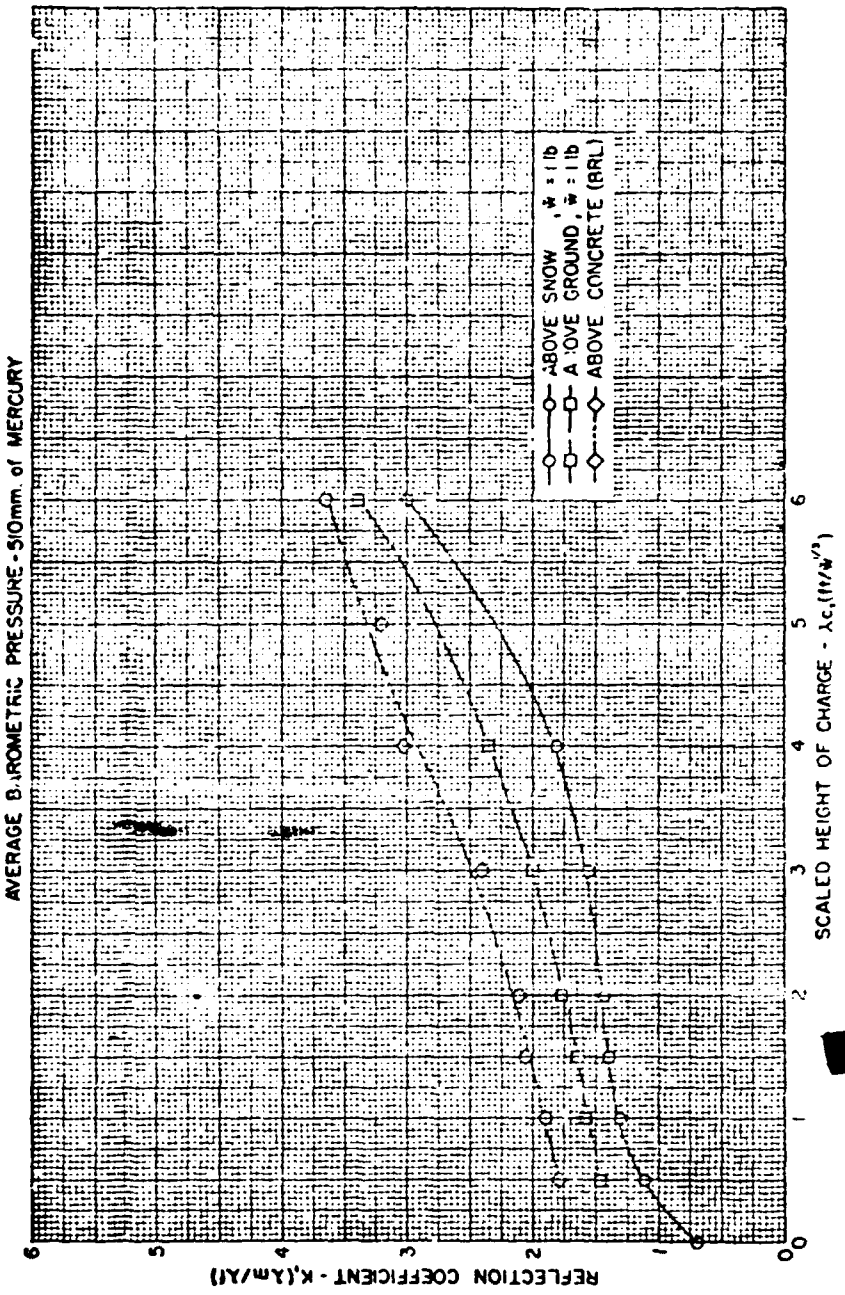

EFFECT OF SNOW AND BARE GROUND SURFACES
ON REFLECTION COEFFICIENT

FIGURE 2-13. (Wisotski and Snyer, 1966)

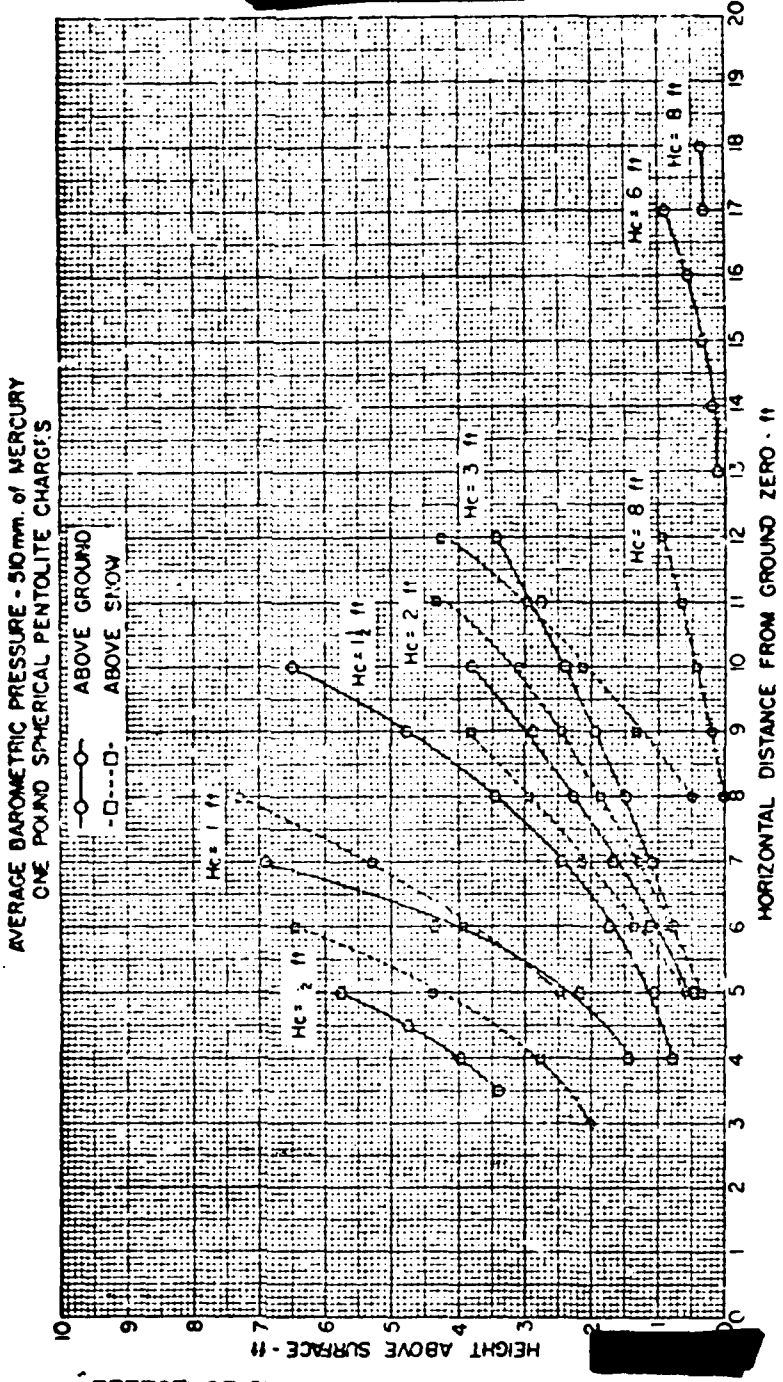

EFFECT OF SNOW AND BARE GROUND SURFACES ON PATH OF THE TRIPLE-POINT

FIGURE 2-14. (Wisotski and Snyer, 1966)

[redacted]

[redacted] 2 ft are not definitive and may not follow this trend. Data on the ground range at which the triple point forms are incomplete; so, no comparison is possible for the snow-covered and bare ground tests.

[redacted] Finally, the DRI data are plotted on a height-of-burst (HOB) chart shown in Figure 2-15. The above-snow curves are supported with more data, and it is possible to be fairly confident as to the form of these curves. The bare-ground data are less extensive, but it is again evident that the snow reduces the distance at which a particular peak overpressure is observed. The magnitude of the distance reduction appears to increase as the overpressure level decreases. There is strong evidence of the over snow contours "pulling in" for the surface burst case (HOB = 0); this is consistent with the fact that a surface detonation over snow loses a large portion of its explosive energy to the snow which is close to the explosion.

[redacted] The Greenland HE series involved a large number of tests from about 1958 to the middle of the 1960s. A large number of WES and Cold Regions Research and Engineering Laboratory (CRREL) reports which were referred to previously were written to describe the results of the various tests. Included were tests over and under the deep snow on the Greenland ice cap, and over and under ice. Shock transmission through snow and ice were measured as well as a large number of cratering shots in snow and ice. A report never widely distributed summarizes these results (Smith, undated).

[redacted] The HOB related shots were primarily 32 and 256 pound charges with scaled heights of burst to 12 ft/lb$^{1/3}$. The instrumentation band width was too narrow to adequately resolve

[redacted]

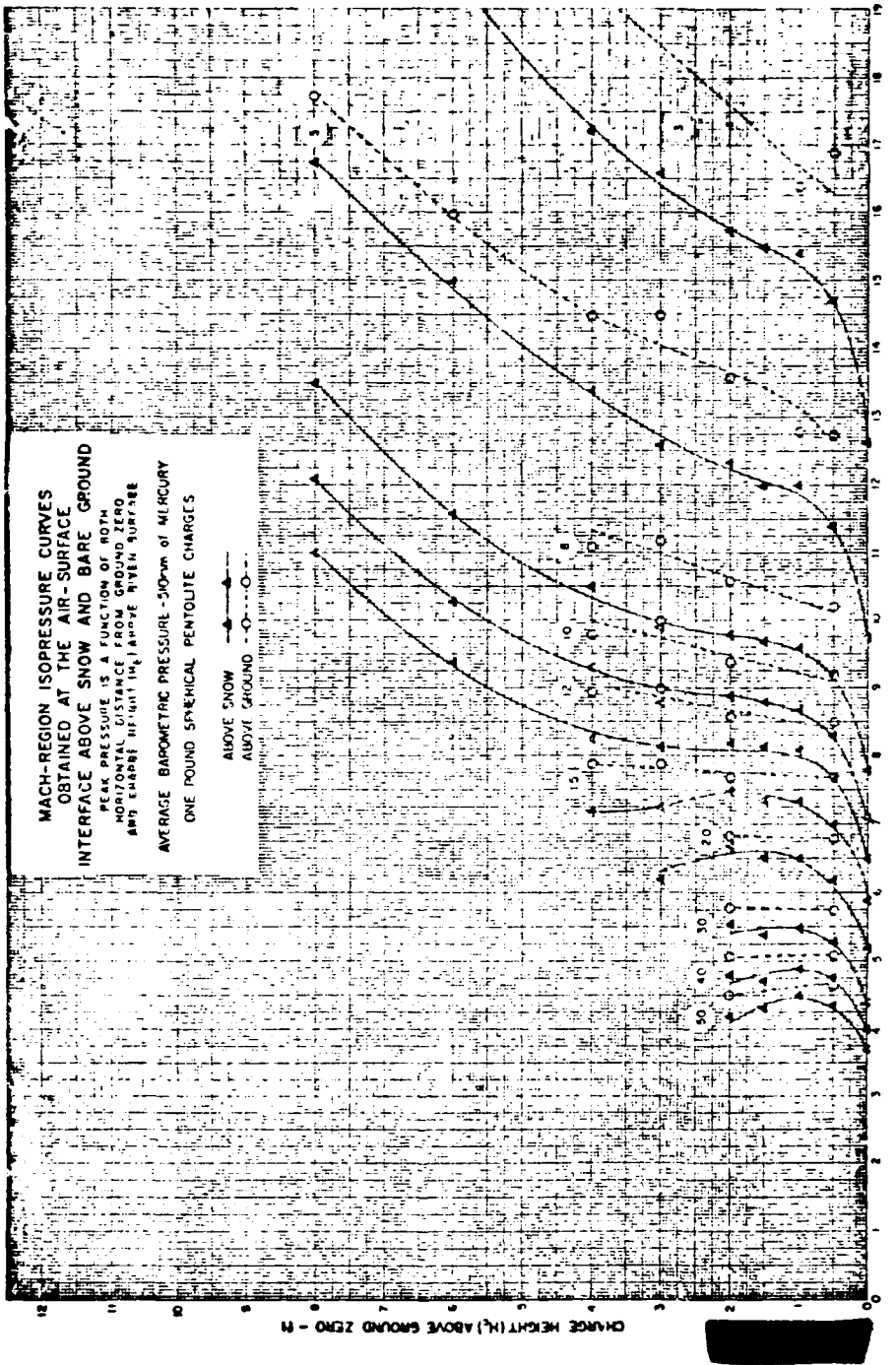

FIGURE 2-15. (Wisotski and Snyer, 1966)

[redacted]

[redacted]

the narrow pulses; so, as is the case with the DRI experiments, one must be very careful in comparing the WES data with other data. In this case, however, no comparison measurements were made over ground with the same instrumentation; so the comparisons are more uncertain than with the DRI measurements.

2.3.4 [redacted] Overpressure Contours from HOB Tests

[redacted] For the military planner, the air blast height-of-burst (HOB) charts are the most useful for prediction purposes. Since the Arctic environment data we have for air blast is from HE tests, we shall emphasize the HE HOB charts; also, maximum overpressure is the principal parameter we shall consider.

[redacted] A series of high explosive (HE) blast tests was conducted jointly by the U.S. Army Ballistic Research Laboratories (BRL) and the Canadian Defense Research Establishment Suffield (DRES) during the fall of 1969. These tests, held at the Watching Hill test range at DRES in Alberta, Canada, were known as the 1969 Height-of-Burst Series (Reisler et al, 1976 and 1969). Later, during the summer of 1975, another series of HOB tests was conducted by BRL as a part of the three-year DIPOLE WEST series (Reisler, 1975).

[redacted] Some of the results from these HOB tests are plotted in Figures 2-16 through 2-18, showing the peak overpressure contours for various overpressure values (Reisler, to be published). These data correspond to air blast wave propagation over bare ground under "near-ideal" conditions, which implies that there are no significant thermal effects.

[redacted] Looking at these figures, the plotted data and the solid-line contours correspond to the BRL tests referred to above. Additional curves are shown to correspond to data collected by other agencies on their tests using various HE

[redacted]

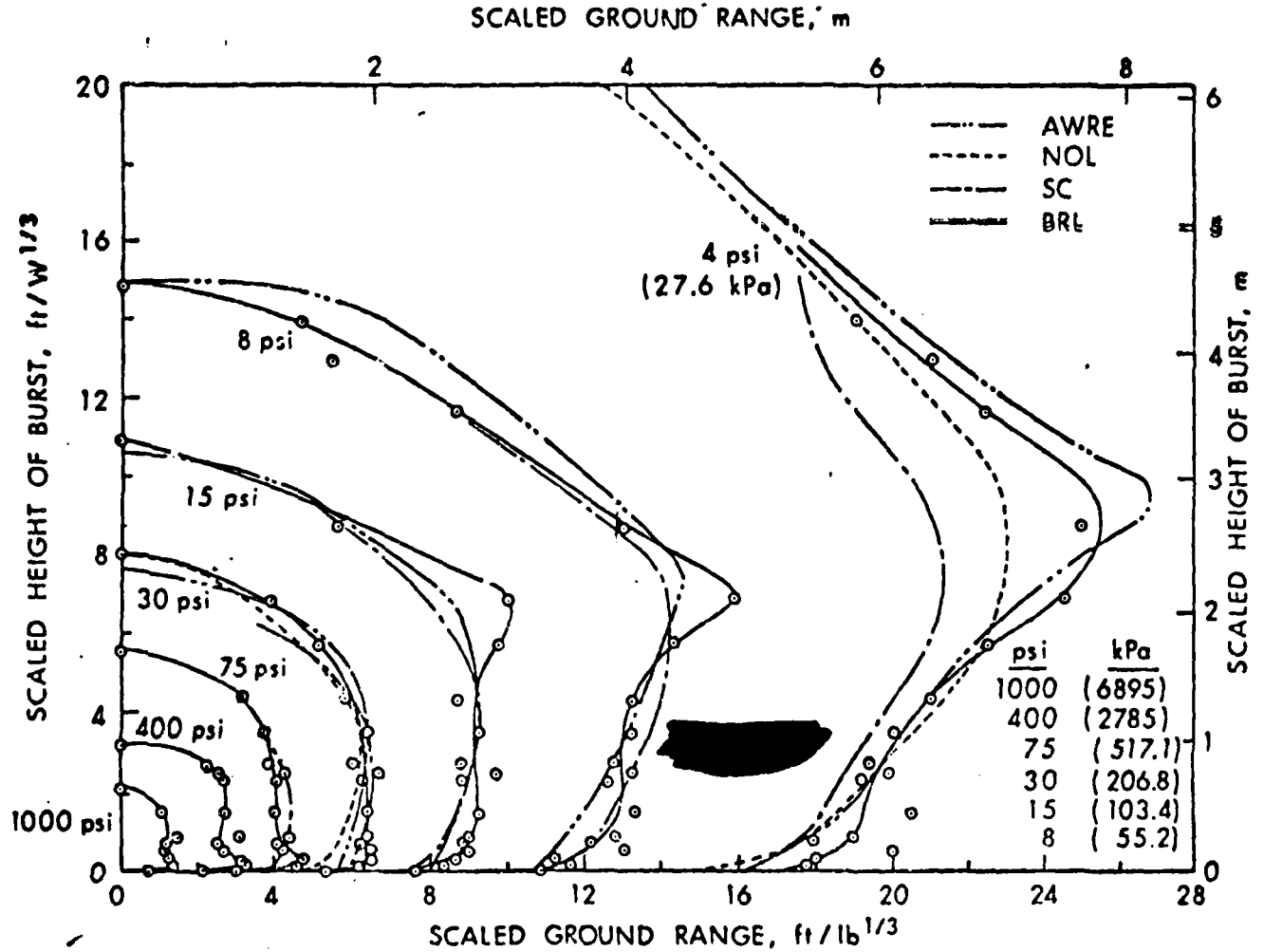

FIGURE 2-16. OVERPRESSURE HOB CURVES, 1000 - 4 PSI
(Reisler, to be published)

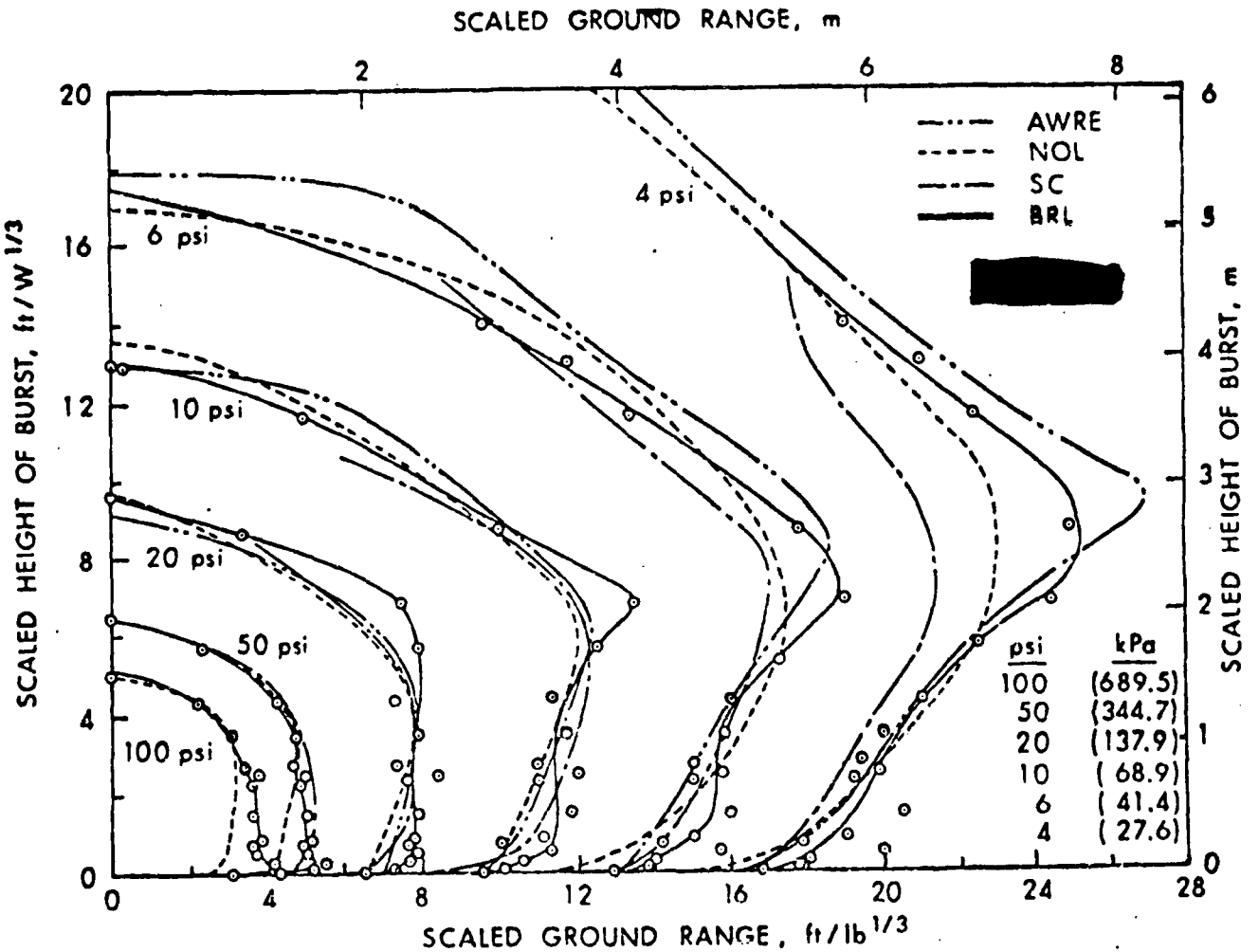

FIGURE 2-17. OVERPRESSURE HOB CURVES, 100 - 4 PSI
(Riesler, to be published)

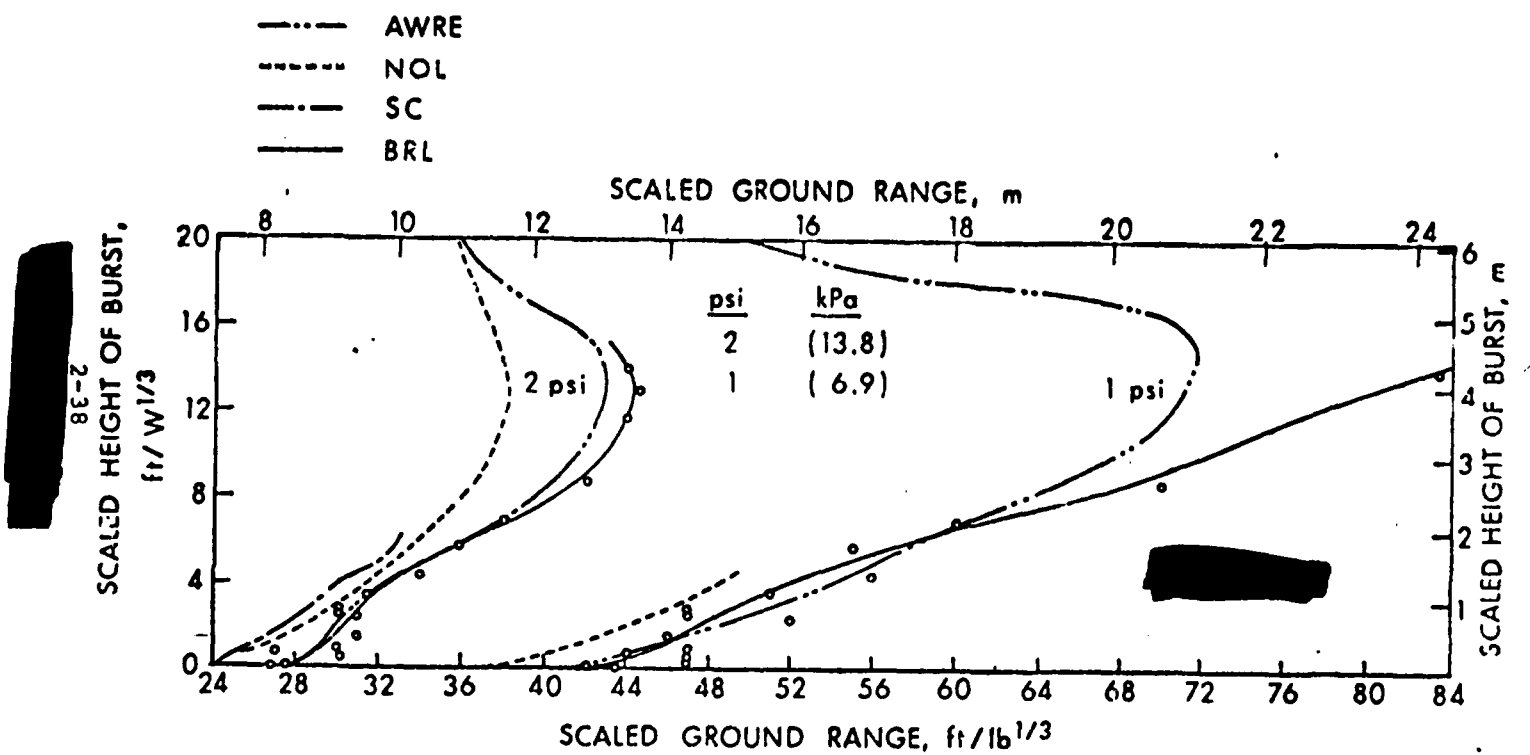

FIGURE 2-18. OVERPRESSURE HOB CURVES, 2 and 1 PSI
(Reisler, to be published)

[redacted]

[redacted]

charge sizes; tests were performed by Sandia Corporation (SC) (Vortman & Shreve, 1976), the Naval Ordnance Laboratory (NOL) (Hartman and Kalanski, 1952), and the Atomic Weapons Research Establishment (AWRE), United Kingdon (UK) (Worsfold, 1957 and 1963). The BRL contours indicate that there is some data scatter around the actual contour lines; as is usually the case, the data scatter is more pronounced for the lower overpressure contours. It is also significant to note that HOB data from other agency tests do not always agree with the BRL curves. In fact, for overpressures of 10 psi and lower, the deviations are significant. For comparison purposes, we shall use the BRL contours, but we should remember that an error band of $\pm$ 10% is estimated for the data.

[redacted] The data plotted on Figures 2-16 through 2-18 are "as read", and although they are scaled to 1 lb TNT, they are not scaled to sea level conditions. The atmospheric pressure at the test site varied from about 13.38 to 13.87 psi. The pressure scaling factor (S_p) for this test series varies from about 1.060 to 1.098. This means that the correction to sea level conditions would be between 6% and 10% for the data shown.

[redacted] Data from both the WES and DRI HE studies have been combined in Figures 2-19 and 2-20 to show how the data over snow compare with the BRL bare-ground HE data. It should be noted that the small-charge data have been Sachs-scaled to BRL average pressure P_o = 13.63 psi. As was discussed in some detail in Section 2.3.3, such data comparisons can be misleading, if taken too literally. This is because the WES and DRI data were obtained by using instruments with inadequate frequency response. Therefore, it is likely that a portion of the obvious displacements of the over-snow overpressure contours

[redacted]

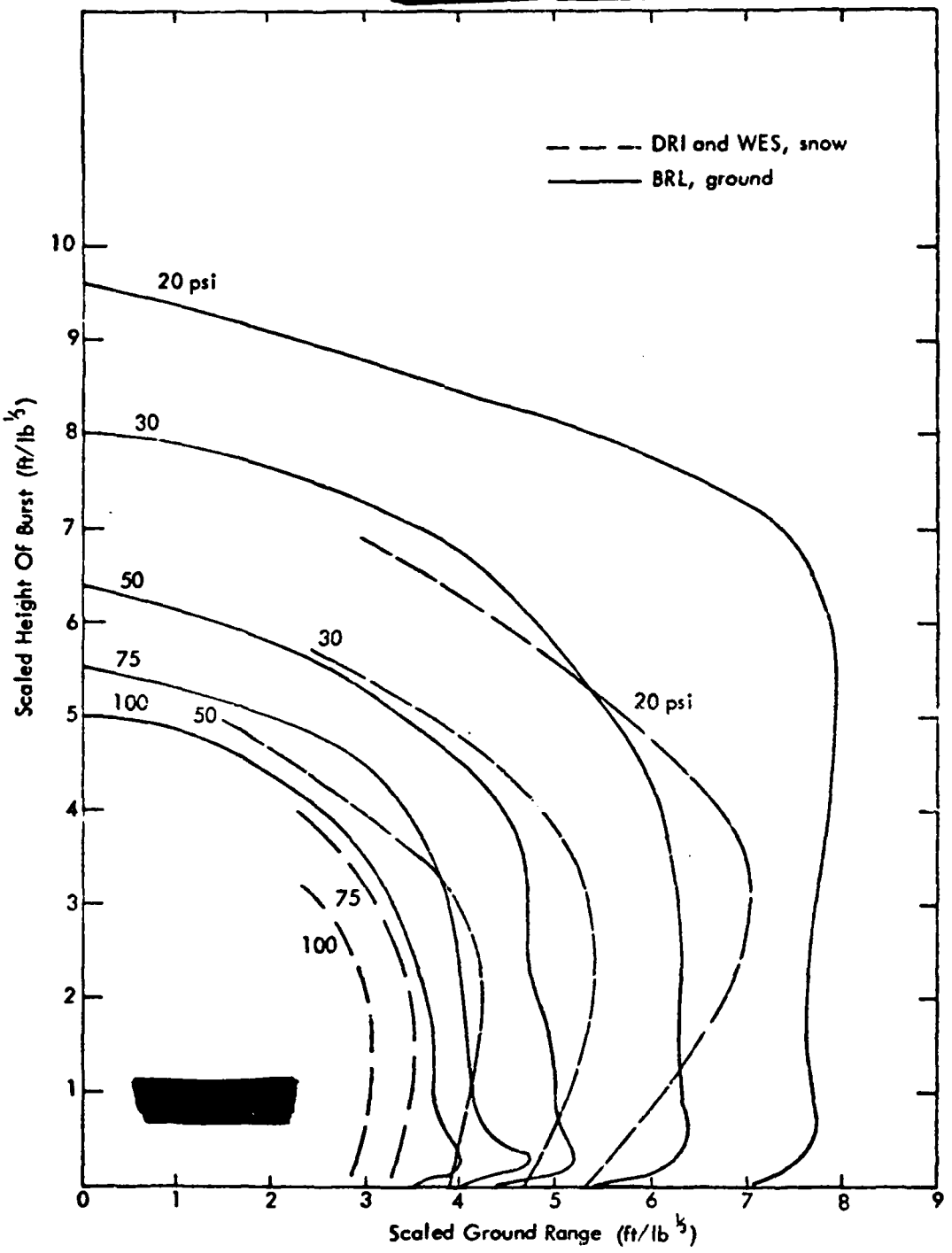

FIGURE 2-19. COMPARISON OF OVERPRESSURE HOB CURVES - HIGH PRESSURE

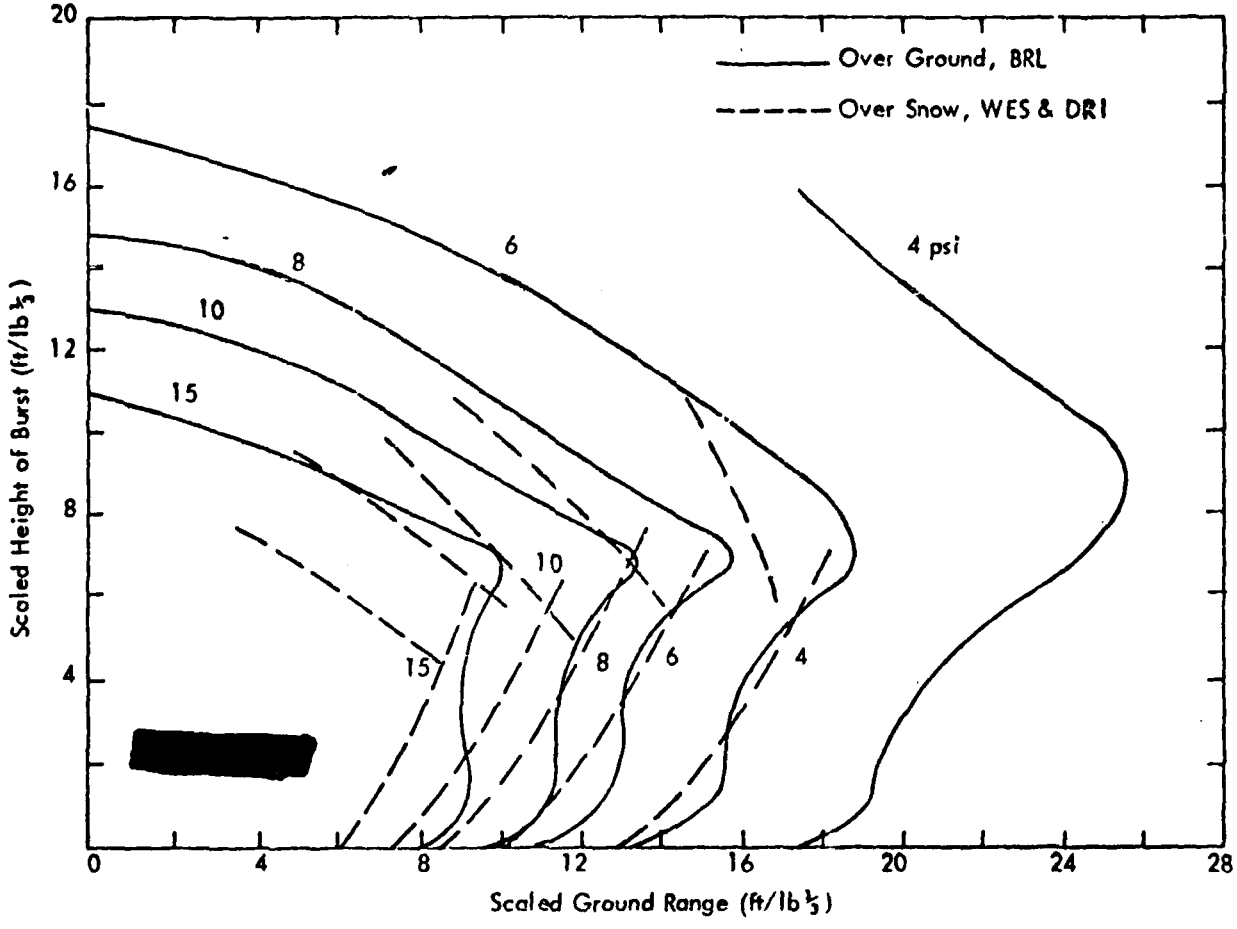

FIGURE 2-20. COMPARISON OF OVERPRESSURE HOB CURVES - LOW PRESSURE

[redacted]

[redacted] from the bare ground contours is due to the limited bandwidths, and it is difficult to determine what portion of each displacement is "real". The conclusion is that there is an effect, shown qualitatively in Figures 2-19 and 2-20; however, to attempt to quantify that effect based on the data available, will probably lead to larger effects than actually exist.

2.3.5 [redacted] Yield Scaling of Snow Depth Effects

[redacted] The minimum snow depth on the various DRI HOB measurements over snow was about $6"/lb^{1/3}$. If this snow depth is scaled to nuclear yields by the $W^{1/3}$ relation, then these HOB curves for a 1 kt would correspond to snow depths of at least sixty feet, which is much deeper than snow encountered in the Arctic except for the snow/ice depths found in the highly glaciated areas.

[redacted] The DISTANT PLAIN winter event snow depth of 4" is equivalent to a depth of about one foot when scaled for a kt. The typical snow depth can range up to 60 cm to 1 m near the end of the winter season over much of the Arctic region. Thus, we are left in a quandary. The HOB curves over deep snow show a marked drawing-in of the curves for surface bursts over deep snow with no dependence on snow depth, while the surface burst over shallow snow showed no effect or at most a questionable effect at high overpressures.

[redacted] There is no real reason to expect a priori that the standard $W^{1/3}$ scaling should be used when considering surface interaction effects due to the snow which is far from an ideal reflecting surface. For an ideal reflecting surface with no energy loss at the surface or for near-ideal situations where only minor effects are expected then the $W^{1/3}$ relation can be justified.

[redacted]

[redacted]

[redacted] Measurements of the response of snow to loading (Napadensky, 1964) indicate an elastic response at overpressures below 10 to 30 atmospheres depending on the snow type, then a crushing region where a large volume decrease occurs with small increases in pressure, then a region with relatively small volume decrease as the pressure increases to 150 atmospheres or so until the density of ice is approached. Thus, for pressures below the yield threshold no permanent deformation of the surface would result.

[redacted] The snow surface does not act like a rigid boundary even in this elastic region. In Figure 2-21 (Ingram, 1962) the magnitude of the reflected shock measured over a snow surface is compared with the theoretical value over a rigid surface for normally incident shock waves. The values of the incident shock are considerably less than the yield strength of snow. Note that the measured shock pressure is about 70% of the theoretical value and the difference seems to be increasing at the higher overpressures. No data were given for non-normal incident shock waves. These measurements were taken in Greenland with 100 foot snow depths; so extrapolation to shallow snow cases is uncertain. The DRI experiments involved snow depths as small as $6"/1b^{1/3}$. The reduction of the pressure over snow as compared to bare ground was about 11% averaged over all ground ranges and burst heights. The DRI bare ground values were less than the rigid surface values as indicated by Figure 2-13, where the reflection coefficient for ground is less than for concrete. No calculations are available to indicate the depth of snow required to induce these effects as a function of yield and specifically to indicate the magnitude of the effect expected for the nuclear case.

[redacted]

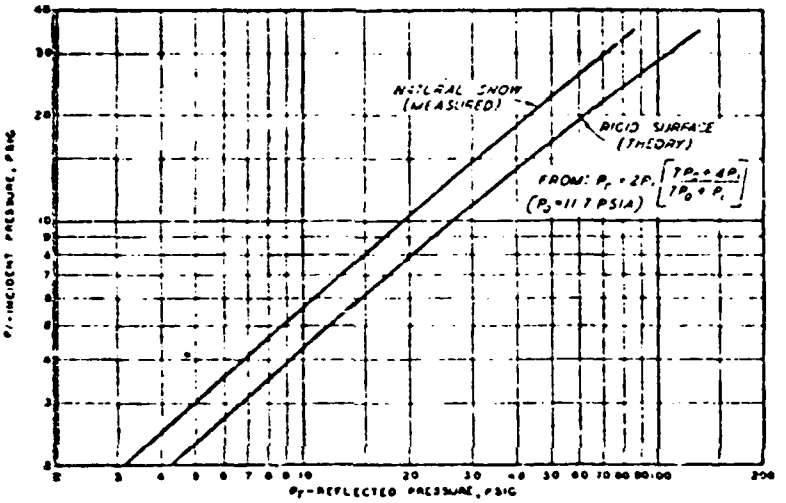

FIGURE 2-21. REFLECTED VERSUS INCIDENT PRESSURE FOR NORMAL INCIDENCE (INGRAM, 1962).

[redacted]

[redacted] For incident pressures above the yield limit, PV work is done by the crushing process and energy is removed from available blast energy. Porzel (1962) gives $Q = 1/2(P-P_o)(V_o-V)$ as an estimate of the energy absorbed by an ideal absorber which will overestimate the energy absorbed. If we use P_o as 150 psi or about 10 atmospheres and (V_o-V) of 2 for compressing snow of density of about .3 g/cm^2 then we get the following estimate of the energy absorbed by a snow layer. The energy loss as a function of range is given by the expression

$$\Delta E = \int_{R_o}^{R} \frac{\Delta E}{\Delta m}\, dm = 2\pi D \int_{R_c}^{R} \frac{\Delta E}{\Delta m}\, r\, dr$$

$$\cong 1.04\times10^{2} D \int_{R_o}^{R} (P-P_o) r\, dr \qquad (2.6)$$

the integral can be evaluated from the 1 kt standard pressure radius curve. If the fractional energy loss is considered and if yields other than 1 kt are allowed we have

$$\frac{\Delta E}{W} = \frac{D}{W^{1/3}} \times \left\{1.04\times10^{-10} \int_{R_o/W^{1/3}}^{R/W^{1/3}} \Delta P\, \frac{r}{W^{1/3}}\, \frac{dr}{W^{1/3}}\right\} \qquad (2.7)$$

where D represents the snow loading in g/cm^2 and the ranges are in cm. The integral has been evaluated from R_o corresponding to the charge radius, and the expression in the braces is shown in Figure 2-22. Beyond the range corresponding to 150 psi the integral is zero; the value of the braces is essentially 7×10^{-4}.

[redacted]

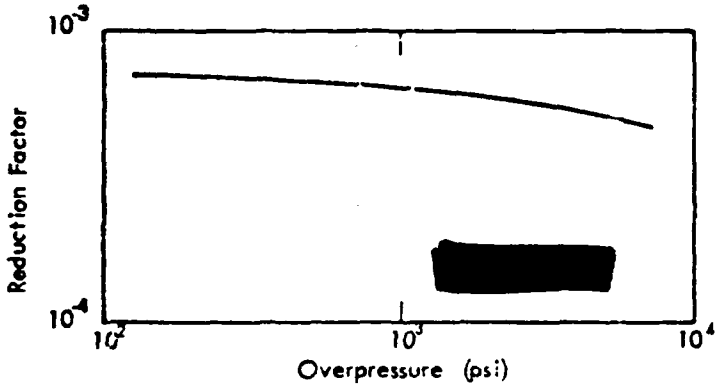

FIGURE 2-22 ENERGY REDUCTION FACTOR DUE TO SNOW LAYER

Thus, one might expect if the above assumptions are correct that the reduction in yield for overpressures below about 150 is given by

$$\frac{\Delta E}{W} = \frac{D}{W^{1/3}} \times 7 \times 10^{-4} .$$

The ranges to these overpressure values might be given by scaling by the expression

$$R'(P) = (W - \Delta E)^{1/3} \, R_{1\ kt}(P) \qquad (2.8)$$

rather than $R(P) = W^{1/3} \, R_{1\ kt}(P)$ (2.9)

so that $R'/R = (1 - \frac{\Delta E}{W})^{1/3}$. (2.10)

Consider the HE charges over deep snow. The snow depth was at least 6" scaled to 1 pound charge. Therefore $D \cong 4.6$ g/cm^2 and $\Delta E/W \sim .4$. Therefore, $R'/R \sim (1 - .4)^{1/3} = .84$

[redacted]

[redacted] or a reduction in range of about 20%, which is of the order of the changes noted in the experiments. In practice one might expect that the ranges would be depressed more for stations closer to the ground and less at the higher altitudes, whereas the above estimate is an average reduction assuming that the blast wave is developing symmetrically from the burst point. Details of the interaction at the surface such as the effect of angle of incidence of the shock wave have been ignored.

[redacted] Recall that the experiment showed no effect of snow depth for snow depths considerably larger than the 6" scaled minimum. Making the same calculations for the 20 ton HE shot with a maximum snow depth of 4" or about 3 g/cm^2 gives $\Delta E/W \sim 7.7 \times 10^{-3}$ or essentially no reduction in yield and no reduction in the pressure-radius relations, confirming the experimental results.

[redacted] Note that the above relation does involve a $W^{1/3}$ scaling of snow depth. Extrapolating to the nuclear 1 kt case and a snow depth of 1 m or a loading of 30 g/cm^2 we obtain $\Delta E/W = .021$ or a negligible effect. The effect would be even smaller for larger nuclear yields. The above general agreement may, of course, be fortuitious and a thorough theoretical investigation of the subject considering the air shock interaction with the nonideal surface should be made.

2.3.6 [redacted]hermal Effects and Precursors

[redacted] Observations on the low-altitude nuclear weapons tests over bare ground show that at a thermal exposure level of 10-30 cal/cm^2 a popcorning effect occurs where particles of the soil are forcibly ejected into the air. This apparently occurs due to the very rapid heating and vaporization of the water entrained in the sand (or other) crystals in the soil.

[redacted]

[redacted]

[redacted] The ejected particles are heated and form a very efficient mechanism for heating the layer of air for a few feet above the surface. A similar effect occurs when rapid heating of organic materials takes place on the surface. The natural convective heat transfer will also be very high and will assist in heating the air layer. These types of effects are certainly strong enough to lead to the formation of a precursor wave.

[redacted] The precursor is characterized by a highly turbulent flow behind the wave front. Dense dust clouds raised by this turbulence tend to follow the shock front as it propagates outward.

[redacted] No empirical evidence is available to indicate the effect of the thermal and shock environment from a nuclear burst over snow. The following assumptions have been made in determining the effect of the thermal pulse on snow. First the energy is assumed to be deposited in the top centimeter of the snow layer. This thickness is arbitrary and the thermal energy is undoubtedly transmitted deeper than this in new light snow and to shallower depths for old packed snow. The actual depth is not critical; however, the point is that very high temperatures that would be obtained by assuming the energy to be deposited in a very thin surface layer are not realistic. Secondly, it is assumed that any melted snow is not heated above the melting point because of the very high conductivity of the slush that will result from surface melting. This means that the energy contained in the thermal pulse will result in melting the maximum depth of snow possible instead of raising the temperature of the melted snow. Of course, if the snow melts completely, the temperature of the surface may begin to increase above 0°C.

[redacted]

[redacted]

[redacted] The characteristics of snow cover a wide range. The reflectivity can vary from .5 to .9, depending upon the condition of the surface so that the absorptivity may vary from .5 to .1. Fresh snow, then, will require about .9 cal/cm^2 deposited to reach the temperature of 0°C and another 8.1 cal/cm^2 to melt each centimeter layer for a total of 9 cal/cm^2 for each centimeter of snow depth. Since only about .1 of the energy is absorbed, an incident exposure of about 90 cal/cm^2 will be required for each centimeter of depth. Assuming packed dirty surface conditions, the required exposure is about the same since the density and the absorptivity can increase about a factor of 5 each.

[redacted] The above estimates indicate that about 2700 cal/cm^2 would be needed to completely melt one foot of snow. No mechanism is available to transfer the energy to the air. This is far above the 30 cal/cm^2 of thermal energy that typically will produce popcorning and other surface effects which serve to transfer energy to the air layer. The conclusion from this discussion is that under most arctic environments, conditions will not be favorable for the formation of a precursor blast wave; that is, the thermal/air-blast interaction effects will be minimal. This conclusion may be substantiated by experimental measurements being performed presently in solar furnaces (Knasel, 1980).

2.3.7 [redacted] Influence of Snow and Water on Dynamic Pressures

[redacted] The air blast dynamic pressure is defined by the relation $1/2\ \delta\ V^2$, where δ is the density of the air behind the shock front and V is the particle velocity of the air. Experiment has shown that blast waves which are "loaded" with dust, e.g., precursor waves, can produce higher-than-expected damage to drag-sensitive targets.

[redacted]

[redacted]

[redacted] The explanation is that the dust picked up by the blast is accelerated to near shock-front velocities, and the increased average density of the air/dust combination results in enhanced pressures.

[redacted] It is expected that the same would be true to some extent for the Arctic environment; however, in this case the blast wave would be loaded with ice crystals and/or water particles. The net effect would be similar to the dust case with density and dynamic pressures increased. In order to determine the magnitude of these increases under various conditions, thorough investigation is needed; some data are available from blast waves propagating over water. Other useful information could be obtained from computer code results.

2.4 [redacted] Air Blast from Underwater Bursts

[redacted] The air shock resulting from an underwater burst has been measured on a few underwater nuclear bursts and several series of small charge conventional explosives tests.

2.4.1 [redacted] Comparison of HE and Nuclear Tests

[redacted] Chapter 7 of DASA 1200 gives analytical techniques for computing the air shock expected from underwater bursts for several DOB, which take into account the available empirical evidence. Prediction curves are given to show the expected air shock for a 1 kt nuclear burst for a wide range of DOB.

[redacted] A series of 5 ton HE tests were made (Pittman, 1970) to determine the air blast from underwater bursts and to correlate with the sparse nuclear data available. Very good correlation with the Baker and Umbrella nuclear data was obtained by using the water column or plume velocity as the scaling parameter for shallow bursts. No correlation of the air blast effects with cavitation closure was possible.

[redacted]

[redacted]

[redacted] NOL has a program to compute the airblast from underwater bursts by using two-dimensional hydrodynamic techniques, but results have not been released for publication (Lorenz, 1980). No calculations including the effects of an ice cover have been made or are planned.

2.4.2 [redacted] Effect of Ice Cover

[redacted] No experiments have been done to determine the effect of an ice cover on the air blast from a nuclear weapon. Consideration of the air blast production mechanisms described in DASA 1200 lead one to expect, if anything, a decrease in the air shock if an ice cover were present. It does not appear that an increase in the air blast due to an ice cover could occur for equivalent DOB as compared with an underwater burst.

[redacted] Contribution to air blast arise from three different mechanisms, the relative importance of which depends upon the DOB. The initial air pulse results from the transmission of the water shock across the interface, another contribution arises from the spray dome, and the third from the plume.

[redacted] The direct transmission of the water shock into the air is the dominant mechanism only for depths below about 700 $W^{1/4}$ feet where the spray dome and plume effects are minimal. In this region the water pressures are low enough that acoustic theory can be used to provide an estimate of the coupling at the interface. DASA 1200 explains several techniques of varying complexity to describe the energy transfer across the interface and propagation into the air. The expected air shocks are very weak ($\leq$ 1 psi).

[redacted] Replacement of a layer of water with ice at the surface would result in a decrease in the coupling efficiency because of the introduction of a second interface where mis-

[redacted]

matching and energy loss can occur. Using the values of the ice, water, and air acoustic characteristics given in Section 1.2, we can estimate the size of the effect as follows:

The overpressure in the air is given by the expression

$$\frac{\Delta P_a}{\Delta P_w} = \frac{2\ P_a\ C_a\ \cos\ \phi_w}{P_a\ C_a\ \cos\ \phi_w + P_w\ C_u\ \cos\ \phi_a} \qquad (2.11)$$

where a and w subscripts refer to air and water values of the parameters, P is the density, C is the sound speed and ϕ is the angle from the normal to the wave front. The angles are related by Snell's law:

$$\frac{\sin\ \phi_a}{\sin\ \phi_w} = \frac{C_a}{C_w}\ . \qquad (2.12)$$

For simplicity consider normal incidence, then substitute values for parameters and we have $\Delta P_a/\Delta P_w = 5.6 \times 10^{-4}$ which indicates the reason why such small air blast occurs with deep bursts.

If we have an ice layer between the water and air then we have

$$\frac{\Delta P_a}{\Delta P_w} \cong \frac{\Delta P_a}{\Delta P_i}\frac{\Delta P_i}{\Delta P_w} \cong \frac{2x428}{2.95x10^6} \times \frac{2*2.95x10^6}{1.54x10^6+2.95x10^6} = 3.8x10^{-4}. \qquad (2.13)$$

Therefore the effect of the ice layer is to reduce the air blast pressure by about 1/3.

The spray dome results when the water shock pressure is strong enough when it reaches the surface that the resultant tension in the water from the combination of the reflected tensile wave and the incident compression wave exceeds the tensile strength of water. This results in cavitation and the separation of a layer of water from the surface with some imparted upward momentum. The spray dome then produces an air shock which can be predicted by the techniques noted in DASA 1200.

[redacted]

[redacted] Introduction of an ice layer for an equivalent layer of water on the surface would obviously cause changes in spray dome development. The pressure pulse transferred to the ice and reflecting as a tensile pulse at the upper ice surface could lead to ejection of a layer of ice whenever the tensile strength of ice is exceeded. Since the tensile strength of ice is much larger than that of water, this will occur only for much larger values of water shock pressures than are needed for spray dome development. This probably will imply a smaller value of air shock than produced from the spray dome. If the tensile strength of the ice is not exceeded, no air shock from this type of mechanism would be expected.

[redacted] The plume or water column is the dominant air blast mechanism when the DOB is less than about $75W^{1/3}$ ft. The plume is treated as a supersonic body moving through the air, and the air shock is computed as described in DASA 1200 by standard hydrodynamic considerations of the bow shock from a blunt body. At the depths where this mechanism is important the water shock pressures are so large ($>10^4$ psi) that a considerable thickness of ice would be shattered. If the entire thickness were shattered, the effect of the ice on plume development would probably be similar to an increased DOB equivalent to the ice thickness. If the ice layer were not completely shattered, then some of the energy of the plume would be expended in breaking up the ice layer and the air blast would be expected to be less.

[redacted] In the above considerations, the effect of the ice cover, if any, would reduce the magnitude of the air blast. It is not expected that more detailed calculations involving hydrodynamic considerations would change these qualitative conclusions. Detailed calculations would be necessary to determine safe escape ranges for aircraft delivering for instance an ice penetrating ASW nuclear burst.

[redacted]

2.5 [redacted] Energy Coupling to the Surface from a Low Altitude Burst

[redacted] The coupling of energy into the surface from a low altitude burst is obviously very intimately connected to the cratering problem which is considered in Section 3 and also is related to the air blast HOB curves which are considered in Section 2.3.

2.5.1 [redacted] Ground Coupling Effects

[redacted] Two cases are of interest involving a snow-ice-ground configuration. In the first the burst occurs above the snow layer so that the shock must traverse the snow layer to reach the underlying ground or structure. In the other case a burst occurs below the snow layer as might happen with an impact fuze which is not actuated by the less dense snow layer. In the first case the snow layer will act as an attenuating medium and will reduce the energy transferred to the underlying medium. In the second case a tamping action might occur and an increase in energy coupled into the underlying material may occur.

[redacted] Both the WES and DRI HE test series included shots in snow with an attempt to measure shock wave parameters in the snow as well as the movement of the snow (acceleration, velocity and displacement). A common problem of these measurements was a very large scatter in the data as evidenced in Figure 2-23 (Wisotski, 1966) and Figure 2-24 which shows the bounds for the data points for shock measurements in ice and snow (Ingram, 1960). The long dashed lines in Figure 2-23 are the limit lines for the snow data from Figure 2-24. The two sets of data are seen to be in essential agreement and suffer from the same order of uncertainty. The source of the data uncertainties include possible quenching of the charge by the snow surrounding the charge and the difficulty of getting good coupling between snow and the gages since snow is a mixture of air and suspended ice crystals.

[redacted]

PEAK PRESSURE AS A FUNCTION OF BOTH HORIZONTAL DISTANCE FROM GROUND ZERO AND CHARGE DEPTH IN SNOW LAYER

MEASUREMENTS TAKEN AT MID-DEPTH OF SNOW LAYER

AVERAGE BAROMETRIC PRESSURE - 510 mm of MERCURY
ONE POUND SPHERICAL PENTOLITE CHARGES

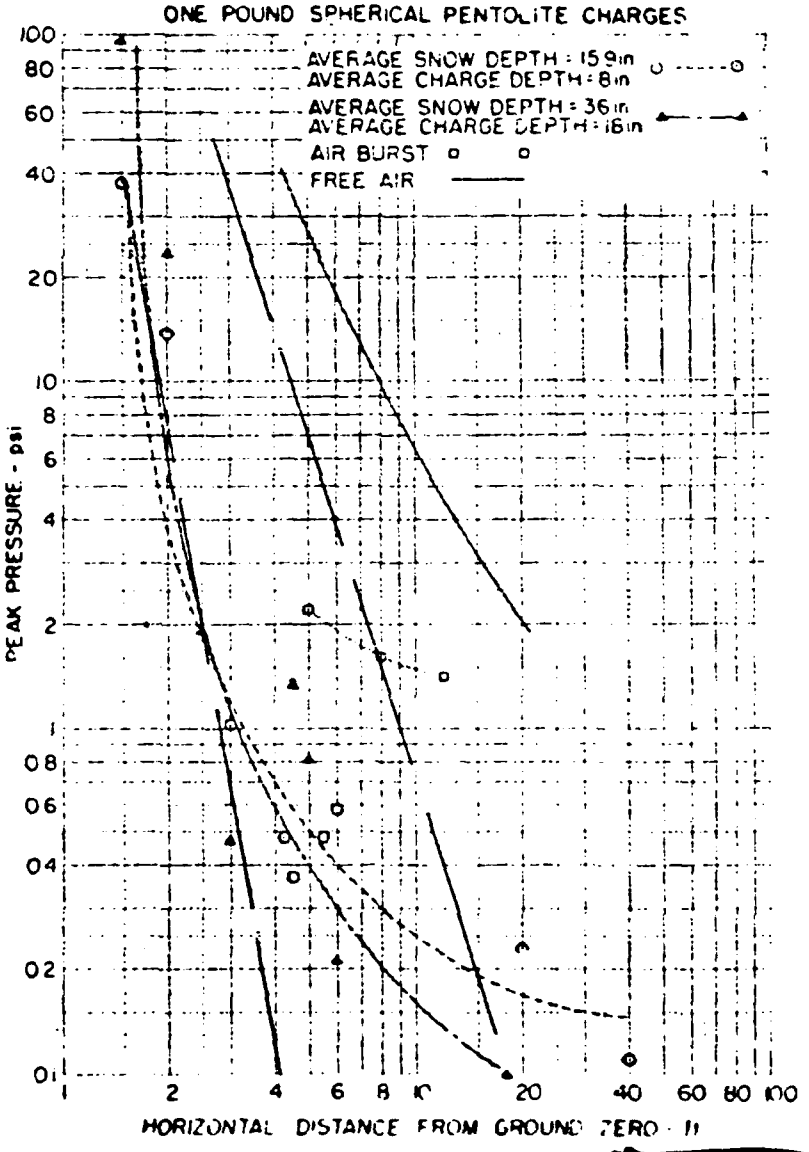

FIGURE 2-23

[redacted]

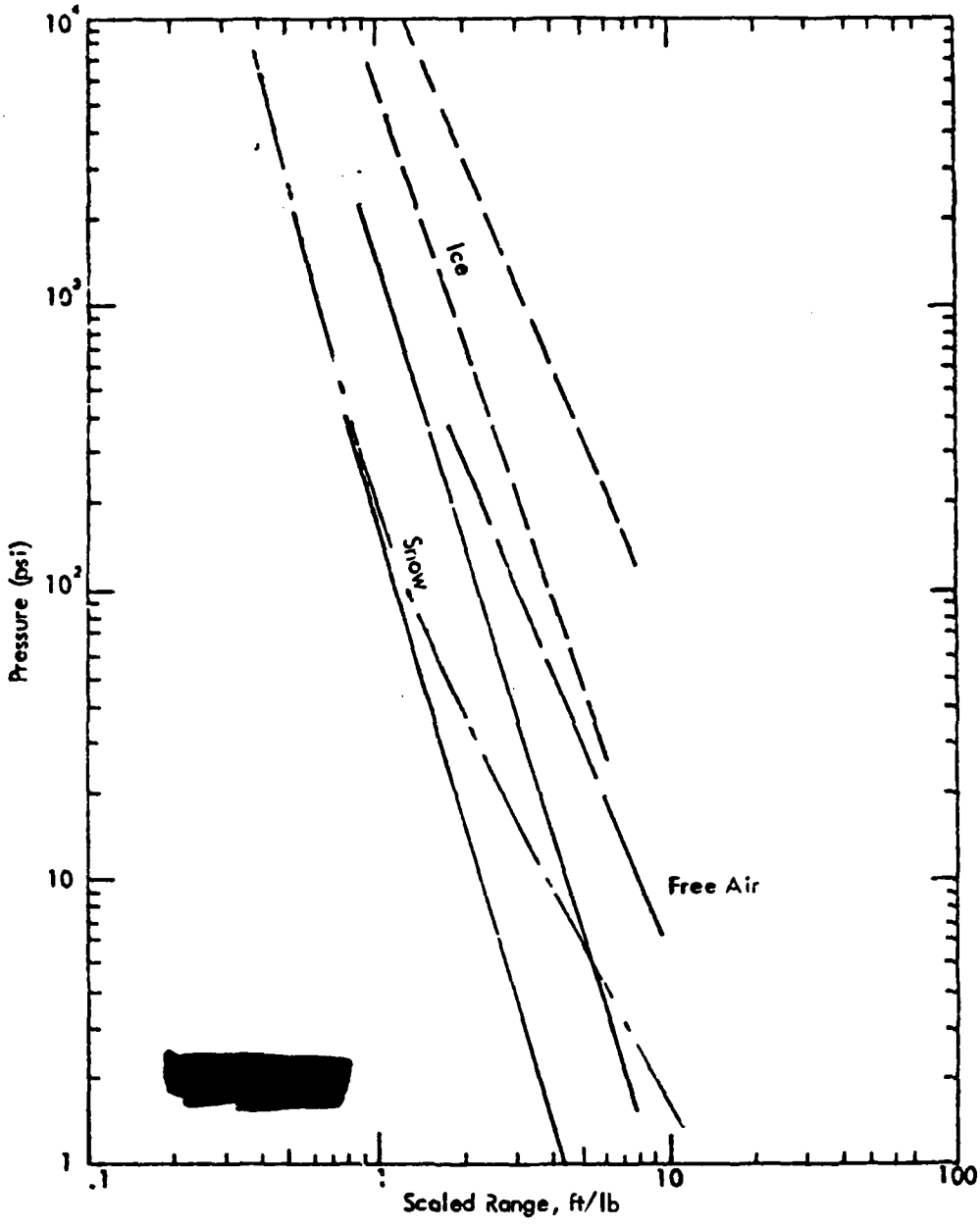

[redacted]

FIGURE 2-24

PRESSURE IN ICE AND SNOW FROM HE EXPLOSION

[redacted]

[redacted]

[redacted] The slope of the snow curve is much steeper than that of air showing that more attenuation of shock energy is taking place. A decay of pressure as $R^{-3.8}$ has been suggested (Smith, undated) as being a reasonable fit of the snow shock measurements. The DRI measurements at pressures less than 1 psi show a marked reduction of the slope, but the curves drawn to represent the data are very subjective.

[redacted] Note that for pressures well under the yield limit there is appreciable attenuation of blast energy. Calculations of the attenuation of blast energy by precipitation referred to in Section 2.2.4 considered energy transferred to water droplets and resulting in vaporization of the suspended water for overpressures as low as 13 psi. The cutoff pressure was assumed to be a function of water droplet size but independent of water concentration. However, the highest concentration considered was about 5% by weight. Scaling of these results to a snow density of .3 g/cm^3 results in attenuations much larger than noted in Figures 2-23 and 2-24. Friedberg considered evaporation of the water requiring about 700 cal/g. It is possible that the shocks in snow involve melting of the snow, which would require about 80 cal/g and which might occur at lower overpressures since smaller temperature rises are involved. Then, however, one should ask why the shock in ice shows no indication of attenuation. If the energies involved are large enough to involve phase change effects then an attenuation in ice shocks would be expected.

[redacted] If we assume attenuation is due to energy lost in crushing the snow, then the effect can be estimated by using the same general procedure as in Section 2.3.4. The energy lost up to a range R is given by

$$\Delta E = \int_{R_o}^{R} \frac{\Delta t}{\Delta m}\, dm = 4\pi\rho \int_{R_o}^{R} \frac{\Delta E}{\Delta m}\, r^2 dr = 2.073\times10^{-2}\rho \int_{R_o}^{R} \Delta P r^2 dr. \quad (2.14)$$

[redacted]

[redacted]

[redacted] for a particular yield W (kt) we have

$$\frac{\Delta E}{W} = 2.0073 \times 10^{-2} \rho \int_{R_o/W^{1/3}}^{R/W^{1/3}} \Delta P (r/W^{1/3})^2 \, d(r/W^{1/3}) \qquad (2.15)$$

where ΔP is the overpressure minus the yield strength. If the above expression is evaluated for a 1 pound charge, then the dash-dot line in Figure 2-24 is obtained. The shock falls progressively lower than the free air curve until the assumed yield strength of 140 psi or about 10 atmospheres is reached then parallels the free air curve. This is of course only a very crude estimate of the effect, but again it is interesting that it is in the range expected.

[redacted] In the nuclear case we do not have a burst in a large amount of snow, but are interested in the attenuation of the blast wave crossing a depth of snow of order of a meter or less in thickness. The above calculation shows that the energy losses in a spherical case scales as $W^{1/3}$. This would imply distances about 126 times larger for 1 kt than for the 1 pound HE charges and would indicate that the snow depths normally encountered in the Arctic would have essentially no effect on the coupling.

[redacted]

[redacted]

[redacted] This is to be expected if the shock energy density is considered. A one thousand psi shock wave has an areal energy density of about 5×10^4 cal/cm^2. The energy loss per gram of snow is 1.65×10^{-3} Δp or 1.65 cal/g for 1000 psi. Since the snow loading is of order 30 g/cm^2 at most, the energy loss is insignificant. Of course we are assuming that no PV work is done for pressures below the yield strength so the attenuation to low pressure blast waves would be zero. This does not agree with the experiments which do show attenuation as compared with the air curve. The stress-strain curves of Napadensky may not be accurate at low overpressures and there may be no well defined yield point as he measured. Unconsolidated snow would be expected to have a very low yield strength. At the present time a quantitative measure of the protection of the snow layer is not possible but the effect is expected to be small for typical Arctic snow depths for nuclear yields.

[redacted] The possible tamping action of snow if a burst is detonated below the snow layer has been considered by Science, Systems & Software (Allen, et al, 1975). In Figure 2-25 the results are shown for a snow depth of 6 g/cm^2. At 6 μsec there is about a 15% enhancement of energy coupled to the ground and the energy in the air is somewhat less for the snow case as would be expected. The calculations were not carried out to later times but the difference might well disappear by later times. However, note that the snow loading is considerably less than the 30 g/cm^2 that can be present in the Arctic. A larger coupling efficiency might be found at lower yields. In practice, the snow layer above the burst would be perturbed which would tend to reduce the tamping effect. A sample calculation with deeper snow should be made to later times to determine the magnitude of this effect even though a large effect is not expected.

Page 2-60 was deleted

[redacted]

[redacted]

2.5.2 [redacted] Water Coupling Effects

[redacted] The coupling of energy from a low altitude or surface burst has been considered experimentally as well as theoretically. However, there is not a large amount of data in this area and certainly none that considers the complications due to an ice layer. For low altitude bursts where the coupling of the air blast into the water is of interest, one would expect the presence of the ice cover to decrease the shock transmitted into the water because there are two surfaces with impedance missmatches instead of only one.

[redacted] For near surface bursts where there is interaction of the weapon outputs with the surface, the situation is much more complicated. There were several nuclear weapon tests involving very small heights of burst over sea water in the Pacific. However, the weapons were mounted on barges in the tests. The area covered by the barge was large enough to have a strong effect on the coupling to the sea water. For this reason, any underwater shock measurements in these tests would probably be different than for a burst directly over the water.

[redacted] Systems, Science and Software has performed a series of calculations to determine the early time coupling of energy from a 1 MT burst to various surfaces. The coupling of energy to sea water was compared to that with NTS Tuff (Allen, et al 1974). At very early times the energy in the sea water is about 50% higher than that in Tuff. The calculations did not continue to late times to consider the underwater shock formation and growth. The increase in coupling was due to the lower opacity of sea water as compared to soil. The presence of salts in sea water does affect the opacity. The salinity of sea ice is less than sea water but is highly variable depending on the ice history. Because of the vast energy available and the high temperatures that are reached, one would

[redacted]

[redacted]

expect the ice calculations to be very similar to the water calculations. Radiation-hydrodynamic calculations of the subsequent shock development would be necessary to determine the effectiveness of this method of coupling energy into the water pressure pulse as compared to an underwater burst.

[redacted] The presence of snow cover on the ice canopy could affect the coupling of energy to the ice then into the water as discussed in Section 2.5.1. The magnitude of the tamping action versus snow depth and yield is unknown. This effect could have implications in ASW. If a technique for locating Soviet submarines under the ice is developed, then the necessity of using an ice penetration weapon must be addressed. In this case the coupling efficiency for the various ice surface configurations will be of great interest.

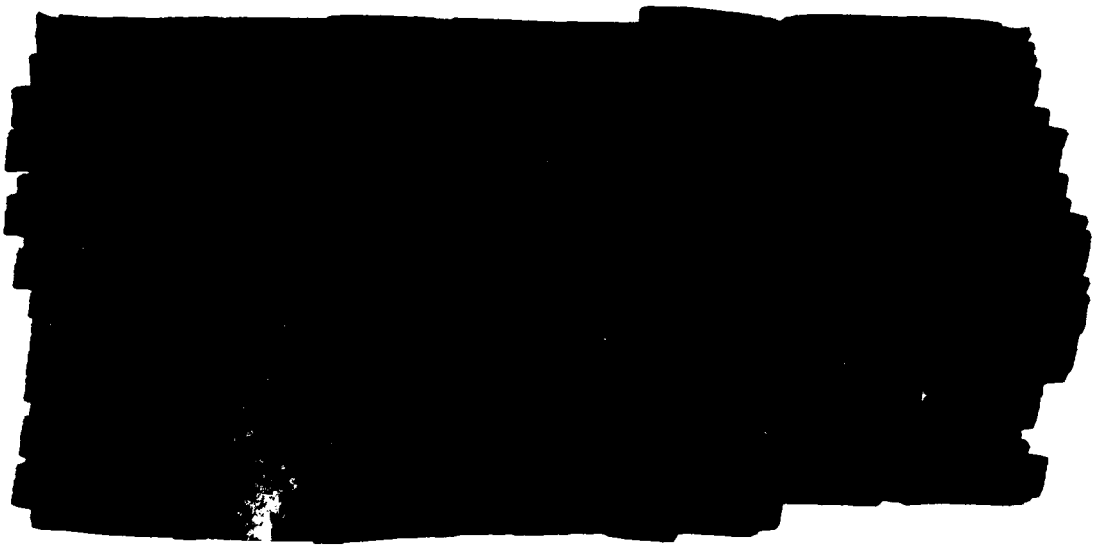

Page 2-63 was deleted

[redacted]

[redacted]

[redacted] There is much uncertainty connected with the underwater shock from near surface nuclear bursts even if the ice cover is not present. A large dependence on the details of the surface configuration may exist even for the late time air and water shocks. In the past there has been little incentive for work in this area. Increased Soviet use of patrols and the current nonavailability of ASW techniques for the polar area may result in an interest in these problems. In order to develop effective airborne tactical nuclear ASW techniques it will be necessary to consider the surface effects on underwater shock.

2.6 [redacted] Air Blast Target Damage Effects

[redacted] The two most important environmental effects on targets or target response in the Arctic are the snow cover on targets and the temperature of the materials used to build the targets. A possible effect is an increase in dynamic pressure due to snow loading of the shock wave.

2.6.1 [redacted] Snow Cover on Targets

[redacted] It is a fact of life in the Arctic that target structures, even those built above ground, will be covered with a layer of snow and/or ice. In fact, most structures designed for arctic use are built to take the most advantage of this cover layer. Snow cover over surface or buried structures affords protection to the structures because it attenuates the air blast load transmitted to the structure. Air-blast-induced accelerations in a snow layer from detonations above the surface attenuate rapidly with depth. Peak vertical downward accelerations at 2 feet below the snow surface are 3 or 4 times greater than those at 5 feet. Much of the air blast energy is absorbed in compacting the snow layer.

[redacted] For structures and equipment above ground, the most effective snow cover protection is afforded by a snow berm over the top of the structure. This berm eliminates any corners

[redacted]

[redacted]

[redacted] or vertical walls and presents a smooth aerodynamic surface to the air blast wave; this has the advantage of preventing large reflected pressure loading of the structure. Also, as the snow berm becomes somewhat compacted, it can contribute to the overall structural strength of the target.

[redacted] For underground (or undersnow) structures and equipment, the snow cover, in addition to providing attenuation of the shock loading, again contributes to the structural strength. This strength contribution can be traced to the "bridging" effect of the snow arch over the buried structure. In a sense, this snow arch acts as an additional structural member when a load is applied.

[redacted] The protection afforded by the snow cover is, of course, a functi.. of the geometry of the snow cover in relation to the construction of the target in question and is dependent on the properties (density, moisture/ice content, etc.) of the snow cover vs depth. Therefore, it is not possible to present useful generalized predictions of the effectiveness of snow cover protection; each case must be considered individually.

[redacted] During the Greenland HE test series, the resistance of snow arches was considered (Smith). A summary of the results obtained is shown in Figure 2-27. As one would expect, the damage level depends primarily on the ratio of arch span to the crown thickness. A strong word of caution is necessary because these were HE tests, and the width of the pressure pulse is much less than would be experienced from nuclear tests at the same overpressure levels. No calculations have been made predicting the magnitude of this effect.

[redacted]

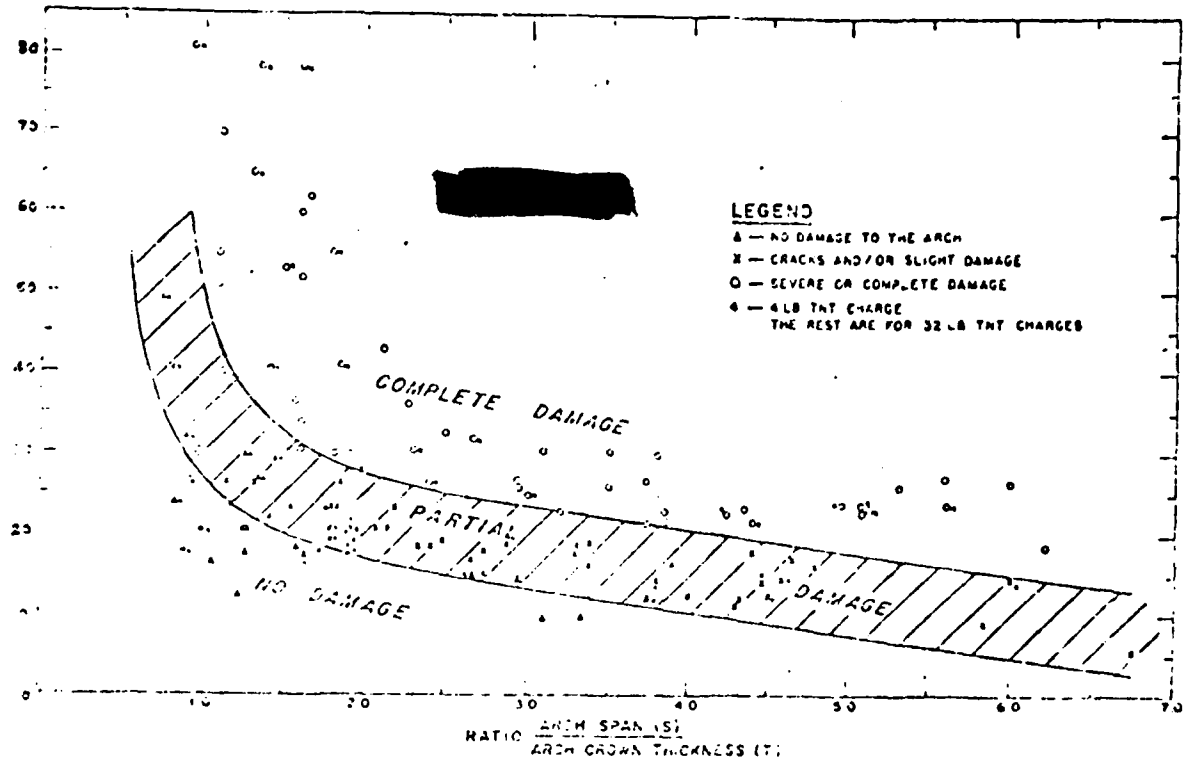

Figure 2-27. Summary of data for damage to model snow arches. Real arches withstood considerably higher overpressures than the model arches. (From Szostak and Benert, ref. 11) (Smith, undated)

[redacted]

2.6.2 [redacted] Effect of Target Temperature

[redacted] Those structural materials which are used on targets essentially the same in Arctic climates as they are elsewhere may react to cold in such a manner as to alter their vulnerability to nuclear effects. Specifically, metals, rubber, plastics, ceramics, and fabrics will undergo changes in their strength, elasticity, impact resistance, and other related characteristics. These changes will increase the susceptibility of the material to damage. Steel is an important material for military targets. The mechanical properties of steel vary with temperature in a non-uniform fashion. However, the most important effect of low temperatures on steel is to reduce its ductility. This property change can cause brittle fracture to occur in structures exposed to relatively small static loads. A significant reduction in impact resistance will also accompany a loss in ductility.

[redacted] During the series of HE tests conducted by WES on the Greenland ice cap, some military equipment was inadvertently exposed to air blast loading. However, during those tests, no measure of the loads and/or response of these targets was obtained. Thus, without any definitive data on the subject, we could only speculate on the quantitative effect of the reduced temperatures of the target materials with regard to damage criteria. This is a technical area which requires more thorough investigation.

2.6.3 [redacted] Enhanced Dynamic Pressure

[redacted] It has been speculated that air blast dynamic pressures in the Arctic would be "loaded" with ice crystals and/or particles for many situations of military interest. These waves impinging upon drag-sensitive targets could impose enhanced forces, which would result in more severe damage than one would predict for the unloaded waves.

[redacted]

[redacted]

[redacted] Virtually no pertinent data are available pertaining to this effect; before one could attempt to quantify the effect, a great deal of effort would be required to collect data and perform computer code calculations to check the data consistency.

2.7 [redacted] Conclusions and Recommendations

[redacted] In the previous sections the current status of knowledge of air blast and surface effects predictions under arctic conditions were considered including the free air blast parameters, precursor effects near the surface, the effects of precipitation, clouds and inversion layers, changes in the height-of-burst curves over shallow and deep snow, and surface coupling considerations including the attenuation or possible tamping effect of a snow layer and the effect of the snow/ice canopy on shock transmission accross the air-water interface. The uncertainties in the various subjects can be corrected by a recommended research program.

2.7.1 [redacted] Conclusions

[redacted] The cold temperatures in the Arctic cause a slight increase in the time of arrival, time duration and impulse expected from a free air burst. If one were considering the effect of attacking a specific impulse sensitive target in the coldest area of Siberia, the change might be worth including. The overpressure-radius and dynamic pressure-radius relations are unchanged since the atmospheric pressure and the variations in the Arctic are essentially the same as in temperate climates. In conclusion, the free air prediction values given in EM-1 are adequate for Arctic free air values, and scaling to arctic pressure and temperate values is not necessary.

[redacted] The attenuation of blast wave energy by precipitation, fogs, and clouds is considered in EM-1 and has been treated in later studies. The amount of precipitation and the precipitation rates in the Arctic are in general less than in most

[redacted]

[redacted]

[redacted] temperate areas. The fact that the precipitation will likely be snow will not increase the magnitude of the effect. Light rain and fogs reduce the effective blast yield of at most 10% even for large yields at overpressures as low as 1 psi. For most studies the attenuation could be ignored since it is very difficult to have accurate knowledge of precipitation patterns and rates.

[redacted] If a burst occurs below a temperature inversion refractive effects can cause a focusing action and increase the extent of blast effects along the ground for very small overpressures (<1 psi). If the burst occurs above the inversion layer, the opposite effect is noted. The high probability of strong inversion layers in the Arctic would lead to an enhancement of these effects noted in temperate climates. Since the effects are only noted at very small overpressures, the military effects of inversions could be important only for low overpressure targets. Inversion effects should definitely be considered in determining fail-safe ranges for HE testing. An experimental program concerning the effect of temperature inversions and wind on blast has recently been completed and a definitive report on this subject will be published during 1980. Calculations have been proposed to determine whether temperature inversion effects can occur for overpressure values as high as 1 psi.

[redacted] In EM-1 the recommendation is made to treat frozen ground, snow, and ice as thermally ideal surfaces and, therefore, not to expect any classical precursor effects as discussed in EM-1. This is a result of the very large amounts of energy required to produce water vapor and heat up a layer of air near the ground and the fact that these surfaces will

[redacted]

[redacted]

[redacted] usually have a large albedo implying absorption of a small fraction of the incident thermal energy. Experimental confirmation of this fact is expected in the very near future. Frozen soil, ice and snow samples will be exposed in the French solar furnace to determine their response to thermal loading and their capability of transferring heat to the near surface air layer.

[redacted] Even though snow is expected to be a thermally ideal surface, because of the strong attenuation in snow, significant reduction of air blast over snow has been measured for bursts over deep snow. Reductions in ranges of 25 - 40% to the overpressures less than 100 psi were noted in these experiments. Scaling the snow depths to nuclear yields would result in depths of about 50 ft/kt$^{1/3}$. Depths this deep would only be found in Greenland or other highly glaciated areas. However, the validity of scaling the snow depths with yield in this manner is very questionable. No theoretical work has been done in this area to determine exactly what interaction is occurring in the snow layer and to determine the proper scaling method.

[redacted] Comparisons have been made of the air blast from 20 ton surface shots over bare ground and with a snow depth of 4", which scales to 1.25 ft/kt$^{1/3}$. No change was noted in dynamic pressures on impulse. A possible reduction was noted in the overpressure over 600 psi over the snow. This difference was not explainable and could be due to data uncertainties.

[redacted] Thus, we have two sets of data, one with scaled snow depths of 50 ft/kt$^{1/3}$ where large differences were noted in the overpressure contours, and another with a scaled snow depth of 1.25 ft/kt$^{1/3}$ where no change was noted for a surface burst.

[redacted]

[redacted]

The typical arctic snow depth will usually be less than 3' which is in the shallow scaled regime. However, there is no assurance that this type of scaling is valid.

[redacted] The presence of deep snow can affect the coupling of blast energy in two ways. In the first, if a low altitude air burst is used to attack a hardened structure either above or below the ground covered by a layer of snow, then one would expect a decrease in the blast energy coupled to the structure and a decrease in the damage. Large numbers of measurements of shock in snow from HE shots have been made. The scatter in the data range over an order of magnitude. The experimental uncertainties are large and involve an effect on the HE burning due to the snow and the difficulty of getting a good match between the snow and the measuring instruments. There have been experiments performed to measure the basic shock properties of snow and the data again show a very wide scatter depending on the state of the snow. No calculations of the attentuation to be expected from snow layers have been located. Theoretical predictions have been made that snow shock values are very similar to NTS Tuff. At the present time, no predictions on the attenuation properties can be made.

[redacted] In the second case, if a weapon were detonated below a snow layer (for example by having an impact fuze that does not actuate in snow) the tamping action of the snow because of the larger opacity as compared with air could result in a larger coupling of energy into the ground. Likewise, if a weapon were detonated on the surface of the snow, the decrease in opacity as compared to ground might result in a larger transfer of energy into the snow and ultimately into the ground than for a ground surface burst. A single calculation of the tamping effect showed

[redacted]

[redacted]

about a 15% increase in the (6 μsec) ground coupling for a 1 MT burst under 4 g/cm^2 of snow. Considering that a typical Arctic case involves about 5 times this amount of snow, one might experience a significant increase in the ground coupling. However, until calculations are extended to later times, no predictions of the magnitude of the effect are possible.

[redacted] Both of these snow effects could have implications for attacking targets in northern USSR. In the first case, the snow may tend to decouple the air blast energy from the target and lead to less damage and attack effectiveness than expected. In the second case, the snow may enhance the damage and attack effectiveness. The second case may have implications in ASW also. Currently, one desires a burst at a sufficient DOB so that little energy is dissipated above the water surface to maximize the submarine damage range. This would require an ice penetrating weapon in the Arctic. However, because of the snow and/or ice tamping effect, it may be possible to fuze the weapon to go off under the surface of the snow or ice and enhance the coupling of energy to the water so that an under water burst may not be required.

2.7.2 [redacted] Recommendations

[redacted] Significant uncertainties which may be important for systems in the Arctic were found to exist in the following areas:

- o The effects of precipitation, fogs, clouds and temperature inversions on the air blast
- o HOB curves over snow for nuclear yields
- o Effects of snow cover in altering the coupling of energy to the surface versus HOB/DOB
- o Air blast from underwater bursts through an ice canopy.

[redacted]

[redacted]

[redacted]

Note that all of the above items involve shock propagation through and interaction with lossy materials consisting of air mixed with quantities of water in various states (vapor, liquid or solid). No recent hydrodynamic calculations were found considering these materials. Resolution of uncertainties in all of the above areas could be obtained by a three part research program.

Preliminary Analytical and 1-Dimensional Hydrodynamic Calculations

[redacted] During this phase equation of state information should be collected on snow, ice and frozen ground materials. Analytical calculations using the developed theories of shock propagation through lossy materials should be made to determine the attenuation of shocks through these materials and to provide confirmation of hydrodynamic runs. A series of 1-d hydrodynamic calculations should be made addressing the attenuation of shocks in air-water mixtures and snow, the coupling of shocks from air to the ground and structures through various snow depths, and to compare the response of frozen grounds with rocks. These calculations might provide resolution of some of the uncertainties in the above areas and would provide guidance in setting up multidimensional hydrodynamics runs.

[redacted] Specifically the effects of precipitation, fog and clouds in causing attenuation to the air shock could be determined and compared with current calculations and predictions. The runs showing the coupling of air shock through various snow depths into the ground and structural materials will show the degree of protection provided by snow cover. These calculations should be done for various incident shock strengths to show the effect on both very hard targets such as silos (1000 - 2000 psi) as well as softer structures (<100 psi). The

[redacted]

[redacted]

[redacted] incident shock angle should be varied to see what effect this has on the coupling and air interaction process. This will provide guidance in the effect of the snow layer on the air blast and effects expected in HOB studies.

Two-dimensional Hydrodynamic Calculations

[redacted] The results of the phase 1 calculations would be used to determine what 2-d hydrodynamic runs are necessary to resolve the remaining uncertainties.

[redacted] A series of runs may be necessary to produce HOB curves over snow. The effect of the snow depth on the air blast may be yield dependent and it may be necessary to generate curves for more than one snow depth.

[redacted] Calculations of the shock transmitted to hard targets covered by a snow layer from a low altitude air burst may be necessary depending upon the results of the 1-d coupling and attenuation calculations.

[redacted] The tamping effect of a snow layer should be determined by repeating the calculations of S^3 for depths of snow representative of Arctic conditions. If a coupling significantly greater than 15% is noted at the early times, then the calculations should be carried to later times to determine the increase in the ground shock.

[redacted] The tamping effect for smaller yields representative of ASW weapons should be determined in a snow-ice-water geometry to determine if ice penetrating weapons would be required in attacking submarines beneath the ice.

[redacted]

[redacted]

[redacted] Depending on the results of the phase 1 calculations 2-d calculations of the air blast from underwater bursts with an ice canopy may be warranted. If ice under strong shocks loses its integrity then these calculations will not be necessary, and the ice can be treated as an increased equivalent water layer for air blast predictions.

Experimental Program

[redacted] During phases 1 and 2 of the program requirements for experiments to define the basic physical properties of snow, ice, and frozen ground can be determined. Information in this area exists, but in the ten years since these experiments were performed better techniques have been developed.

[redacted] Depending on the results of the computer calculations a series of HE tests in an Arctic environment may be warranted. The subjects of interest would be effect of depth of snow on air blast measurements at the surface and above the surface, effect of inversions, correlation if any between yield and depth of snow, effect of ice canopy on water and air shock from underwater bursts and coupling of airshock through the snow to the ground for a burst above the ground. Such a series should include static overpressure and dynamic pressure versus time measurements and have an instrumentation system with an adequate band width to resolve the narrow pulse widths.

[redacted]

[redacted]

[redacted].8 Bibliography

Allen, R. T., Bailey, L. E., and Schneyer, G. P., Energy Coupling for Near Surface Nuclear Explosions, DNA 3400F, Systems, Science, and Software, LaJolla, CA, November 1974, SECRET RD CNWDI.

Allen, R. T. and Baker, J. C., Energy Coupling with Sea Water, DNA 3550F, Systems, Science and Software, LaJolla, CA, 11 October 1974, SECRET RD.

Allen, R. T., et al, Energy Coupling for Near Surface Nuclear Bursts (U), DNA 3564F, Systems, Science and Software, LaJolla, CA, 2 April 1975, SECRET RD.

Carpenter, J. and Brode, H. L., Height of Burst Blast at High Overpressure, Paper, Fourth International Symposium, The Military Applications of Blast Simulation, September 1974, R & D Associates, Marina del Rey, California, UNCLASSIFIED.

Defense Atomic Support Agency, Nuclear Weapons Blast Phenomena (U), DASA 1200, Defense Nuclear Agency, Washington, D.C. 1 March 1971, SECRET RD.

Defense Nuclear Agency, Capabilities of Nuclear Weapons (U), DNA EM-1, Defense Nuclear Agency, Washington, D. C., 1 July 1972 (change 1, 1 July 1978), SECRET RD.

Friedberg, R., Weather Effects on Blast, NWEP-1138, Naval Weapons Evaluation Facility, Albuquerque, NM, July 1976, UNCLASSIFIED, AD-B012752L.

Hartman, G. K. and Kalanski, P. Z. The Optimum Height-of-Burst for High Explosives, NAVORD Report 2451, July 1952, Naval Ordnance Laboratory, White Oak, Maryland.

[redacted]

Ingram, L. P., Blast Effects on a Snow Tunnel, Camp Century, Greenland, WES MP 2-378, U. S. Army Engineer Waterways Experiment Station, Vicksburg, MS, February 1960, UNCLASSIFIED.

Ingram, L. P., Air Blast in an Arctic Environment, WES TR 2-597, U. S. Army Engineer Waterways Experiment Station, Vicksburg, MS, February 1962, UNCLASSIFIED, AD-274722L.

Joachim, C. E., Structures in an Arctic Environment, Airblast and Subsurface Shock of High Explosive Tests, U. S. Army Engineer Waterways Experiment Station, Vicksburg, MS, October 1964, UNCLASSIFIED, AD-450624.

Joachim, C. E., Shock Transmission Through Ice and Snow, WES TR 1-794, Report 3, U. S. Army Engineer Waterways Experiment Station, Vicksburg, MS, September 1967, UNCLASSIFIED, AD-659774.

Knasel, M., private communication, results expected in mid 1980.

Lorenz, R. A., private communication, February 1980.

Napadensky, H., Dynamic Response of Snow to High Rates of Loading, CRREL RR-119, Cold Regions Research and Engineering Laboratory, Hanover, NH, 1964, UNCLASSIFIED, AD-600075.

Pittman, J., Airblast from Underwater Explosions; Mono Lake, NOLTR 70-212, United States Naval Ordnance Laboratory, White Oak, MD, 12 November 1970, UNCLASSIFIED.

Porzel, F. B., Cratering in Snow, Technical Note Number 62-35, Institute for Defense Analyses, July 1962, UNCLASSIFIED AD347266.

Reed, J., private communication, report to be published during 1980.

Reisler, R. E., Giglio-Tos, L., Teel, G. D., and LeFevre, D. P., Air Blast Parameters from Summer and Winter 20-Ton TNT Explosions, Operation Distant Plain, Events 3 and 5, BRL MR 1894, Ballistic Research Laboratories, Aberdeen Proving Ground, MD, November 1967, UNCLASSIFIED, AD-830308.

Reisler, R. E., et al, Air Blast Measurements from the Detonation of Large Spherical TNT Charges Resting on the Surface (Operation DISTANT PLAIN, Events 6A and 6), BRL Memo Report No. 1955, USA Ballistic Research Laboratories, Aberdeen Proving Ground, Maryland 21005, January 1969.

Reisler, R. E., et al, Air Blast Data From Height-of-Burst Studies in Canada, Volume II - 1975 Dipole West Series (HOB 45.4 to 144.5 Feet), BRL Report No. RM 1990, USA Ballistic Research Laboratory, Aberdeen Proving Ground, Maryland 21005.

Reisler, R. E., Pettit, B. A., and Kennedy, L. W., Air Blast Data from Height-of-Burst Studies in Canada, Volume I HOB 5.4 to 71.9 Feet, BRL Report No. 1950, USA Ballistic Research Laboratory, Aberdeen Proving Ground, Maryland 21005, December 1976 (AD #B016344L).

Reisler, R. E., HE Height-of-Burst Blast at Moderate to Low Overpressures, USA Ballistic Research Laboratory, Aberdeen Proving Ground, Maryland 21005 (to be published).

Smith, J. L., Effects of Frozen Surfaces on Air Blast Phenomena, Cold Regions Research and Engineering Laboratory, Hanover, NH, undated, UNCLASSIFIED.

Vortman, L. J., and Shreve, J. C., The Effects of Height of Explosion on Blast Parameters, Sandia Corporation Report SC-3858 (TR), June 1976, Sandia Laboratories, Albuquerque, New Mexico.

Wells, P. B., et al, Air Blast from Special Weapons in Homogeneous and Non-Homogeneous Atmospheres (U), DNA 2751P, Kaman Sciences Corporation, Colorado Springs, CO, 30 April 1971, SECRET RD CNWDI.

Wisotski, John and Sayer, W. H., A Study of the Effects of Snow Cover on High Explosive Blast Parameters, DU-DRI-2303, Denver University, Denver Research Institute, Denver, CO, March 1966, UNCLASSIFIED.

THIS PAGE IS INTENTIONALLY LEFT BLANK.

[redacted]

SECTION 3
CRATERING PHENOMENA

[redacted] The mechanisms producing a crater for near surface, surface or subsurface bursts are closely allied to the air blast and surface effects considered in Section 2. There have been no nuclear tests by the U.S. in cold climates; so the U.S. has no experimental data base for nuclear cratering phenomena in the Arctic. As discussed in EM-1 the data base for nuclear craters consists entirely of large yield bursts in the Pacific and small yield bursts in Nevada. Thus, cratering from nuclear bursts is a very uncertain subject at best. Adding the complexity of Arctic conditions increases the uncertainty.

3.1 [redacted] Arctic Environmental Differences

[redacted] The difference of importance in cratering is the large probability of occurrence of snow, ice and frozen ground in the Arctic. In heavily glaciated areas the snow/ice thickness will be deep enough that the entire crater forms in these materials. Most of the area, however, will have only 1 m or less of snow or ice over frozen ground; so a layered geometry must be considered in the cratering predictions. For large yields the scaled depths of snow or ice are negligible, and as will be shown later, the crater in the ground will be little affected by the snow layer.

[redacted] The ice canopy may influence the underwater crater development. The existence of underwater permafrost may be important. Adequate experimental data are not available in these cases.

[redacted]

[redacted]

3.2 [redacted] Cratering Mechanisms in Arctic Media

[redacted] In the Arctic environment, it is obvious that the medium in which the explosion crater is created can take many different forms. Some of the forms are bare ground (frozen and/or underlain with permafrost), frozen ground covered with snow and/or ice, thick ice layers over water, and shallow bodies of water. In the latter case, the crater could form in the solid medium under the water.

[redacted] Figure 3-1 is a schematic illustration of a crater formed by a surface burst, showing descriptive nomenclature. Since crater size varies primarily with charge yield, depth of burst (DOB), and the cratered medium, it is desirable that tests be conducted with as many different charge geometries and in as many different media as possible. This also involves the development of suitable scaling relations by which results of small-scale tests can be used to predict the results to be obtained with much larger yields. Thus far, attempts to correlate theory with empirically developed exponents, or scaling laws, have met with only limited success.

[redacted] Figure 3-2 shows some ideal crater cross sections from nuclear bursts, illustrating the effect of HOB and DOB on crater volumes. If a nuclear or HE burst is sufficiently high above the ground surface, only a shallow compressional crater is formed and no ejecta produced. As the height of burst decreases, the crater volume increases and an increasing fraction of the crater is due to excavation and ejection of material from the crater region.

[redacted]

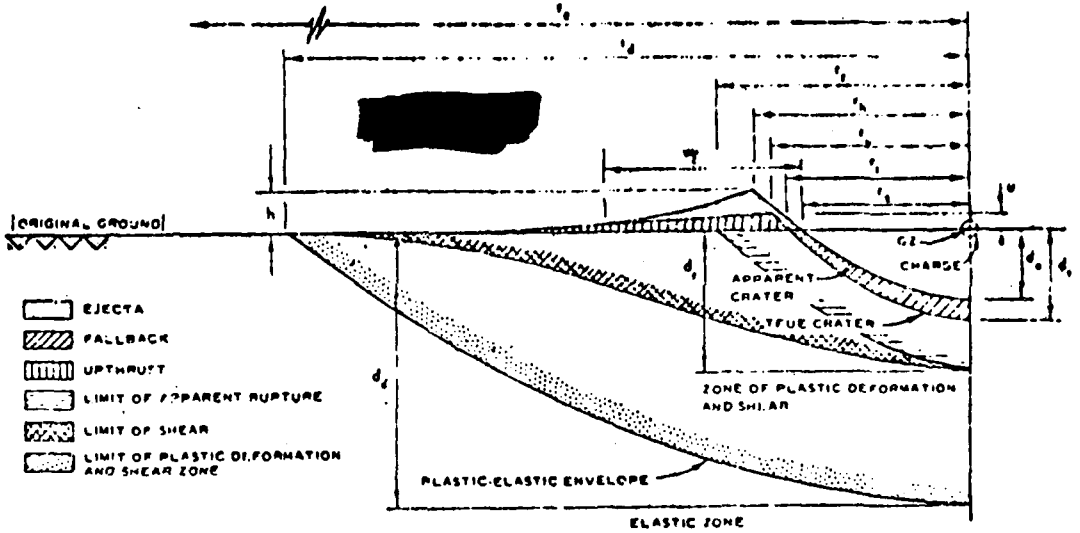

Figure 3-1 Typical half-crater profile and nomenclature for surface burst. Profiles and dimensions are symmetrical about the centerline.

[redacted]

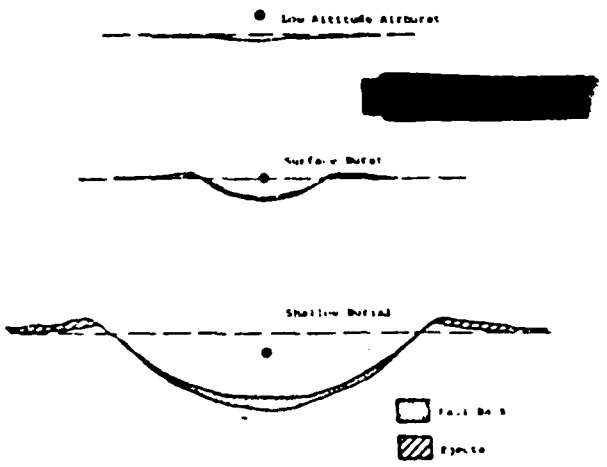

[redacted] FIGURE 3-2. EFFECT OF DEPTH OF NUCLEAR BURST ON CRATER SIZE AND SHAPE

[redacted]

[redacted]

[redacted] The large difference in energy density (ratio of explosive yield to explosive mass) between high explosive and nuclear devices can cause substantial differences in cratering efficiency (the ratio of volume of crater to explosive yield) and in the relative importance of various cratering mechanisms between the two types of sources.

[redacted] The material properties of the medium in the crater region influence the crater volume primarily through their compressibility and shear strength under dynamic loading conditions. Water content plays a large role in determining shear strength, especially in soils. The largest crater volumes are found in wet soils and the smallest crater volumes are found in rock. Jointing is an important factor in determining the crater size in rock geologies. Geologic layering is a rough indicator of material properties with depth and must be considered when predicting crater volumes. Frozen ground or ground interspersed with ice lenses and/or permafrost will behave like rock as far as crater formation is concerned.

[redacted] The failure process in snow differs from that in glacial ice, frozen ground, rock, and certain types of soil. Characteristic features of this failure (referred to here as "viscous-damping failure") are: 1) damping of the disturbance during the rise to peak pressure, and 2) substantial recovery of stored potential energy during unloading. Due to the unique physical properties of snow, craters formed by explosions in snow will be unusual in appearance and size compared with craters formed in other media. Snow is a composite material that consists of a relatively incompressible crystalline solid (ice) and a compressible gas (air).

[redacted]

[redacted]

[redacted] The air is found in the interconnecting voids in the ice matrix and comprises up to 70% of the volume of snow near the surface of the ice cap. Other properties of snow of importance in cratering are low melting and vaporizing temperatures.

[redacted] Immediately after detonation, as the hot gas bubble begins to form a cavity by vaporization, the surrounding snow is compacted radially, and the air in the voids is compressed. Cavity walls are fractured and an ice skin is formed by fusion. During this loading of the snow, a significant amount of the explosive energy is expended in compacting and deforming the snow without destroying cohesion. Some snow is dissociated and thrown out as ejecta.

[redacted] Much of the energy used to compress the air during loading is recovered during unloading (after the pressure wave has passed), which results in fracturing and deforming the snow. The primary cavity then exhibits a reversal in the direction of displacement (implosion) as the snow attempts to regain its original location. This part of the mechanism is referred to as pseudo-elastic rebound. Simultaneously, the compacted snow zone and the ice skin are fractured.

[redacted] A sensitively balanced transition condition appears to exist at critical depth. The balance determines under what conditions fractures during the rise of pressure and the outward expansion of the gas bubble predominate over fractures formed as a result of implosion. Implosion is closely followed by a vortex within the snow and scouring action as the gas bubble emerges from the rising column defined by the vortex. This scouring largely determines the final shape of the apparent crater.

[redacted]

[redacted]

[redacted] At a charge depth less than that at which maximum scouring occurs, more of the energy of the explosion is expended in the atmosphere and less is available to the snow. An apparent crater is formed in the air blast range and the secondary zone of the fragmentation range. Refer to Figure 3-1. The volume of the apparent crater per pound of explosive charge is maximum at the transition limit between the two ranges, where scouring is a maximum. Dimensions of the apparent crater are neither predictable with accuracy by conventional cube root scaling nor usable as a basis for predicting undersnow damage because 1) it is difficult to determine the proportion of the explosive energy partitioned to loading the snow, and 2) the apparent crater in snow occurs subsequently to loading and is the result of the scouring action of the vented gas bubble.

3.3 [redacted] High Explosive Cratering Experiments

[redacted] There have been many HE cratering experiments performed in the Arctic or sub-Arctic. The surface materials include snow, ice and frozen ground of various types. Many of the experiments have been designed to determine the optimum depth of burst of various HE types and charge sizes for producing the largest crater for mining and excavating. In Figure 3-3 (Bauer et al, 1973) representative cratering efficiencies are given as a function of depth of burst for several arctic materials. For purposes of nuclear cratering emphasis on shallow or surface bursts would be of more interest.

[redacted] The large differences in the lower and upper limits for frozen materials noted in Figure 3-3 are typical in cratering experiments due to variations in local geology and material properties. The cratering efficiency of HE charges increases with increasing water content. As discussed in EM-1 this has also been noted in unfrozen ground materials.

[redacted]

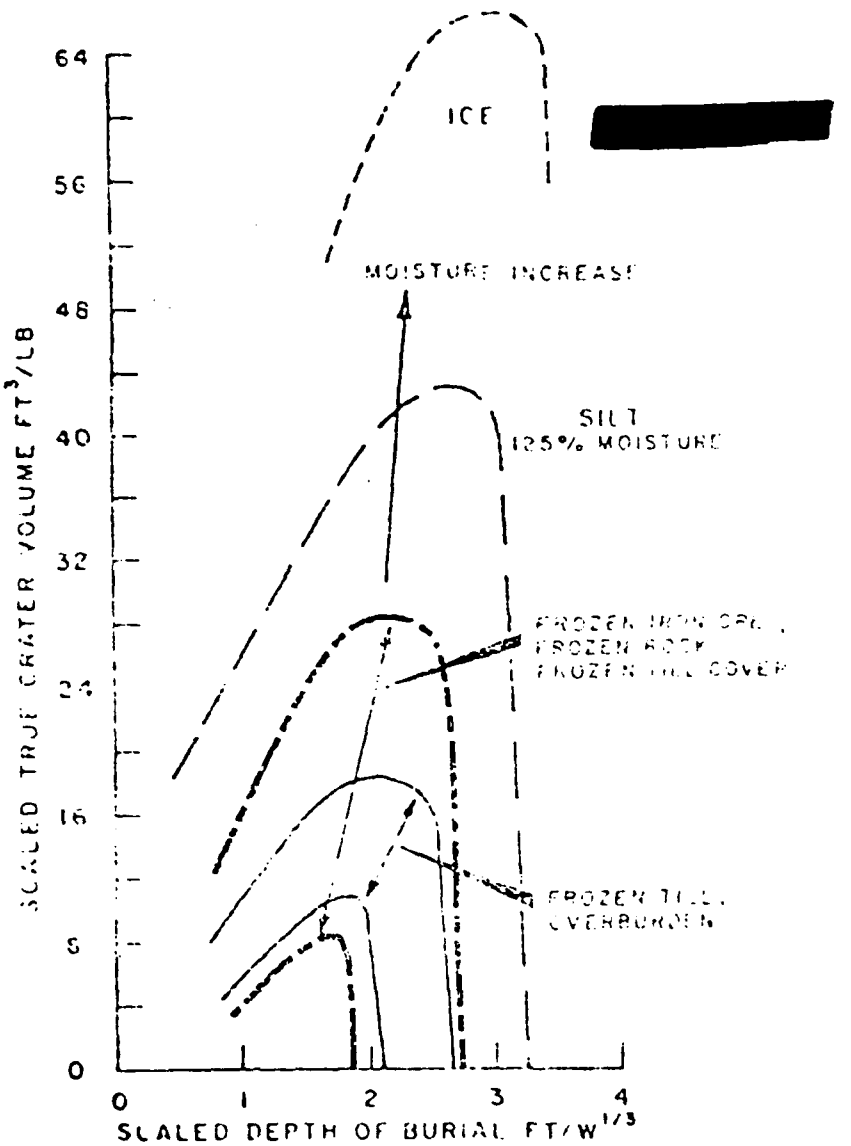

FIGURE 3-3. SCALED CRATER VOLUME VS SCALED DEPTH OF BURST FOR VARIOUS FROZEN MATERIALS AND EXPLOSIVE COMBINATIONS.

[redacted]

[redacted] In conjunction with the WES and CRREL air blast experiments in Greenland, extensive measurements (Livingston, 1970 and 1968) were made of craters in deep snow and ice. The depths were such that the entire crater was in the snow or ice. Shallow and even above ground burst heights were used in addition to depths of burst extending below the optimum depth of burst.

[redacted] In Figure 3-4 the efficiencies of HE cratering in ice and snow as a function of the scaled DOB are compared. The very wide bounds shown in the figure result from several different types of explosives and several charge sizes. Thus, the scatter is due to material properties and differences in efficiencies of explosives as well as possibly to inapplicability of cube-root scaling of the charge weight. Note that at optimum depth of burst the snow crater will be about 3 times as large as a crater in ice. The optimum depth of burst in ice is somewhat deeper. For a surface burst the snow crater is about twice as large as an ice crater. No data were provided for near surface air bursts over ice.

[redacted] In Figure 3-5 the scaled radius of snow and ice craters are compared as a function of scaled depth of burst. The radius of the snow crater is much larger than ice especially at the deeper depths. For a surface burst the radius for snow is about 50% larger than for ice. In Figure 3-6 the scaled crater depths in snow and ice are compared. The differences for deeper depth of burst are not as large as for the radii but for a surface burst the crater depth in snow is about twice that in ice.

[redacted] Surface bursts are very important militarily; so the Greenland surface burst experiments have been analyzed as a function of charge weight (Conway and Meyer, 1970). The apparent crater depths and radii are summarized in Figure 3-7; also included on these figures are data from Sager (1960 and 1961). Figure 3-8 shows the apparent crater volume as a function of charge weight. Other cratering data from surface events in snow are virtually non-existent.

[redacted]

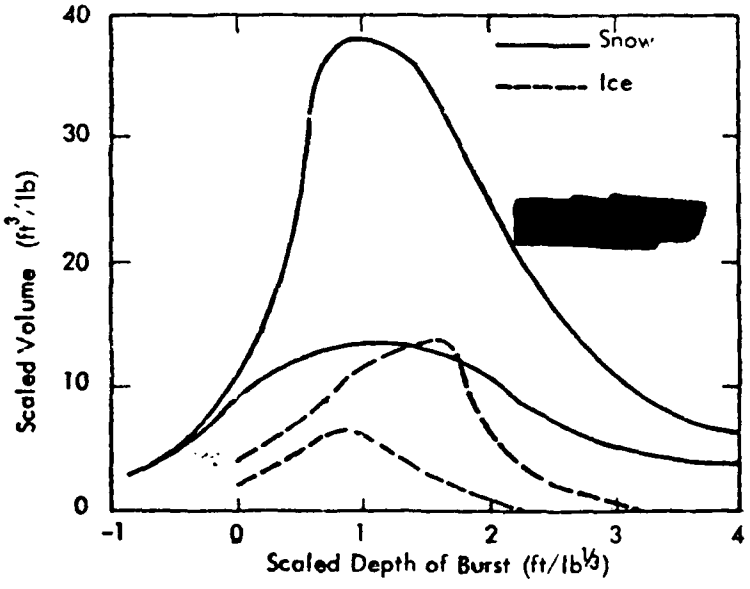

FIGURE 3-4 HIGH EXPLOSIVE CRATER VOLUME IN SNOW AND ICE

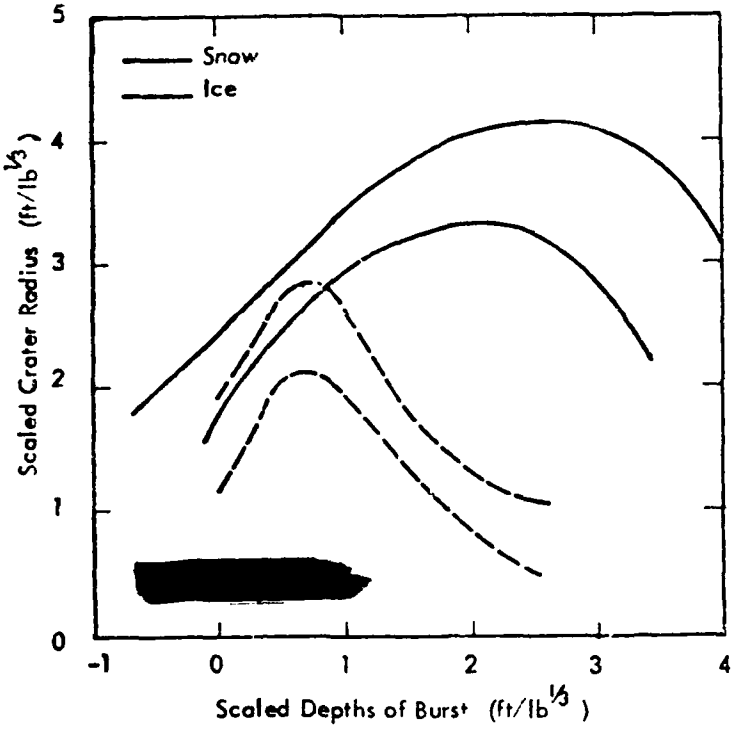

FIGURE 3.5 HIGH EXPLOSIVE CRATER RADII IN SNOW AND ICE

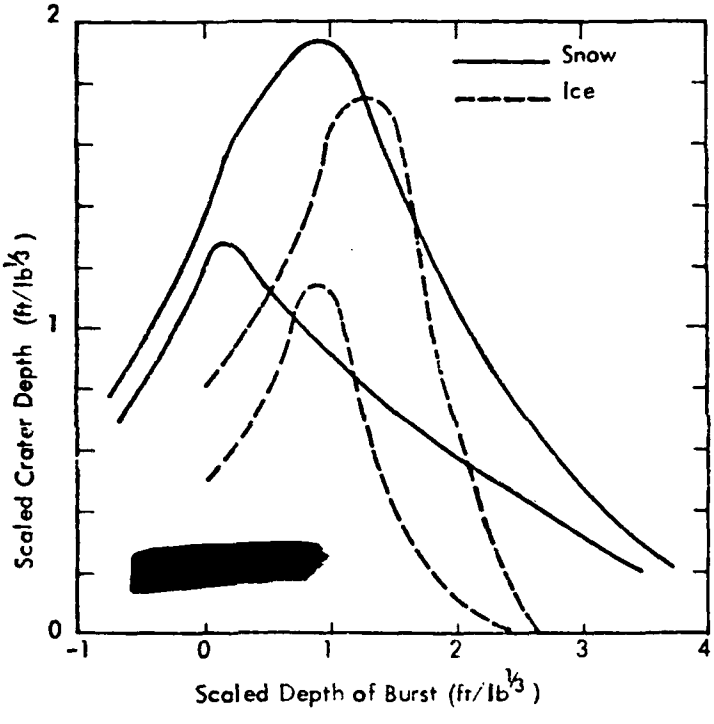

FIGURE 3-6 HIGH EXPLOSIVE CRATER DEPTHS IN SNOW AND ICE

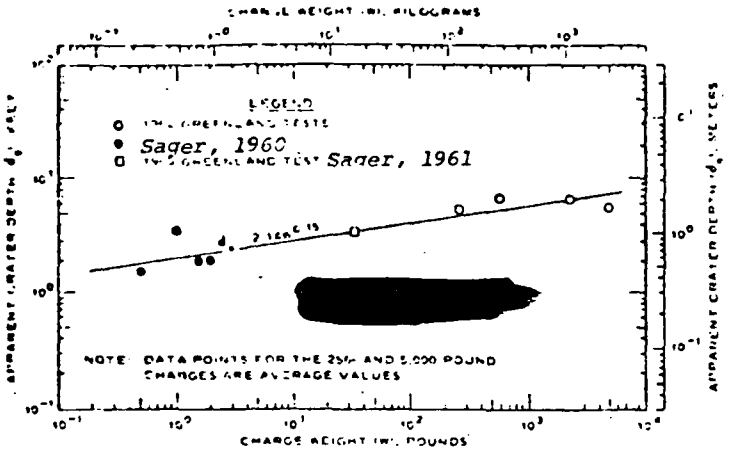

a. APPARENT CRATER DEPTH (d_a') VERSUS CHARGE WEIGHT (W)

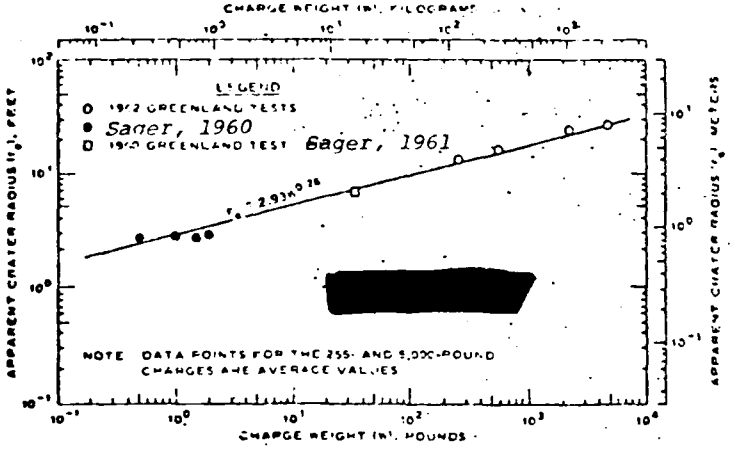

b. APPARENT CRATER RADIUS (r_a') VERSUS CHARGE WEIGHT (W)

Figure 3-7 Apparent crater dimensions as functions of charge weight.

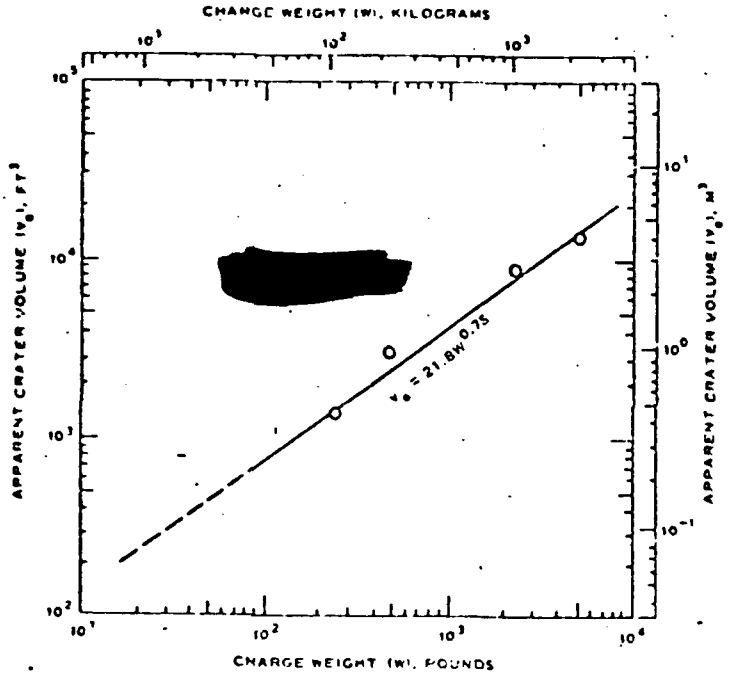

[redacted] Figure 3-8 Apparent crater volume as a function of charge weight.

[redacted]

[redacted]

[redacted] Figure 3-9 shows the variation of apparent crater radius with charge weight for surface bursts in snow as compared with craters from surface TNT events in clay, sand, basalt and shale. Similarly, Figure 3-10 presents a comparison of apparent crater depths versus charge weights. These figures show that craters in snow tend to be larger than craters in other media for the same charge yield.

[redacted] This increased size appears to be due to the greater amount of material vaporized and compacted during the explosion. Although no ejecta measurements were made, examination of the crater lip profiles indicates that the contribution (to volume) of the ejection mechanism in snow craters is correspondingly less than in craters in other media. Craters in snow have a characteristic wide shallow appearance. The magnitude of the pseudo-elastic rebound in snow is greater directly under the charge than in the material pushed laterally outward because of the greater lateral confinement of the material under the charge.

3.3.1 [redacted] Scaling Considerations

[redacted] Equations for scaling crater dimensions in snow within a range of yields of 0.5 to 5,000 lbs, as determined by the use of the method of least squares, are presented in Figures 3-7 and 3-8. These equations show a significant departure from the common cube-root scaling. For the apparent crater radius, a slightly smaller scaling exponent of 0.26 is indicated. The scaling exponent for apparent crater depth, 0.15, is considerably smaller than that normally applied to craters in soil. These unusual scaling exponents are probably best explained by the mechanism of pseudo-elastic rebound in snow. A correspondingly low scaling exponent of 0.75 is evident (Figure 3-8) for the apparent crater volume. It should be noted that these empirical

[redacted]

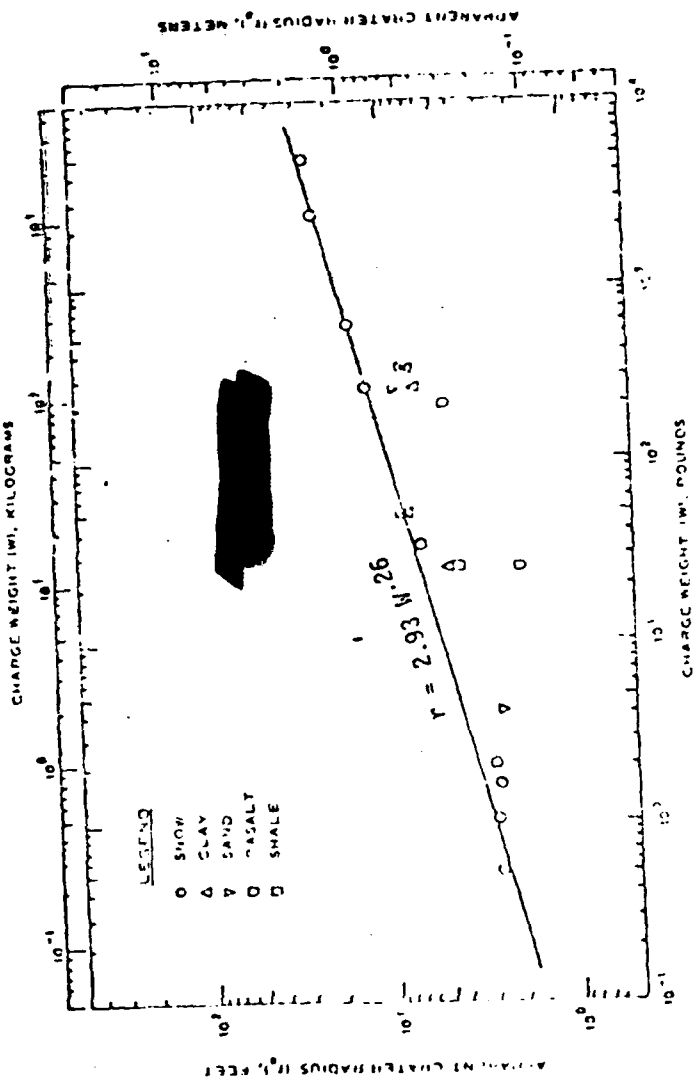

FIGURE 3-9. COMPARISON OF APPARENT CRATER RADIUS VERSUS CHARGE WEIGHT FOR SURFACE-BURST CRATERS IN VARIOUS MATERIALS

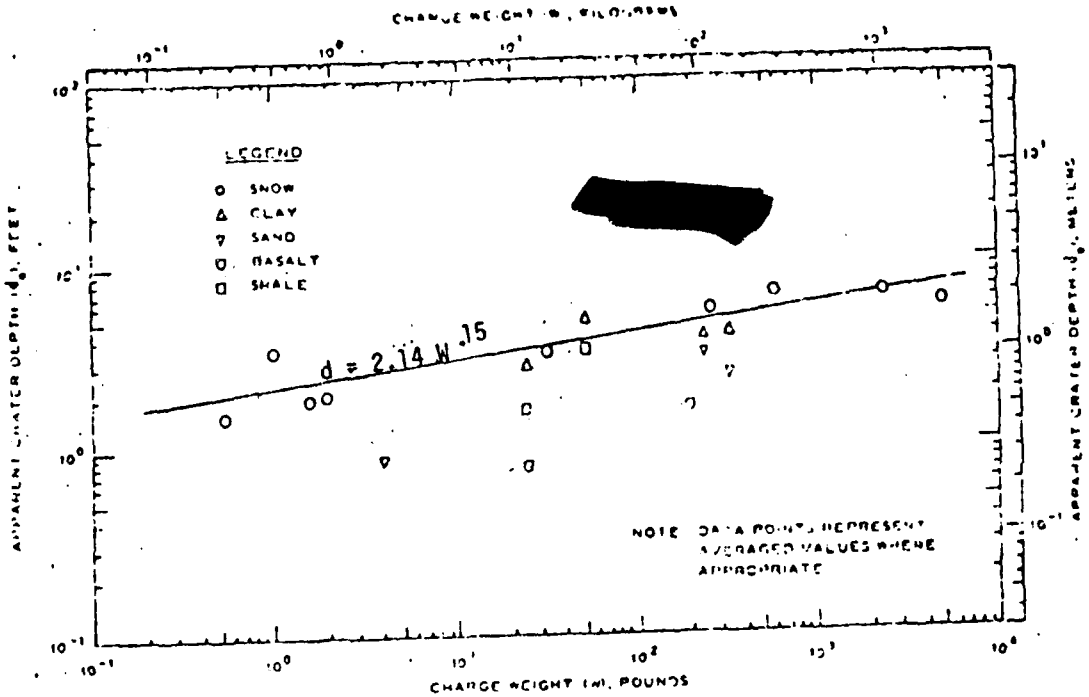

FIGURE 3-10. COMPARISON OF APPARENT CRATER DEPTH VERSUS CHARGE WEIGHT FOR SURFACE-BURST CRATERS IN VARIOUS MATERIALS.

[redacted]

[redacted] scaling components are based on a limited amount of data and should be considered as approximations. The use of these exponents to scale HE data to nuclear explosions would be questionable because of the magnitudes of the NE yields and the differences in thermal energy release, which appears to influence crater formation in snow significantly.

[redacted] Even though the scaling rules for the snow radius and depth are very uncertain when extended to nuclear yields, it is instructive to compare these results with the wet soil EM-1 predictions. Using the relations in Figures 3-9 and 3-10 a crater from a 1 kT surface burst over snow would have a radius of 127 ft and a depth of 19 ft. Using the relations given in the revised cratering section of EM-1, a crater from a 1 kT burst in wet soil would have a radius of 101 ft and a depth of 42 ft. Thus, a wide shallow crater is predicted by the HE snow data when scaled to nuclear yields.

[redacted] Snow efficiency varies from about 7×10^{3} to 3×10^{4} ft^3 per ton, being equivalent to wet sand or muck. Ice varies from 4×10^{3} to 8×10^{3} ft^3 per ton. Frozen soils range from 3×10^{3} to 6×10^{3} ft^3 per ton. The highest efficiencies are found in frozen silts which are equivalent to wet soft rock, and the lower efficiencies are for frozen aggregates which are equivalent to hard rocks. As is normal for cratering measurements, a wide range of values is noted. It is suggested that for want of a better method these efficiencies be used in conjunction with the prediction methods in EM-1.

[redacted]

[redacted]

[redacted] The effect of the increased thermal yield of nuclear bursts as compared with HE is unknown. For typical soil materials small yield nuclear devices (<1 kt) are assumed to be about 1/7 as efficient as HE and large yield devices (≥1 kt) are assumed to be 1/20 as efficient as HE charges. Thus, a 1 kt nuclear burst would produce a crater volume of about 3×10^5 to 1.5×10^6 ft^3 per kt. A kt of energy is capable of melting about 1.5×10^6 ft^3 of snow (ρ = .3 g/cm^2, melting energy about 80 cal/g) and vaporizing about 1.7×10^5 ft^3 of snow (vaporizing energy about 700 cal/g). If a fraction of this energy were available to increase the cratering efficiency for nuclear bursts, then the efficiencies obtained using the current prediction methods may be too low by as much as a factor of two.

3.3.2 [redacted] Layered Geometry Considerations

[redacted] Consider the 19 ft. crater depth found for a 1 kT burst in snow. This is much deeper than typical snow depths except in highly glaciated areas. Thus, the cratering data considered above must be modified to include the effects of the shallow snow. HE experiments considering a layered geometry of dry soil over wet soil have been represented by the expression

$$(V-V_L)/(V_U-V_L) = 1 - \exp(-5.4\ d/V^{1/3})$$

where

- d = depth to base material (water table or cemented layer)
- V = apparent crater volume in the layered geology
- V_U = apparent crater volume in the surface material when $d = \infty$
- V_L = apparent crater volume in the base material when $d = 0$.

In Figure 3-11 the data for a sand over a cemented soil layer is shown. The upper curve will represent a case with a definite boundary between the surface and base layer such as would occur for snow over frozen ground. The dashed line is the equation given above.

[redacted]

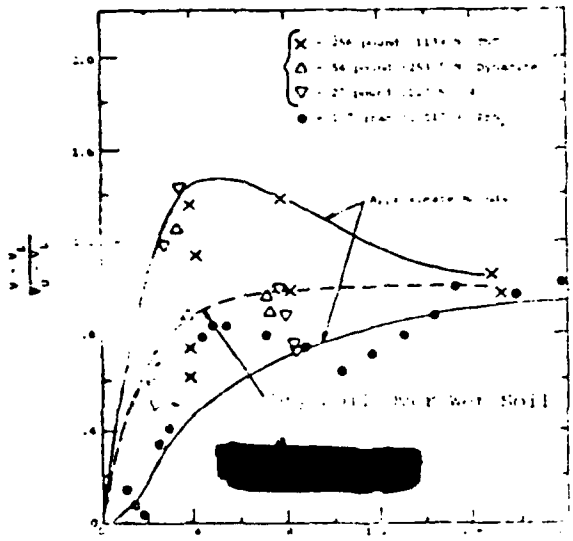

Scaled Depth to Layer ($d/V^{1/3}$)

FIGURE 3-11. CRATERING DATA: SAND OVER A CEMENTED LAYER

[redacted]

[redacted] In using the technique given above an iterative process is necessary since the volume appears on both sides of the equation (or on both axes in Figure 3-11). The volumes V_U and V_L are obtained by using the HE efficiencies along with the proper nuclear yield and efficiency ratio factor. When this is done for the typical Arctic case of 1 m of snow over frozen ground then the following observations can be made. For 1 kt $V_U = 1 \times 10^6$ ft^3 and V_L could be as low as 2×10^4 ft^3. The value of V would be about 2.5×10^5 ft. The scaled snow depth is only about .05. In this case the volume of the crater in the base material would not be altered appreciably by the thin snow layer. For larger nuclear yields this depth of snow would be insignificant.

[redacted] The calculations for the layered geometry are very uncertain, and we are applying the results of layered geometry cases far outside the original configuration.

3.4 [redacted] Underwater Cratering

[redacted] Underwater cratering is discussed as a major topic in Chapter 2 of DNA EM-1 and in Chapter 8 of the Underwater Handbook. However, existing manuals do not discuss any effects that may be caused by conditions peculiar to cold-weather regions, nor do there appear to have been any experimental investigations into this matter. The discussion that follows must therefore be regarded as conjectural. The factors that might cause variations under Arctic conditions from what is predicted under temperate conditions are differences in bottom composition, if any, and the presence of ice.

[redacted] Reference to Table 2-12 in Problem 2-36 of DNA EM-1, wherein soil correction factors are given for various bottom materials, reveals that the range of bottom materials covered encompasses the range of materials expected to be found in any

[redacted]

[redacted]

[redacted]

of the world's oceans, including the Arctic. It is known, however, that subsea permafrost exists in several of the seas of the Arctic, the Laptev, Kara, E. Siberian, Chukchi and Beaufort Seas for example (Lewellen, 1973, 1974, 1977). The extent of the subsea permafrost is not known, and there is a limited amount of information as to its characteristics (Chamberlain et al., 1978). Of particular importance is whether the permafrost in a given area is bonded, with ice in the interstices, or unbonded, saturated with brines that have a depressed freezing point. The soil correction factors may well be different for the two states, and different from that applicable to the basic material forming the permafrost.

[redacted] Underwater cratering from an underwater detonation occurs when the first expanding bubble interacts with the bottom. The presence of an ice cover would affect the early time history of this bubble only if the bubble interacts with the ice layer as well as with the bottom, and then only to the extent that the energy required to vaporize ice differs from that required to vaporize seawater. Depending upon whether the ice is old ice of low salinity, or more recently-formed ice of higher salinity, the latent heat of fusion may vary from less than 40 cal/g to the 80 cal/g of ice of zero salinity at -1°C (Neuman and Pierson, 1966). The energy used to vaporize ice is thus some 6-12% more than would be used to vaporize an equivalent amount of seawater at 0°C.

[redacted] In analogous fashion, for a surface burst or low air burst over water to create an underwater crater, the expanding fireball must vaporize the water layer beneath and interact with the bottom. Again, the presence of ice cover may require 6-12% more energy for vaporization than if no ice were present. Except in extremely shallow water, the volume of ice to be vaporized, even in the case of a relatively thick solid ice pack, would be

[redacted]

[redacted]

[redacted] a small percentage of the water to be vaporized. The decrease in energy available for cratering would therefore be expected to be extremely small in most cases.

[redacted] It is concluded that, except where the bottom is subsea permafrost, the methods of predicting underwater crater dimensions given in Problem 2-36 of DNA EM-1 are valid under Arctic conditions, regardless of the amount of ice present. The uncertainties in crater dimensions given are of the order of plus 150-160% to minus 50-60%. These are large enough to encompass any additional uncertainty due to ice cover. In very shallow water, if the crater lip height were such that it extended above the water or ice (unwashed crater), or to just below the water surface, the scouring action of broken ice caused by its wave-induced motion would be expected to hasten the erosion of the crater lip. If the bottom is composed of subsea permafrost, the proper soil correction factor to use is not currently known.

3.5 [redacted] Conclusions and Recommendations

[redacted] The following conclusions are drawn from the rather scant information applicable to arctic cratering and recommendations of research necessary to reduce the uncertainties are given.

3.5.1 Conclusions

[redacted] Equations for scaling crater dimensions in snow within a range of yields of 0.5 to 5000 lbs TNT show a significant departure from the customary cube-root scaling. For apparent crater radius, the scaling exponent 0.26 is indicated, which is close to fourth-root scaling. The scaling exponent for apparent crater depth is 0.15, which is considerably smaller than that usually applied to craters in soil. A correspondingly low scaling exponent of 0.75 is derived for apparent crater volume.

[redacted] It should be noted that these empirical scaling exponents are based upon a limited amount of data and should be considered as approximations. The use of these exponents to scale up to nuclear explosion craters would be questionable because

[redacted]

[redacted]

[redacted] of the magnitudes of the nuclear burst yields and the profound differences in thermal energy release, which appears to influence crater formation in snow significantly. When comparisons of apparent crater radii for TNT tests in snow are made with craters from TNT tests in clay, sand, basalt, and shale, the comparisons show that craters in snow tend to be larger than craters in other media for the same charge size. This increased size appears to be due to the greater amount of material vaporized and compacted during the explosion and to a scouring action.

[redacted] Although no ejecta measurements were made in the WES tests, examination of the crater lip profiles indicate that the contribution of the ejection mechanism (to volume) in snow craters is correspondingly less than in craters in other media. Craters in snow have a characteristic wide, shallow appearance. The magnitude of the pseudo-elastic rebound in snow is larger directly under the charge than in the snow pushed laterally outward, because of the greater lateral confinement of the snow directly under the charge.

[redacted] Craters in frozen soil or permafrost have similar appearance and dimensions to craters formed in hard rock. It is speculated that the mechanisms for the formation of these craters are similar to those in other soils.

[redacted] Since all of the available cratering data obtained under Arctic environmental conditions have been collected from HE charge tests, the main questions which remain when one uses these data to predict craters from nuclear weapon bursts are:

1. Does the enhanced thermal radiation associated with the nuclear burst have a profound effect on the partition of the total energy going into the snow and/or ice cap?

[redacted]

[redacted]

2. Further, does this enhanced thermal radiation significantly alter the mechanisms of crater formation which are associated with the crater formed in snow by the relatively small HE charges?

[redacted] In areas where subsea permafrost is not present, the methods of EM-1 are adequate for predicting crater dimensions, using the soil factor appropriate to the bottom composition. Other arctic environmental factors are not expected to have a significant effect on underwater cratering.

3.5.2 [redacted] Recommendations

[redacted] To establish whether or not it is valid to scale HE-charge crater data to the nuclear burst cases, computer code calculations should be performed for the different charge output characteristics and sizes. The results of the HE-charge calculations can be checked against test data to verify the accuracy of the code(s).

[redacted] Should a large-charge HE test (100-ton TNT or more) be implemented in the Arctic, the crater and ejecta measurements should be obtained. Early-time photography of the crater formation should be obtained also. Additional crater dimension data from small-charge HE explosions should be collected on a "test of opportunity" basis, but a test series performed specifically to obtain crater data is not recommended.

[redacted] The recommended series of calculations, experiments and field tests described in Section 2.7.2 should be planned such that the above questions will be answered.

[redacted] A research program to narrow the uncertainties in underwater cratering should take a dual approach - to support the collection of data to delineate the areas of bonded and unbonded permafrost, and to determine the appropriate soil

[redacted]

correction factor to use for each type. Whether seismic methods can be used to delineate the two types of permafrost areas or whether a program of subsea coring is required should be investigated by experts in the field. The determination of soil correction factor should be accomplished by analytic means if possible, but laboratory or field testing might be required. This question should be studied by experts in the area before embarking on a program of field testing.

3.6 Bibliography

Bauer, A., Calder, P. N., MacLachlan, R. R., and Halupka, M., Cratering and Ditching with Explosives in Frozen Soils, DREV R-699-73, Queens University, Kingston, Ontario, for Defense Research Establishment, Valcartier, Quebec, July 1973, UNCLASSIFIED, AD-913283.

Conway, J. A. and Myer, J. W., Cratering in Greenland Icecap Snow, WES MP N-70-6, U. S. Army Engineer Waterways Experiment Station, Vicksburg, MS, July 1970, UNCLASSIFIED, AD-711861.

Chamberlain, Edwin J., Sellmann, P. V., Blouin, S. E., Hopkins, D. M., and Lewellen, R. I., Engineering Properties of Subsea Permafrost in the Prudhoe Bay Region of the Beaufort Sea, Report of the Third International Conference on Permafrost, pp. 629-635, National Research Council of Canada, 1978.

Defense Nuclear Agency, Capabilities of Nuclear Weapons (U), DNA EM-1, Defense Nuclear Agency Effects Manual Number 1, Headquarters, Defense Nuclear Agency, Washington, D. C., 1 July 1972 (Change 1, 1 July 1978), SECRET RESTRICTED DATA.

Defense Nuclear Agency Handbook of Underwater Nuclear Explosions (U), DNA 1240 H, Defense Nuclear Agency, Washington, D. C., November 1971, SECRET RESTRICTED DATA.

Lewellen, Robert I., The Occurrence and Characteristics of Nearshore Permafrost, Northern Alaska, in Permafrost: The North American Contribution to the Second International Conference, pp. 131-136, National Academy of Sciences, Washington, D. C., 1973.

Lewellen, Robert I. Offshore Permafrost of Beaufort Sea, Alaska, in The Coast and Shelf of the Beaufort Sea, J. C. Reed and J. E. Sater (ed.), pp. 417-426, The Arctic Institute of North America, 3426 N. Washington Blvd., Arlington, VA 22201, 1974.

Lewellen, Robert I., Subsea Permafrost Research Techniques, Geoscience and Man, Vol. XVIII, pp. 29-34, December 30, 1977.

Livingston, C. W., Explosions in Ice, Technical Report 75, USA SIPRE, now Cold Regions Research and Engineering Laboratory, Hanover, NH, December 1960, UNCLASSIFIED.

Livingston, C. W., Explosions in Snow, Technical Report No. 86, Cold Regions Research and Engineering Laboratory, Hanover, NH, 1968, UNCLASSIFIED.

Neuman, Gerhard and Pierson, Willard J. Jr., Principles of Physical Oceanography, Prentice-Hall, Inc., Englewood Cliffs, NJ, 1966.

Sager, R. A. et al, Cratering from HE Charges: Compendium of Crater Data, Tech. Report No. 2-547, May 1960, U. S. Army Engineer Waterways Experiment Station, CE, Vicksburg, Miss.

Sager, R. A., Cratering Data from 1960 Greenland Test Series of HE Charges in Snow, Feb. 1961 (unpublished), U. S. Army Engineer Waterways Experiment Station, CE, Vicksburg, Miss.

THIS PAGE IS INTENTIONALLY LEFT BLANK

SECTION 4
THERMAL RADIATION

About a third of the yield of a nuclear weapon detonated at low altitudes in the atmosphere is emitted as infrared, visible and ultraviolet radiation with a pulse width depending on the yield and altitude typically lasting for a few seconds for a megaton weapon. This thermal energy can be transmitted to large ranges in the atmosphere and is usually readily absorbed in a thin surface layer on most target material causing large surface temperature increases which can cause damage to the targets. The types of damage usually of concern result from fires that start due to ignition of combustible materials and from burns to personnel but also can involve thermo-mechanical loading due to very large fluences incident on hardened facilities such as radars.

4.1 Arctic Environmental Differences

A large variability is expected in the effects of thermal radiation in an arctic environment because extreme variations in clouds, atmospheric moisture, visibility, precipitation, and the earth's surface occur more commonly in the arctic region than elsewhere in the world. These variations create conditions that can as much as double significant thermal effects or reduce them by even larger factors. The following briefly described effects will be discussed further in subsequent sections of the handbook.

4.1.1 Visibility

Surface visibility in arctic and subarctic climates during clear seasons is often exceptionally good because of the low humidity coincident with cold temperatures and the absence of dust in the air. The northern and coastal regions during the warmer months are subjected to extensive sea fog and low cloud-

[redacted]

[redacted]

iness. Falling or blowing snow can reduce the visible range to less than a mile during stormy periods. These extremes of atmospheric conditions require examination of their effects on transmission of thermal energy.

4.1.2 [redacted] Fog

[redacted] Arctic fog and precipitation generally reduce the range of thermal phenomena. At the very low temperatures of the arctic winter the atmosphere is capable of holding very little mosture. Such low temperatures as a rule are accompanied by minimal surface wind, and these conditions together are favorable to the formation of fog. Ice-fog crystals consist of many spherical particles and some hexagonal plates and columns of 2μ to 30μ diameter formed at about -40°C in high concentration that reduces visibility significantly. In addition ice fog can cause extinction of the infrared beam of an infrared guidance system.

4.1.3 [redacted] Albedo Surfaces

[redacted] Ground surfaces covered by snow and ice have a much higher albedo than bare ground in temperate climates. The transmission of thermal radiation is considerably enhanced by the presence of these high albedo surfaces. Layers of cloud, smoke, or haze are other common albedo surfaces.

4.1.4 [redacted] Cloud Cover

[redacted] The low dense cloud cover characteristic of arctic areas can result in significant enhancement of thermal environment for targets at low altitudes from a low altitude burst. A high albedo ground surface is very likely in the arctic. The combination of a high albedo ground surface and a low cloud cover results in a definite channeling of thermal energy and a marked increase in thermal fluences.

[redacted]

[redacted]

4.1.5 [redacted] Humidity

[redacted] Even though t' e relative humidity is generally high in the arctic especially over the ocean areas because of the low temperatures, the absolute conce ration of water vapor is much lower than in temperate areas. This results in less absorption of thermal radiation in the important infrared water vapor absorption bands and tends to increase the thermal transmission.

4.1.6 [redacted] Low Temperatures

[redacted] The low temperatures in themselves do not result in changes in the thermal transmission except for their influence in producing ice fogs, ice/snow surfaces, etc.

[redacted] Materials used for clothing and supplies in arctic climates do not possess the same vulnerability to thermal effects as materials used in less severe temperatures. Furthermore, cold temperatures reduce somewhat the vulnerability of most materials to thermal effects.

[redacted] Besides a reduction in flammability with reduction in temperature, combustible material is less susceptible to thermal damage when protected by snow and frost covering. Characteristic low humidity of the arctic air will somewhat mitigate the reduction of combustibility. In some of the tundra, expanses of coarse vegetation growing on a thick peaty layer might be subject to surface fires started by nuclear detonations.

4.2 [redacted] Transmission Effects

[redacted] The quantity and effectiveness of thermal radiation that reaches a target is dependent on a large number of parameters whose variability in an arctic environment is sufficiently great to produce a significant change in thermal radiation transmission. The parameters to be considered here may be grouped

[redacted]

into two general categories; first, those parameters which determine the manner in which thermal radiation is scattered and absorbed and in the atmosphere are discussed here, and secondly, those that determine the manner and extent of its reflection will be considered in Section 4.3.

The thermal irradiance, H, received at a distance R from a nuclear burst is given by the expression

$$H = \frac{PT}{4\pi R^2} \cos \lambda, \tag{4.1}$$

where P is the total power radiated by the burst as a function of time, cos $\lambda = 1$ if the receiver area is normal to the burst, and T is the transmission factor. T is used here in a very general sense and includes such effects as atmospheric attenuation, surface albedo effects (ground, water, or clouds), and source asymmetries.

The radiant exposure, Q, during time from zero to t is then defined to be

$$Q_t = \int_0^t H \, dt, \tag{4.2}$$

where in general P, T and R may depend upon time. If we assume that the transmission T and the radius R to a unit area facing the burst are constant, then

$$Q = \frac{fWT}{4 R^2} \tag{4.3}$$

where W is the yield of the weapon in calories and f is the thermal partition or efficiency, and fW = E is the thermal

[redacted]

[redacted]

yield. Even though both T and R are seldom truly independent of time, sufficient accuracy may often be obtained by using the values corresponding to the time of peak radiated power. Often it is assumed that defining T = 1 will give the worst case environment. This assumption is usually good unless the conditions include source asymmetries and albedo from clouds and ground surfaces.

[redacted] In order to determine the amount of thermal energy actually transmitted to the receiver, allowance must be made for the attenuation of the radiation by the atmosphere. This attenuation is mainly of two forms - absorption and scattering. There are no strong absorption processes for the visible wavelengths but strong absorption bands exist in the ultraviolet and infrared. Scattering occurs with radiations of all wavelengths. The state of the atmosphere in the visible region can be represented by what is known as daylight visibility.

4.2.1 [redacted] Arctic Visibility

[redacted] There are several highly variable climatological characteristics that could significantly change the absorption and scattering of thermal radiation in the arctic and subartic atmosphere. As indicated although the arctic and subarctic regions are generally areas of comparatively low absolute humidity and little industrial dust, characterized by good visibility; the northern and coastal regions are seasonally subjected to extensive sea fog and low clouds, and falling or blowing snow can reduce visibility to less than one mile for extended periods in some areas.

[redacted] There is no single correct value of the attenuation coefficient μ for any given set of atmospheric conditions. The value of μ is a function of both the nature and distribution of the scattering and absorbing particles, and also of the wave

[redacted]

[redacted]

[redacted]

length of the radiation involved. There is no simple average value of μ because the spectral distribution of the radiation will change with the distance "R" involved. In spite of the variable nature of μ, an assumption is often made that reasonable average values of μ can be determined in terms of visibility. This is not too unreasonable an assumption since that portion of the spectral distribution of radiated energy which penetrates any considerable distance in the atmosphere is concentrated mostly in the visible and near visible wave lengths. The conventional visibility as given in weather forecasts is generally the distance at which the transmission is reduced to 5.5%, i.e., $T = e^{-V\mu} = .055$.

[redacted] It is convenient to calculate the visibility on the basis of the above approximation to illustrate the dependence of atmospheric transmission and attenuation on visual properties of the atmosphere. There is wide discrepancy among values assumed for the distance called visibility and in relating that parameter to the optical properties of the atmosphere one should be aware of its very approximate and necessarily subjective nature. In most technical literature on atmospheric transmission the term meteorological range is defined as that distance where the transmission is 2%, i.e., $T = e^{-m\mu} = .02$. Unfortunately some authors use the terms visibility and meteorological range interchangeably.

[redacted] The international code for correlating the condition of the atmosphere with visibility is given in Table 4-1. In temperate climates one may see variations in the visibility from the highest to lowest visibilities depending upon the concentration of aerosol particles from pollution sources. In most areas of the arctic the background level of pollutants at the surface is low leading to very high visibilities. However, the occurrence of certain weather conditions such as blowing snow, ice fog, etc. result in very low visibilities of one mile or less.

[redacted]

[redacted]

[redacted]

[redacted]TABLE 4-1 INTERNATIONAL VISIBILITY CODE

Code Number	Description	Visibility From	Visibility To
0	Dense Fog	----	50 m (55 yds)
1	Thick Fog	50 m	200 m (220 yds)
2	Moderate Fog	200 m	500 m (550 yds)
3	Light Fog	500 m	1 km (0.6 mi)
4	Thin Fog	1 km	2 km (1.2 mi)
5	Haze	2 km	4 km (2.5 mi)
6	Light Haze	4 km	10 km (6 mi)
7	Clear	10 km	20 km (12 mi)
8	Very Clear	20 km	50 km (30 mi)
9	Exceptionally Clear	50 km	280 km (170 mi) (Glasstone, 1977)

[redacted] When one is considering the transmission for a broad spectrum as results from a nuclear weapon, the relation between the visibility and transmission is not as straightforward as indicated above. Scattering and buildup effects occur which result in a non-exponential falloff of the transmission. The various interaction cross sections vary as a function of wavelength so that integration of results across the broad wavelength must be considered. Extensive discussion of all aspects of this problem are presented in the DNA Thermal Sourcebook (Keith, 1973) and EM-1 (DNA, 1978) which is currently under revision.

[redacted] Figure 4-1 (Keith and Sachs 1977) shows predicted transmission as it varies with visibility of one to 30 miles. In the figure the variation of transmission with the ground level visibility is noted as a function of ground range for a large yield weapon

[redacted]

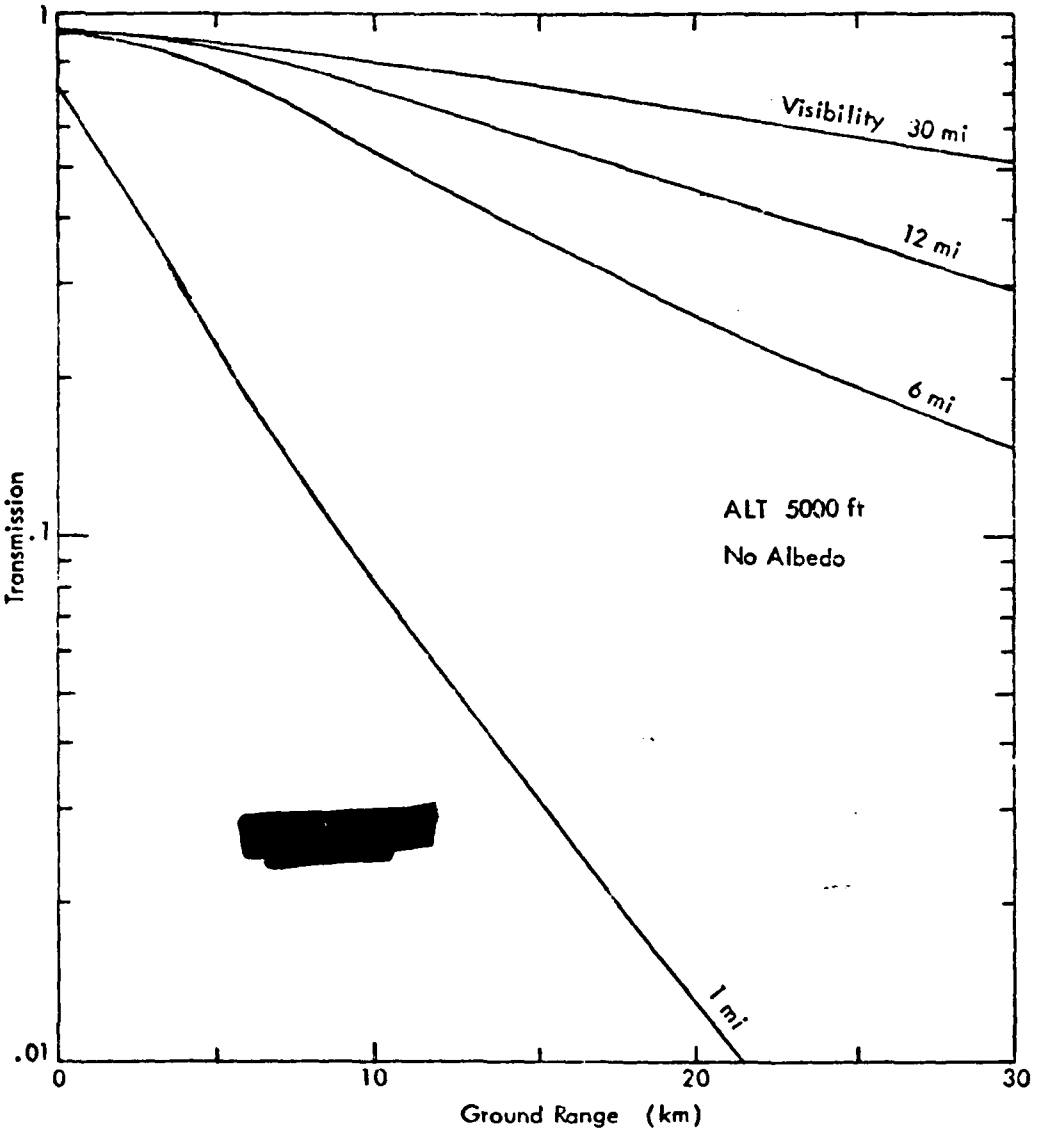

FIGURE 4-1 VARIATION OF TRANSMISSION WITH VISIBILITY

[redacted]

[redacted]

detonated at 5000 ft above the ground. The atmospheric profiles for every quantity except the aerosol concentration are unchanged for the various calculations. The aerosol concentration at ground level is adjusted to give the desired visibility; then a constant exponential lapse rate is defined between ground level and 5 km. The aerosol concentration profile, as in most atmospheric models, is assumed to be unchanged above 5 km altitude regardless of the visibility at the surface. This implies that essentially none of the particulate contaminants are carried above 5 km altitude.

[redacted] The calculated transmission increases as expected with increasing visibility. These curves represent a burst at 5000 ft with no albedo surfaces present. The representative arctic humidity is 1 g/m^3, and the spectrum corresponds to a high-yield burst. At a range of 10 km the transmission for 30-mile visibility is about 50% higher than that for 6 miles and 10 times that for visibility of 1 mile. At a range of 30 km the transmission for 30-mile visibility is about 3.5 times that for 6-mile visibility, and transmission for 1-mile visibility is practically negligible.

[redacted] The transmission curves given above refer to a ground level absolute humidity of 1 g/m^3. As shown in Table 1-5 the absolute humidities of the standard atmospheres are .46 in January and 5.6 in July. The effect of the humidity for a particular visibility is very small in the visible region of the spectrum but can strongly affect the portion of the weapon energy emitted in the infrared. The clear visibility curves from reported results correspond to a water vapor concentration that is considerably in excess of that normal for an arctic winter.

[redacted]

[redacted]

[redacted] In Figure 4-2 the effect of changing the absolute humidity at ground level is shown. All quantities except the water vapor concentration are held constant. The ground level concentration is set equal to the desired value and an exponential lapse rate is defined between ground level and 5 km. The profile above 5 km is assumed to remain the same for the various humidities. As expected the effect is not as large as noted with changing the visibility. A surface burst where the entire path is along the ground should show the maximum effect. The overall slope of these curves is determined by the visibility, which here is 30 miles, and the relative placement shows the effect of the water vapor. For the higher concentrations the water vapor absorbs strongly within the first km of the path until the infrared energy is depleted; then the transmission versus range is determined by the visibility. Note that increasing the concentration beyond 5 g/m^3 has a relatively small effect.

[redacted] The large yield bursts have a relatively larger fraction of the yield in the infrared region where humidity effects are important, therefore, these results represent a reasonable upper limit to the effect of humidity on the transmission. The differences shown are not of importance considering the uncertainties in the other meteorological parameters.

4.2.2 [redacted] Ice Fog

[redacted] Some of the effects of ice fog on infrared transmission in Alaska have been reported (Kumai and Russel, 1969). Besides reducing visibility significantly, ice fog can cause attenuation of the infrared beam in an infrared guidance system. The optical properties of fog depend on the number concentration and size distribution of the particles, which can vary significantly during different meteorological conditions. Ice-fog crystals appear as initial stages in the formation of snow crystals at about -40°F. At the very low temperatures often occurring during

[redacted]

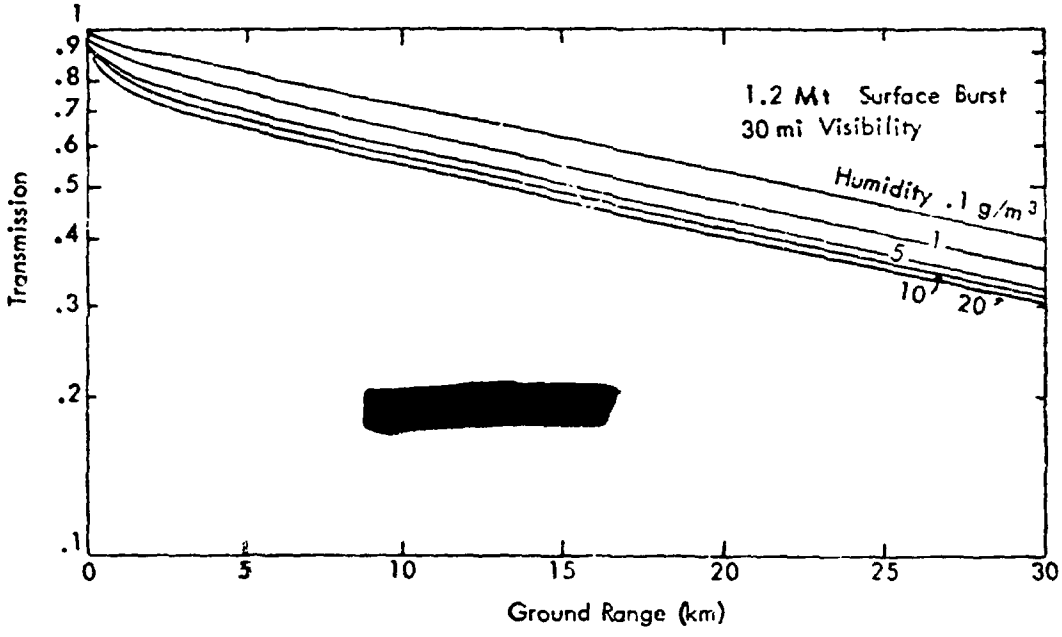

FIGURE 4-2 VARIATION OF TRANSMISSION WITH HUMIDITY FOR A SURFACE BURST.

[redacted]

[redacted]

the polar winter, the atmosphere can hold very little moisture and surface wind is almost invariably calm. Since conditions are frequently conducive to formation of ice fog from any source of water vapor, the frequency of ice fog has increased with human activity in the arctic.

[redacted] Table 4-2 from the report summarizes the important physical properties of the ice fog at -39°C and -41°C. The ice-fog distribution at -39°C is shown in Figure 4-3. The number of particles and the mass of fog per unit volume are shown as a function of particle diameter.

[redacted] TABLE 4-2

PHYSICAL PROPERTIES OF ICE FOG AT FAIRBANKS, ALASKA

Observations	N (no./cm^3)	r_{mode} (μ)	r_{min} (μ)	r_{max} (μ)	Δr (μ)	Air temp (°C)	L.W.C. (g/m^3)
No. 1(Fig 4-3)	140	3.0	1.5	12.0	0.5	-39	0.08
No. 2	90	1.5	1.5	12.0	0.5	-41	0.02

UNCLASSIFIED

N = total concentration

r_{mode} = mode radius = radius corresponding to the maximum number of ice-fog crystals

r_{min} = minimum radius

r_{max} = maximum radius

Δr = radius interval containing n(r) crystals, where $N = \sum_r n(r)$

L.W.C. = liquid water content

[redacted]

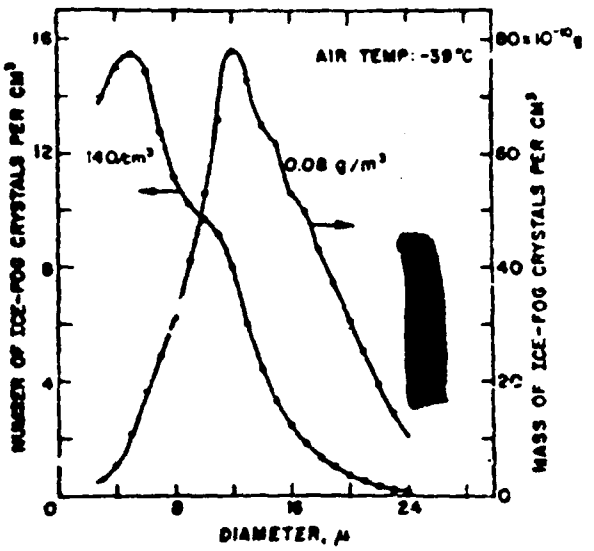

Figure 4-3. Size and mass distribution of ice-fog crystals formed at -39°C ambient temperature.

Computer calculations of the attenuation and back-scattering of radiation by ice fog alone showed them to be within the same order of magnitude as those for water fog of equivalent fog concentrations and observed wavelengths. The optical constants used in the calculations were considered to be known much less exactly for ice than for water. Calculations made for the distribution in Figure 4-3 were presented and are reproduced as Table 4-3 (Kumai and Russell, 1969).

These calculations were done for narrow wavelength intervals in the infrared and do show detailed differences at specific wavelengths due to the different scattering characteristics of the ice crystals and water droplets with equivalent amounts of water involved. The same size distributions were assumed for these calculations which may not be a realistic assumption since the size distribution of the ice fog is considerably different from other types of fog.

[redacted]

TABLE 4-3

INFRARED ATTENUATION COEFFICIENTS (m^{-1})

Concentration no./cm^3	Water Content g/m^3	Wavelength, Microns 2.2	2.7	4.5	5.75	9.7	10.9
			Ice-Fog				
70	.039	.01153	.01212	.01321	.01304	.00513	.00679
140	.077	.02306	.02424	.02642	.02608	.01026	.01359
280	.15	.04611	.04848	.05283	.05216	.02052	.02717
420	.23	.06917	.07272	.07925	.07824	.03078	.04076
			Water-Fog				
70	.039	.01153	.01217	.01314	.01282	.00784	.00546
140	.077	.02305	.02434	.02628	.02564	.01568	.01091
280	.15	.04611	.04868	.05256	.05127	.03137	.02182
420	.23	.06916	.07303	.07885	.07691	.04705	.03273

[redacted]

[redacted] Another paper on visual range in polar regions (Mitchell, 1958) also states that the visual range in ice fog is characteristically very low, frequently less than a quarter of a mile. The total particulate water content of ice fog is comparable to that of other fogs, as shown in Figure 4-4, but the average ice-fog particle is smaller. Thus the ice-fog contains more particles and favors greater optical scattering. Because ice fog is often a man-made phenomenon, it is a particular problem at arctic military installations.

[redacted] The details of the transmission of thermal energy in the atmosphere depend upon the aerosol particle distribution as well as the concentrations. The scattering phase functions determine the details of the thermal transport including the angular distributions and transmission factors. The

[redacted]

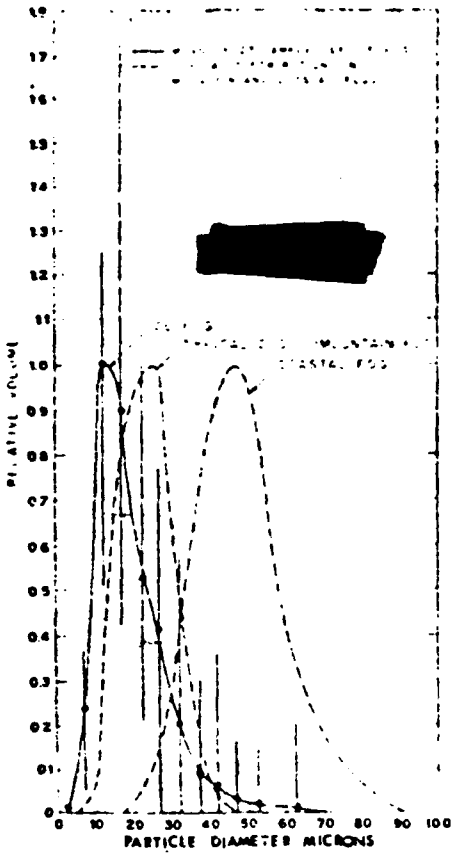

Figure 4-4. Comparison of typical particle volume distributions for ice fogs and water fogs (Mitchell, 1956).

phase functions depend upon the particle properties and size distribution. No calculations of the Mie scattering functions have been made for distributions peculiar to the arctic region. All transmission curves in this section were prepared by using available phase functions derived to represent the aerosol distributions found in temperate polluted areas.

4.3 Albedo Surface Effects

The nature of the clouds and the condition of the surface in the vicinity of a nuclear detonation can considerably alter the amount and direction of thermal radiation reaching a target. Although there is great geographical and seasonal variability throughout the world in these parameters, more extreme variations occur in arctic and subarctic areas. The number of variables involved and the range of possible variations in these parameters make a comprehensive consideration of the reflection or albedo problems very complex.

In terms of thermal radiation, surfaces or atmospheric anomalies which reflect radiation are known as albedo surfaces. Surface albedos range from 0 to 1, where the value 1 indicates a perfect reflector. Typical albedo surfaces are the ground plane, especially when covered by snow, ice or water, a cloud layer, and a smoke or haze layer. Dense clouds may have albedos as high as 0.9.

Even if albedo surfaces are not present, all sides of an object will receive radiation even though the side facing the fireball will usually receive the dominant exposure. A portion of the radiation traveling upward is lost to space with relatively little being scattered downward unless clouds are present above a burst. If a cloud layer is present a large portion of the incident radiation will be diffusely reflected from the surface with a small fraction being diffusely transmitted. A typical ground surface also reflects the radiation diffusely with the albedo varying from near zero to near unity for snow or ice surfaces. Some materials such as water or ice may also have a fairly large specular reflection. The thermal exposure for targets bounded by clouds and a high albedo ground surface can be several times the vacuum exposure value.

[redacted]

[redacted] Seasonal aspects of the albedo of arctic surfaces north of 65° N latitude have been examined (Larsson and Orvig, 1962) from data in the literature. At high latitudes seasonal variations in albedo are largely determined by the presence or absence of snow cover. In the tundra zone the contrast is greatest. In forested tundra albedo from snow cover beneath the trees is approximately twice as great as from the ground vegetation except in a close-crown forest where snow is caught on the surface for a relatively short time. Different types of ice reflect differently, and although open water and low cloud cover usually are found coincidentally, little information is available on the albedo of open water containing ice. Albedo stereograms in Figure 1-16 represent the seasonal and latitudinal changes in arctic surface albedo.

4.3.1 [redacted] Experimental Results

[redacted] A series of arctic transmission measurements were made by the United States Army Electronics Command, Fort Monmouth, New Jersey (Cantor and Petriw, 1964) in Greenland under various weather conditions with particular emphasis given to the albedo effects of the ground surface and cloud layers.

[redacted] Under many atmospheric and surface conditions, the indirect radiation effects can equal or exceed the direct radiation. A 2π detector is used to simulate a flat plate receiver so that the full indirect as well as the direct transmission can be measured.

[redacted] Such a receiver, near ground level, was employed with a 6500°K point light source about 400 feet above the surface, under generally hazy atmospheres on the New Jersey shore from October 1960 to February 1961. These tests indicated sharp increases of radiation under relatively high surface albedos. The maximum surface albedos, however, are readily obtainable in the arctic or antarctic regions. This led to studying trans-

[redacted]

[redacted]

[redacted] mission effects of an energy source located between two high albedo surfaces, a snow-covered surface and an extensive cloud cover at Camp Century, Greenland.

[redacted] Cantor and Petriw give a very complete description of the experiments of thermal transmission made at Camp Century, Greenland in March, October, and November 1962, where measurements were made on the Greenland icecap to try to maximize the effect of albedo. The terrain was essentially flat and had an albedo of almost unity extending for about 100 miles in all directions.

[redacted] The light source was a xenon flash tube surrounded by a 10"-diameter opal-covered sphere about 100 feet above the surface. The blackbody temperature of the source was about 6500°K. Photomultiplier tubes were used as 2π detectors with no variation in the field of view possible. Occulters were used to block the direct irradiance. Measurements were made at ranges of 0.13, 0.5, 1., 4.5, 7.6, and 10.3 miles whenever conditions permitted.

[redacted] Their report gives a detailed explanation of the weather conditions, experimental configuration, and data obtained each night measurements were made. Plots of the total and scattered transmittance for each night and many of the signal variations as a function of time are also given. Very large, short-term variations of up to 160% were noted in the intensity in time intervals of less than 30 seconds. These largest variations occurred in periods of high visibility and steep temperature inversions with smaller variations occurring for smaller temperature inversions.

[redacted] Figure 4-5 is derived from the summary graph from the report and gives the transmission as a function of range. The labels refer to the visibility in miles followed by the altitude of the cloud layer in feet. Several interesting effects can be

[redacted]

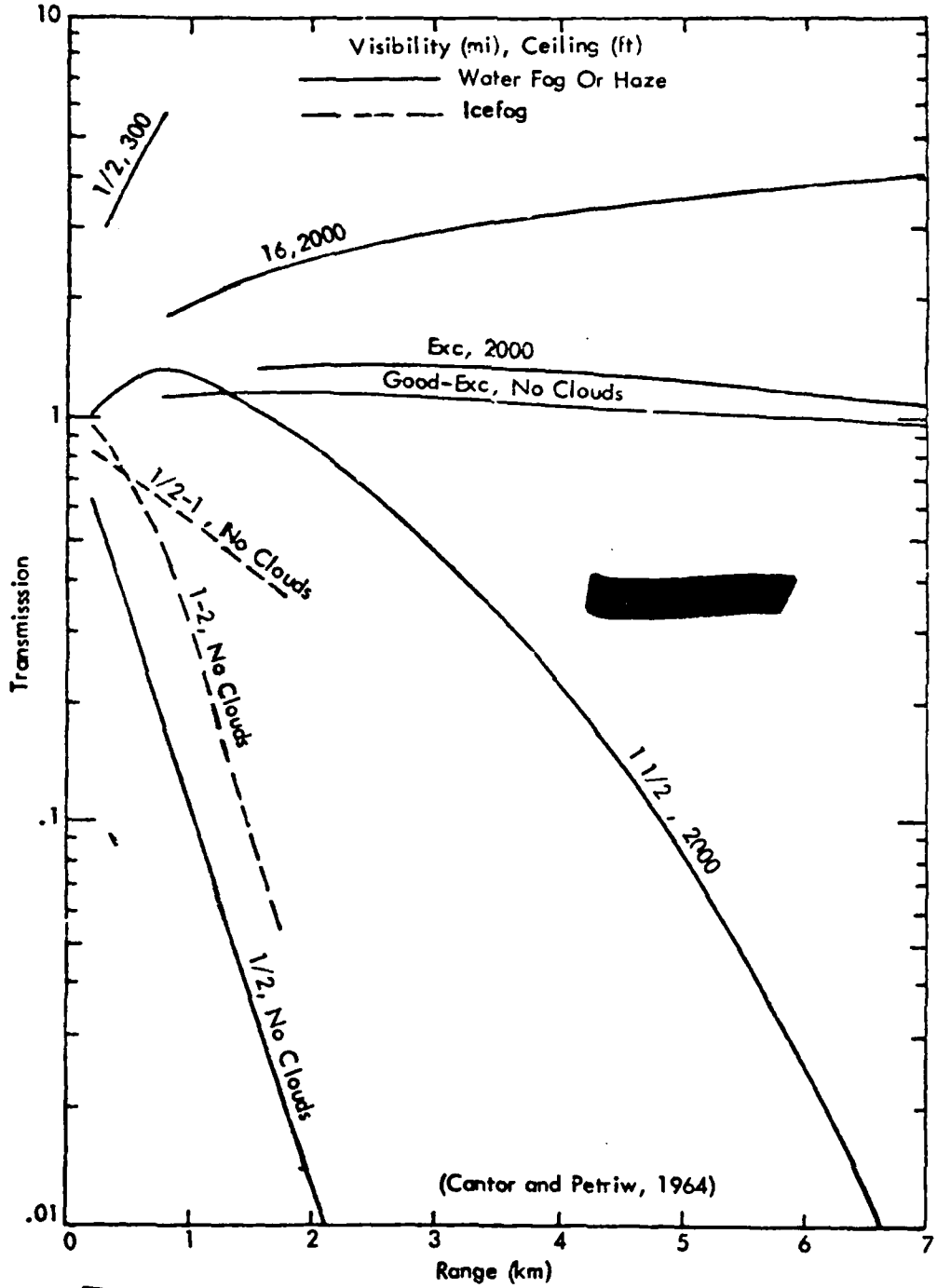

FIGURE 4-5 EXPERIMENTAL TRANSMISSIONS IN GREENLAND

[redacted]

[redacted] seen by comparing the transmissions for the different atmospheric conditions. First note that the case referred to as good to excellent visibility with no clouds shows essentially no transmission variation with range over the fairly short range of the experiment. The addition of a cloud layer at 2000 feet did introduce an increase due to the ducting effect but the change is of the order of only 25%. A much larger increase is noted for the case with 2000 ft cloud layers and a lesser visibility of 16 miles. This general type of behavior is noted in Monte Carlo calculations of this effect as will be discussed in the next subsection, but the calculated effects are much less extreme. Note that for a visibility of 1 1/2 miles and clouds at 2000 ft there is an initial increase in the transmission above unity followed by a decrease in the transmission.

[redacted] For the 1/2 mile visibility case with no clouds a rapidly decreasing transmission is shown. For a cloud layer at 300 feet and 1/2 mile visibility the transmission increases to over 5 at a range of about 1 km beyond which no measurements were made. One would then expect a precipitious drop with increasing range.

[redacted] The dashed curves refer to cases in which the visibility reduction was due to ice fog rather than water fog. There is an indication that for the same visibility the transmission may be higher for ice fog indicating larger scattering contributions and differences in the scattering phase functions.

[redacted] The experimental uncertainty is fairly large; so quantitative measures of the effects should not be derived from these experiments. The measurements do not extend to long ranges as are necessary for nuclear weapon thermal prediction methods. The general trend of the results does agree with results of Monte Carlo calculations of thermal transmission including the effects of albedo surfaces.

[redacted]

[redacted]

4.3.2 [redacted] Monte Carlo Calculations

[redacted] This section will summarize work at RRA (Wells, Collins, Marshall, 1969; Wells, Collins, Cunningham, 1966) begun in the mid 1960's and the further work at KSC (Keith, 1973) in developing Monte Carlo codes describing the thermal radiation transport model atmospheres. Given a complete specification of the atmospheric parameters a calculation of the transmission with these codes will probably be the most accurate that can be obtained theoretically.

[redacted] Monte Carlo calculations (Wells, Collins, Marshall, 1969) have been made of the transmission for a 6000°K blackbody source at 1 km altitude for the model atmospheres representing meteorological conditions for an arctic case and three mid-latitude cases - summer, winter, and a winter inversion. Calculations were run with and without a ground albedo factor. Table 4-4 lists some parameters used in the four atmospheres compared on the graph. The only difference in the summer and winter midlatitude case is in the absolute humidity. The winter case with the inversion added the very low visibility region of aerosols below 2 km. The arctic case was chosen to provide exceptionally high visibility and zero humidity, which as noted previously will increase the transmission by a relatively small factor. A snow-covered surface with cloud distribution was also assumed.

[redacted] In Figure 4-6 the results of their calculations for a target on the ground surface are summarized and replotted. The differences between the summer and winter midlatitude clear visibility cases are relatively small as expected. The exceptionally clear visibility assumed for the arctic case gives a much larger transmission factor. The winter inversion case for a haze visibility of 2.2 km or 1.4 miles results in significant attenuation even at fairly small ranges. The effect of changing the ground albedo from 0 to .9 is seen to result in a significant

[redacted]

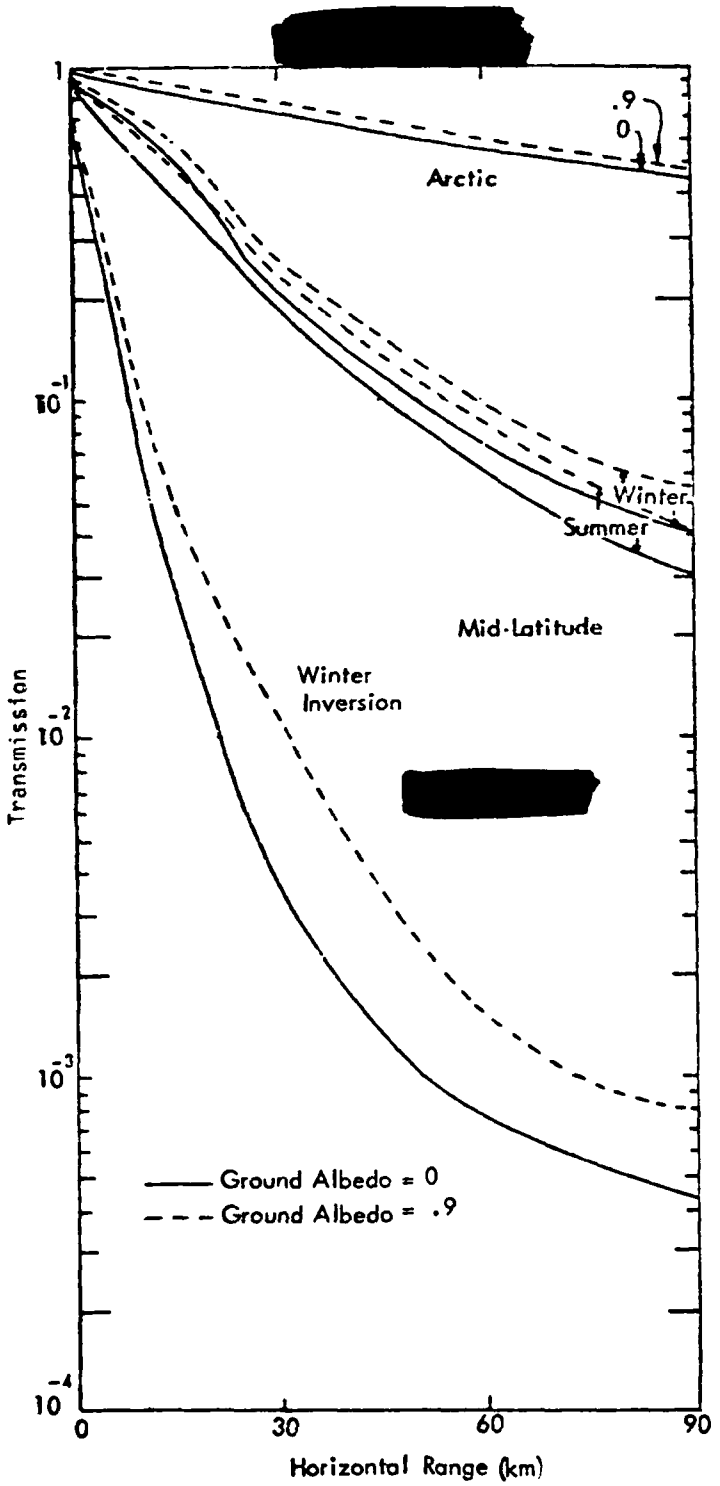

FIGURE 4-6. TRANSMISSION IN MODEL ATMOSPHERES (from Wells, 1969)

[redacted]

TABLE 4-4
METEOROLOGICAL CONDITIONS
USED FOR MODEL ATMOSPHERES

[redacted]

Atmospheric Model	Ground Level Absolute Humidity (g/m^3)	Ground Level Visibility (km)	Aerosol Size Distribution
Summer Midlatitude	12	18	$N(r) \propto r^{-4}$
Winter Midlatitude	3	18	$N(r) \propto r^{-4}$
Winter Midlatitude (Inversion Profile to 2 km altitude)	3	2.2	$N(r) \propto r^{-3}$ to 2 km altitude $N(r) \propto r^{-4}$ above 2 km altitude
Arctic	0	148 (Exceptionally clear)	$N(r) \propto r^{-4}$

* r - radius of aerosol particles

N(r) = aerosol concentration as a function of r

[redacted] buildup of the transmission for the midlatitude cases considered. The effect is only about 5% for the arctic case so that the effect of one high albedo surface for exceptionally high visibilities is not large. For targets above the surface a larger effect is noted.

[redacted] In a recent study (Kaman Sciences, 1978) calculations with Monte Carlo computer codes were done including the effect of introducing albedo surfaces. In Figure 4-7 the effects of various combinations of albedo surfaces are compared. The burst conditions

[redacted]

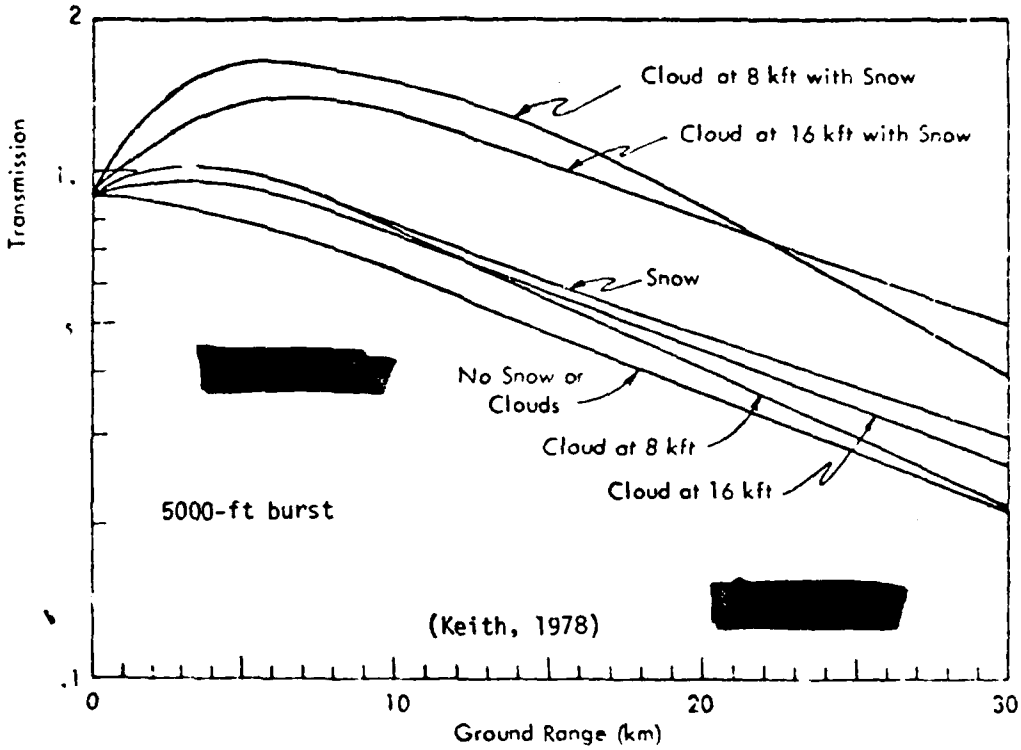

Figure 4-7. VARIATION OF TRANSMISSION WITH ALBEDO SURFACES AT 12-MILE VISIBILITY.

[redacted]

[redacted] are the same as in the transmission figures in Section 4.2 for varying visibilities and humidities. The ground level visibility is 12 miles and the absolute humidity is 10 g/m^3. The addition of a single albedo surface, either snow covered ground or a cloud layer, causes a modest increase in the transmission of about 20% to 30%. The transmission with only snow cover is seen to be somewhat higher than with only cloud cover. The effect of a cloud layer at 8 kft becomes less with increasing range, and for ranges greater than 30 km a reduction in transmission will occur. The effect of a 16 kft cloud layer is similar except the increase and decrease occur over a longer range. The combined effect of snow cover and a cloud layer can be quite large as noted by the two upper curves on the figure. An increase of up to a factor of about 2.5 is possible. The effect is larger at the small ranges for the lower cloud layer. At much larger ranges than shown on the figure a reduction in transmission will result. In Figure 4-8 similar curves are given for a visibility of 30 miles. The same general trends relative to the curve with no albedo surfaces are obtained with the albedo effect being somewhat larger with the higher visibility. The presence of the albedo surfaces causes a large effect in the transmission factors but since the effect depends upon the cloud height, it must be quantified for specific cases of interest.

[redacted] The effect of two albedo surfaces on the transmission is seen to be very large. The calculations of RRA were done with too large a visibility to represent realistic Arctic conditions and the KSC calculations were done with a visibility lower than can be expected in the Arctic. Neither set of calculations was done with aerosol scattering functions representing aerosol concentrations appropriate for arctic conditions.

[redacted]

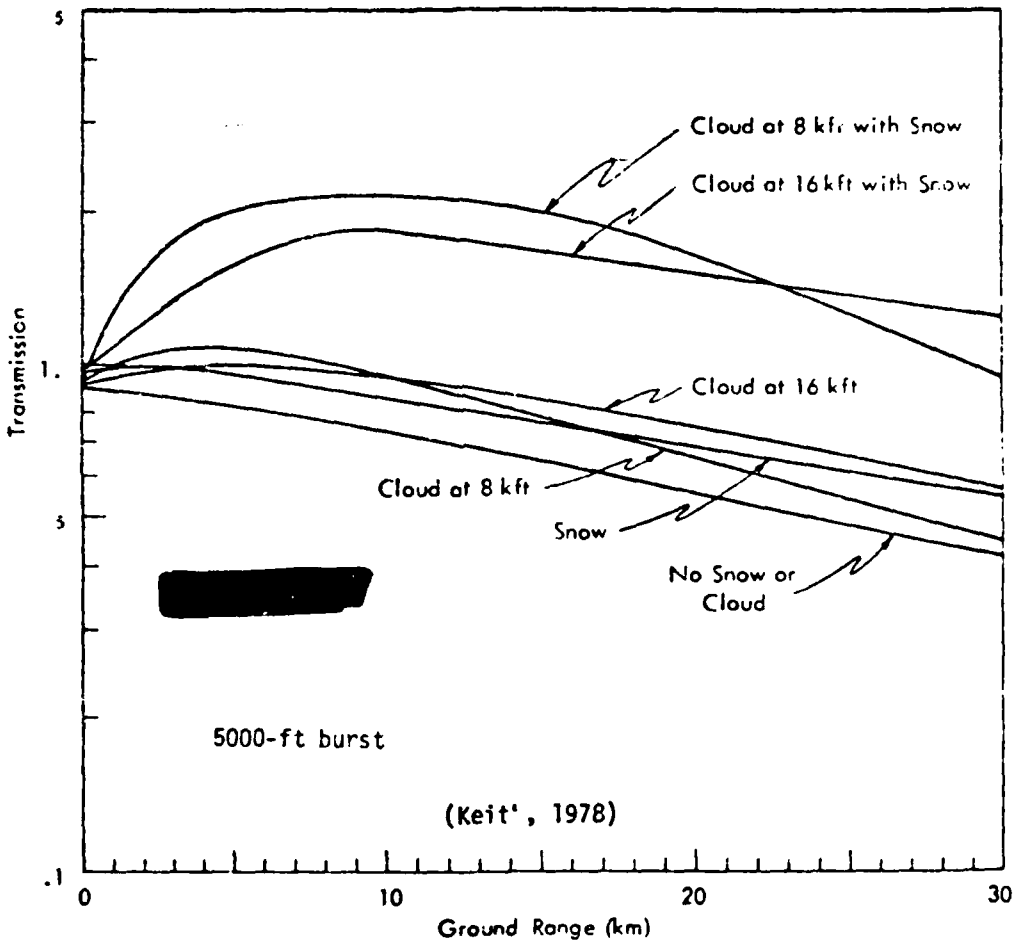

FIGURE 4-8. VARIATION OF TRANSMISSION WITH ALBEDO SURFACES AT 30-MILE VISIBILITY

[redacted]

4.4 [redacted] Example Thermal Exposures

[redacted] Figure 4-9 gives curves of radiant exposure from 1 to 1000 cal/cm^2 versus ground range from the point beneath a high-yield burst at 5000 feet altitude. For a very clear atmosphere (30 mi visibility) the exposure is 10 calories per square centimeter at a range of about 15 miles. This same damaging exposure is seen to occur approximately half as far from the burst in a thin fog with visibility of a mile. The upper curve shows the exposure for a visibility of 30 miles with snow cover and a cloud layer bottom at 8 kft altitude. The 10 cal/cm^2 exposure occurs at a ground range of about 22 km which is about 50% larger than for the 30 mile visibility case with no albedo surfaces and a factor of three larger than for the 1 mile visibility case.

[redacted] A recent study (Keith, 1979) considered the thermal environment for a selection of Soviet cities considering the wide variation of meteorological conditions that may result in this area. Representative and extreme days were defined which happen to be of some interest for considering the thermal environment in the arctic. The results are shown in Figure 4-10. The extreme low day refers to a .3 mile visibility with no cloud cover and medium ground albedo which corresponds roughly to a heavy ice fog with no cloud. The extreme high day refers to a 50 mile visibility with a 16 kft complete cloud cover and a medium ground albedo which corresponds roughly to a clear winter arctic day with no fog or haze. For these extreme cases the range corresponding to 10 cal/cm^2 varies from about 25 km to 4 km which is a somewhat larger spread than noted in Figure 4-9 and is much larger than typical for temperate climates.

[redacted]

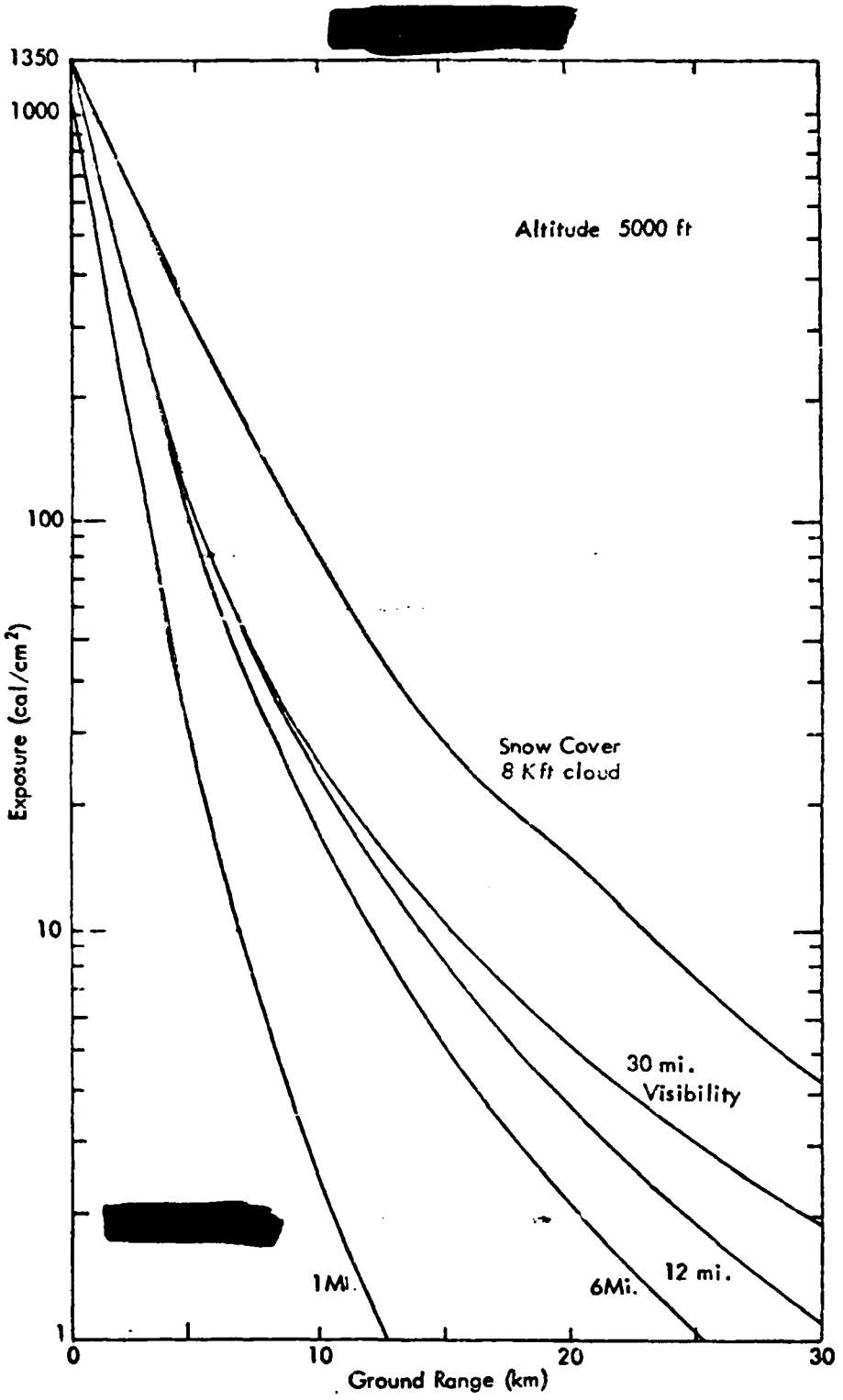

[redacted] FIGURE 4-9 PREDICTED EXPOSURE VS GROUND RANGE AT SAMPLE VISIBILITIES

[redacted] Page 4-29 was deleted

[redacted]

All of the examples given previously refer to the thermal exposure received by a target on the ground surface. An important consideration is the thermal exposure on aircraft in the vicinity of the nuclear burst both for consideration of a safe escape range for a delivery aircraft as well as determining the thermal damage potential for attacks on Soviet airbases in the Arctic. No calculations are available for the specific Arctic cases of interest but the transmission results presented in Figure 4-11 shows the type of effect that will be experienced. The transmission is given as a function of horizontal range and altitude from a burst at an altitude of 1 km. The solid lines give the exposure contours for a case with a cloud bottom at an altitude of 6 km and with a medium ground albedo corresponding to desert sand. The transmission for the Arctic albedo case would be somewhat larger. The dashed lines refer to the same burst conditions without albedo surfaces.

[redacted]

The ratio of the solid to dashed contour values at the same point in space give an indication of the buildup introduced by the albedo surfaces. Note that the dashed contours are all less than unity and tend to decrease with increasing range and decreasing altitude in a regular pattern. The introduction of the albedo surfaces leads to a much more complicated spatial dependence for the transmission because of the complicated interaction occurring between the attenuation and scattering properties of the atmosphere and the diffuse scattering of the two albedo surfaces.

[redacted]

Vulnerability levels of about 100 cal/cm^2 are realistic for aircraft which in previous figures would occur at a range of about 7 km near the ground for the albedo case. Ratios of 1.8

[redacted]

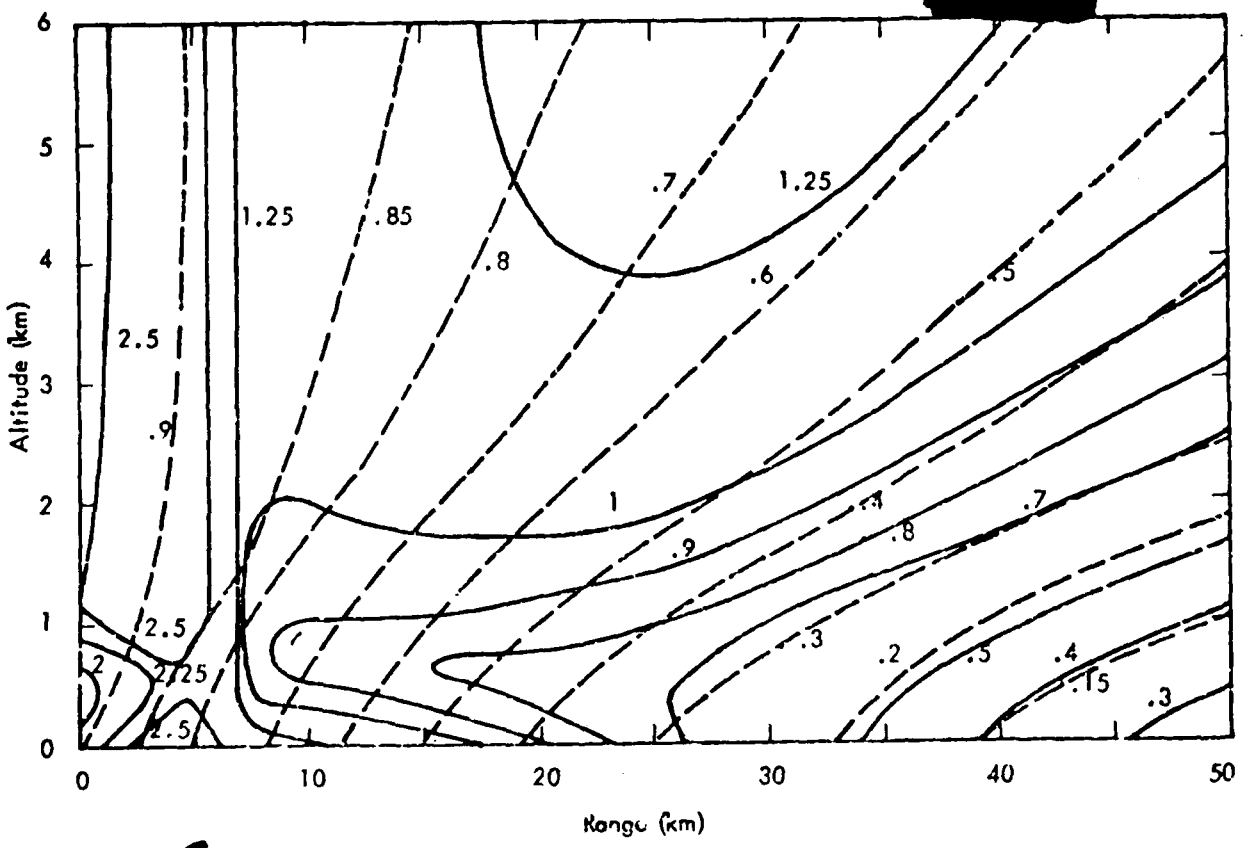

FIGURE 4-11 TRANSMISSION WITH AND WITHOUT ALBEDO SURFACES

[redacted]

[redacted] are noted near the ground for these ranges. At higher altitudes ratios of 1.5 are obtained. These represent large differences in exposure levels and could represent the difference between sure-safe and sure-kill environments.

[redacted] Directly above the burst ratios of 2.5 are obtained. At larger ranges representing lower exposures ratios near 3 are experienced at the lower altitudes. In general thermal effects become more important as the yield is increased and as shown in the last three figures, the effects of the albedo surfaces are largest at the longer ranges.

4.5 [redacted] Thermal Effects of Underwater Bursts

[redacted] Thermal effects of underwater nuclear detonations are generally ignored. In Chapter 3 of DNA EM-1, only land surface and subsurface bursts are treated in any detail. It is stated that in the case of underwater bursts, thermal effects in the atmosphere are usually insignificant, and the fact that a 20 kt burst in 90 feet of water produced negligible thermal radiation is cited. (20 kt at 90 ft is a very shallow detonation -- $\sim 33W^{1/3}$.) The presence of ice in the Arctic would tend to reduce thermal effects in the atmosphere even more.

[redacted] Since the thermal energy of an underwater detonation is largely absorbed by the water, the question arises as to whether there will be left a body of heated water sufficient to create and maintain an ice-free pool in a region of otherwise total ice cover. Neither DNA EM-1 nor the Underwater Handbook addresses this question. A limited amount of experimental data has been collected on the temperature changes produced in water by underwater explosions. While most of the data have been acquired on experiments conducted with a steam-generating explosive (Lithanol), developed for the purpose of simulating the bubble behavior of underwater nuclear detonations, a few parallel

[redacted]

[redacted]

[redacted] tests were conducted with Pentolite, a conventional high explosive, and water temperature data were collected during Operation Wigwam. The high explosive tests were conducted in Chesapeake Bay, Puerto Rico, and Panama City during the period 1965 to 1969. Lithanol charges up to 13,000 pounds were used.

[redacted] None of these data have demonstrated any significant heating of the water. The results of the non-nuclear tests have been published in the open literature (Young, 1971 and 1973). Young and Scott, 1970, summarized the existing experimental and theoretical knowledge of the heating of water by underwater explosions and examined phenomena that had not been treated in earlier studies (e.g., Young, 1968 and Young and Scott, 1968).

[redacted] A simple calculation will show that it is not surprising that significant heating effects of underwater explosions have not been observed. Assume an explosion deep enough that the first bubble at its maximum radius does not penetrate the surface, say $d = 240W^{1/4}$. Assume that 100% of the available energy remains in the bubble and is used to heat the water in the cylinder less half sphere that is between the bubble and the surface. It can be shown that the temperature rise in that volume of water is about $2.4W^{1/4}$ °C, where W is in kt. A 10 kt detonation would heat this water less than 5°C and a 100 kt explosion less than 8°C.

[redacted] The conclusions of Young and Scott, 1970 provide the best summary of what has been found in the investigations of the heating effects of underwater explosions:

[redacted]

[redacted] Page 4-34 was deleted

[redacted]

[redacted]

4.6 [redacted] Thermal Damage Effects

[redacted] Thermal damage effects result from absorption of the thermal energy on the target accompanied by a surface temperature increase during the delivery time of the nuclear weapon pulse. The temperature reached in the target depends upon the thermal characteristics of the material, the thermal pulse amplitude and duration, the thickness of the material and the absorptivity of the surface. The range of magnitude of thermal effects ranges from personnel burns that can occur at levels as low as 2 cal/cm^2 to massive melting and ablation of metals in blast hardened structures requiring a thousand cal/cm^2 or more.

[redacted] Thermal burns on personnel in the Arctic will be reduced because of the amount of exposed skin will be much less than in temperate climates. The degree of incapacitation depends upon the fraction of the body burned as well as on the severity of the burn. First degree burns can result from exposures as low as 2 cal/cm^2 for low yield weapons, but a first degree burn must occur over most of the body to produce a casualty. Thus, one would not expect casualties from such burns in the arctic. A less extensive second degree burn may cause a casualty but this takes about twice the exposure for a first degree burn. A mitigating factor is that the parts of the body most likely to be exposed are the face and hands, and a burn on these portions of the body affects performance more than other parts.

[redacted]

[redacted]

[redacted] Flash blindness casualties may be affected in the artic. During the day, the casualties will probably be less than in temperate climates because the high level of light will generally require some eye protection which will reduce the thermal radiation received by the eye, even under the possibly higher arctic transmission. Even if no eye protection is worn, the pupil of the eye will be very small and will reduce the problem. During the long winter nights, however, the eye will be more sensitive to flash blindness.

[redacted] The type of clothing worn in the arctic will tend to reduce the effects of burns. In temperate climates only thin layers of material are usually worn, and if these ignite or melt as can happen with synthetic fabrics, an extensive burn can result. Dark materials will be affected at levels as low as 10 cal/cm^2 for low yield weapons while white materials may require twice as much exposure because of their smaller absorption. In the Arctic since one would probably be wearing several thickness of material, a burn would be much less likely to reach the skin.

[redacted] The effect of the frost covering surfaces in the arctic will be to reduce the absorption of the thermal energy because of its high reflectance. However, the thickness of the frost would be crucial because the fraction of the energy absorbed during the early part of the pulse could melt the frost and expose the underlying surface to the later portion of the pulse. No discussion of this effect was noted in the literature, but the magnitude of the effect can be estimated as follows.

[redacted] Consider the surface loading expressed as the equivalent g/cm^2 of water on the surface. Then with the assumed standard temperature of -24°C it will take about 24 cal/cm^2 to bring the frost to melt and another 81 cal/cm^2 to completely melt it for each g/cm^2 of water loading, for a total of 105 cal/cm^2 of absorbed

[redacted]

[redacted]

energy. The albedo can be as large as .9 for fresh snow and frost. Therefore, about 1000 cal/cm^2 of incident energy is required to completely remove a frost equivalent to 1 g/cm^2 of water. The hoarfrost and snow buildup can be easily this large under arctic conditions; so that this would result in a very effective thermal shield even at high exposure levels. Note that a frost equivalent to a .01 cm rain would require about a 10 cal/cm^2 exposure to disperse and expose the underlying material. This could be of importance in considering the damage to combustible materials and other materials whose damage level is low such as canvas tents and truck tops.

[redacted] The ignition threshold for materials such as leaves, and newspapers is typically defined for conditions representing a nominal humidity of 30% - 40% in temperate climates. The relative humidity in the Arctic is generally much higher than this, but the absolute humidity or the moisture available in the air is low in the Arctic temperatures. This might result in an effective lower humidity for these materials and a lowering of their ignition threshold.

[redacted] During the warm weather months, one would expect the ignition of fires and their subsequent spread in inhabited areas or forest and dry tundra areas to progress much as in temperate areas. During the cold winters, however, the lower temperatures imply a larger heat input to raise materials to the ignition temperature and sustain burning. Thus, one would expect extensive fires to be a less significant damage mechanism than in temperate climates. Because of the extreme conditions existing in the arctic, however, loss of shelter becomes a very significant factor in survivability and in retaining the capability of performing a mission.

[redacted]

[redacted]

[redacted] The thermal damage threshold for hardened targets such as radars which have been designed to survive large blast overpressures would probably not change under arctic conditions. The amount of energy necessary to raise the temperature from the low arctic value would be negligible compared to that required to cause the relevent material damage. It is possible that for specific designs the high surface temperatures in conjunction with the lower overall structure temperature might result in larger thermo-mechanical loading and an increased warping force. If this occurred in materials that became more brittle at the lower temperatures, then there might be some chance for the structure to suffer damage at a lower exposure due to the lower temperatures. No studies of this applied to weapons effects were found.

4.7 [redacted] Conclusions and Recommendations

[redacted] The arctic is characterized in general as a region of relatively large surface visibilities with the high probability of high albedo surfaces in the form of snow or ice covered terrain and low cloud layers. This combination leads to a very high transmission of thermal radiation as compared to average conditions in temperate locations. At the same time arctic meteorological conditions result in the large probability of occurrence of water and ice fogs and blowing snow which tend to reduce the visibility to less than 1 mile when these conditions are existing. This is a much smaller visibility than will be found in heavily polluted temperate climates. Thus, an extreme variability in possible thermal damage ranges must be expected in the arctic depending upon the specific meteorological conditions at the burst point.

4.7.1 [redacted] Conclusions

[redacted] The low absolute humidity characteristic of the arctic does result in an increase in the transmission of infrared energy as compared with temperate cases with the same visibility. Because of the relatively small amount of infrared energy in the

[redacted]

[redacted]

[redacted] output spectrum of nuclear weapons the increase in overall transmission is small. The uncertainties in the other meteorological parameters are larger than this effect.

[redacted] The experimental data showing the transmission of thermal radiation under various arctic conditions are very limited and can not be used independently as a prediction method for general transmission calculations in the arctic. The data do indicate a very pronounced ducting effect for cases in which a high albedo snow layer exists in conjunction with a cloud layer. Enhancements as large as a factor of 100 over the direct exposure were noted for low visibility cases. However, because the direct exposure may be low for these cases, the total exposure may be less than would be noted at the same position for a high visibility. Enhancements of a factor of two were noted in the high visibility cases.

[redacted] Two different Monte Carlo calculations have been made of thermal transmission including the presence of two reflecting surfaces as well as attempts at handling the problem analytically. The simple techniques result in significant over-estimates of the enhancement due to poor handling of the attenuation in the atmosphere even under high visibility conductions. The Monte Carlo calculations indicate possible enhancements of as much as 2.5 due to the ducting effect over the general region of interest for thermal damage.

[redacted] Reliable Monte Carlo calculations require careful specification of atmospheric parameters including detailed information on the suspended particulate matter. The current standard atmosphere profile tables include a 75° latitude model which is suggested for use at all higher latitudes. For the purpose of low altitude nuclear effects this is not a serious problem since

[redacted]

[redacted]

[redacted]

the available meteorological information gives a good description of the arctic atmospheric conditions near the surface which is of most importance.

[redacted] A few studies have been made of the particle distributions and concentrations for various conditions in the arctic. These have usually been oriented towards providing information on the visibility for aircraft operation. Recent measurements have indicated that layers of aerosols at altitudes of 1 km to 3 km exist often during the winter portion of the year leading to lower visibilities in these layers than observed on the surface. This could lead to predictions of a higher thermal fluence than actually exists for these conditions if the current techniques of using the surface visibility to specify the aerosol distributions are used. One calculation has compared the relative transmission of ice fog and super-cooled water fog. There has been no general study made of the transmission for various wavelengths for the observed particle size distributions and the effects expected in the transmission of nuclear weapon thermal energy.

[redacted] No studies were found relating to the change of thermal damage thresholds due to arctic conditions. The discussion in Section 4.6 reveals that one would expect the thermal damage threshold to be larger under arctic conditions except in particular cases where brittle materials conceivably would be subjected to a more damaging thermo-mechanically induced force than under temperate conditons.

4.7.2 [redacted] Recommendations

[redacted] Analyses of the meteorological information available from arctic sites should be made to define the relative occurrence of high and low visibility conditions on a seasonal basis.

[redacted]

[redacted]

[redacted]

The parameters of interest include visibility, ground albedo, cloud layer definition, aerosol concentrations and distributions and ice and water fog concentrations and distributions.

[redacted] From these analyses reasonable model atmospheres could be defined for purposes of thermal transmission studies. Calculations should be made of the thermal transmission for these model atmospheres emphasizing those cases which result in an enhancement over that expected in temperate climates such as those involving the ducting effect in high visibility conditions.

[redacted] From these calculations, figures showing the predicted exposures under arctic conditions should be prepared. Comparisons should be made with blast HOB charts since in general blast and thermal are competing nuclear damage mechanisms. It may be that considering the reduction that occurs in blast effects over snow that thermal will be of more importance in the arctic even considering the low visibility conditions that can occur.

[redacted] 4.8 Bibliography

Cantor, Israel and Petriw, Andrew, Atmospheric Attenuation of Light Radiation From a Point Source in an Arctic Environment, Technical Report ECOM-2453, U. S. Army Electronics Command, Fort Monmouth, NH, October 1964, UNCLASSIFIED.

Defense Nuclear Agency, Capabilities of Nuclear Weapons, Part I-Phenomenology, Part II - Damage Criteria (U), DNA EM-1 (Change 1), Dolan, P. J., Ed., Defense Nuclear Agency, Washington, D. C. July 1978, SECRET RD.

Glasstone, Samuel and Dolan, P. J., Eds., The Effects of Nuclear Weapons, Third Edition, The U. S. Department of Defense and the U. S. Department of Energy, 1977, UNCLASSIFIED.

[redacted]

Keith, J. R., Nuclear Weapons Thermal Radiation Phenomena, Volume 1 - Analysis, Chapter 2 - Atmospheric Transmission, K-73-534(R), Kaman Sciences Corporation, Colorado Springs, CO., September 1973, UNCLASSIFIED.

Keith, J. R., and Sachs, D. C., Damage Assessment and Strike Burst Environments and Damage Descriptions, DNA 4639P, Kaman Sciences Corporation, Colorado Springs, CO, December 1977, SECRET FRD.

Keith, J. R. Analysis of Soviet Weather Data, K-79-10U(R) Kaman Sciences Corporation, Colorado Springs, CO, February 1979, UNCLASSIFIED.

Kumai, Motoi and Russell, J. D., The Attenuation and Backscattering of Infrared Radiation by Ice Fog and Water Fog, CRREL-RR 264, Cold Regions Research and Engineering Laboratory, U. S. Army Terrestrial Sciences Center, Hanover, NH, April 1969, UNCLASSIFIED. AD-689447.

Larson, P. and Orvig, Svenn, Albedo of Arctic Surfaces, Publication in Meteorology No. 54, Arctic Meterological Research Group, McGill University, Montreal, for Air Force Cambridge Research Laboratories, Bedford, MA, October 1962, UNCLASSIFIED.

Mitchell, J. M., Jr., Visual Range in the Polar Regions with Particular Reference to the Alaskan Arctic, From: Polar Atmosphere Symposium, Part 1. Meteorology Section, Symposium at Oslo, July 1956, Sutcliffe, R. C., Ed., Pergamon Press, Almsford, NY, 1958, UNCLASSIFIED.

Wells, M. B., Collins, D. G., and Cunningham, K., Light Transport in the Atmosphere - Volume I: Monte Carlo Studies, RRA-T63-1, ECOM-00240-1, Radiation Research Associates, Inc., Fort Worth, TX, for U. S. Army Electronics Command, Fort Monmouth, NJ, September 1966, UNCLASSIFIED.

Wells, M. B., Collins, D. G., and Marshall, J. D., Monte Carlo Calculations of the Transmission of Thermal Radiation From Nuclear Detonations in Model Atmospheres, RRA-T810, ECOM-00240-4, Radiation Research Associates, Inc., Fort Worth, TX, for U. S. Army Electronics Command, Fort Monmouth, NJ, March 1969, UNCLASSIFIED.

Young, George A., The Transport of the Products of Very Deep Underwater Explosions (U), NOLTR 67-179, U. S. Naval Ordnance Laboratory, White Oak, Silver Spring, MD, 1968, CONFIDENTIAL, FORMERLY RESTRICTED DATA, AD-388 179L.

Young, George A., The Physical Effects of Conventional Explosions on the Ocean Environment, NOLTR 71-120, Naval Ordnance Laboratory, White Oak, Silver Spring, MD, 3 August 1971, UNCLASSIFIED.

Young, George A., Guide-Lines for Evaluating the Environmental Effects of Underwater Explosion Tests, NOLTR 72-211, Naval Ordnance Laboratory, White Oak, Silver Spring, MD, 13 February 1973, UNCLASSIFIED, AD-758 641.

Young, George A. and Scott, B. W., Explosion Debris Distribution Following Large Lithanol Underwater Explosions (U), NOLTR 68-162, U. S. Naval Ordnance Laboratory, White Oak, Silver Spring, MD, , CONFIDENTIAL, AD-395 126L.

Young, George A. and Scott, Bruce W., Temperature Changes Produced in Water by Underwater Explosions (U), NOLTR 70-29, Naval Ordnance Laboratory, White Oak, MD, 12 August 1970, CONFIDENTIAL, AD-511 453.

[redacted]

THIS PAGE IS INTENTIONALLY LEFT BLANK

[redacted]

[redacted]

SECTION 5

NUCLEAR RADIATION

[redacted] The nuclear radiations considered include the prompt gamma rays, the prompt neutrons, the secondary gamma rays from neutron interactions with air and ground, ground activation products, and the radiation from the fission products from the weapon. The last two components are typically treated together and considered in two time regimes. The initial radiation occurs within a minute or so following detonation while the residual radiation is that which is contained in the rising debris and subsequently is distributed over a wide area as fallout. For the underwater bursts the initial radiation is associated with the base surge, and there will also be some radioactivity remaining in the water which should be considered when considering possible ship or submarine contamination.

5.1 Arctic Environmental Differences

[redacted] The primary atmospheric parameter affecting the prompt radiation dose is the density. As shown in Section 1.2 the January 75° standard atmosphere has a density 16% greater than the midlatitude standard typically used for weapons effects studies. For the temperature extremes noted in Section 1.2 the density will be even larger. For these cases the radiation will tend to be decreased relative to temperate areas.

[redacted] The ground composition can have an effect on the neutron and gamma ray transport in the atmosphere primarily involving the secondary gamma rays. The amount of water in the ground is important.

[redacted] Under arctic conditions involving a snow or ice cover changes might be noted in the neutron and gamma ray dose.

[redacted]

[redacted]

[redacted] Fallout depends upon many parameters which are significantly different in the arctic. The particle size distribution and composition of the swept up debris cloud will be significantly different for the snow/ice situations. The atmosphere profiles of pressure, density and temperature may change cloud rise characteristics. The meteorological conditions in the arctic including wind and precipitation patterns could affect the fallout distributions.

[redacted] The freezing conditions that occur in the arctic area may be important in terms of retaining radioactivity from the base surge on ships near the area.

5.2 [redacted] Prompt Radiation Effects

[redacted] The characteristics of prompt nuclear radiation under arctic conditions will be discussed with regard to effects of the air density, the ground composition, and the depth of burst.

5.2.1 [redacted] Air Density Effects

[redacted] The vast majority of the predictions that are made of the effects of prompt radiation use scaling relationships applied to infinite uniform air transport results. The techniques can involve codes such as ATR (Harris, 1972) or graphical techniques as contained in EM-1. (DNA, 1978).

[redacted] The basic transport results are typically presented as a $4\pi R^2$ dose as a function $F(\rho R)$ of the amount of air between source and receiver (ρR). $F(\rho R)$ will depend upon the particular source spectrum of interest and the particular dose response function desired. The dose at a particular range R is then given by

$$D = \frac{F(\rho R)}{4\pi R^2}$$

where for a uniform density (ρ) case the amount of air is just the product of ρ and R. If the density varies over the path, an

[redacted]

[redacted]

[redacted]

integral of tne density over the path is used in the above expression. At the same range in atmospheres of different densities the dose will be related by the expression

$$\frac{D_2}{D_1} = \frac{F(\rho_2 R)}{F(\rho_1 R)} \quad .$$

The function $F(\rho R)$ typically shows a buildup from zero as contributions from multiple scattering increase the dose, then a decrease with increasing ρR as various extinction processes begin to dominate the transport.

[redacted] At ranges for typical environment levels of interest near sea level the $F(\rho R)$ is a decreasing function of ρR. Thus, if $\rho_2 > \rho_1$ then the dose D_2 is less than D_1. Thus, for the winter arctic conditions where the density is greater than in temperate climates a decrease in the radiation will be expected.

[redacted] Example curves are given for several different prompt radiation doses of interest in military systems. In all cases a 1 MT nominal thermonuclear weapon is assumed for the source function for the radiation. The neutron fission heating is used to assess the vulnerability of warheads. In Figure 5-1 the neutron fission heating is shown as a function of range for several different ratios of the density to the density of sea level standard mid-latitude atmosphere. Ignoring surface effects, the top curve represents the neutron fluence versus range for the weapon chosen near sea level for temperate climates. The curve marked 1.157 represents the neutron fluence expected for the arctic winter standard case. Note that for a 10^{15} heating level a reduction of about 10% is noted in the range. The higher ratios refer to densities corresponding to more severe cold temperatures that might occur in the arctic. For the extreme case corresponding to a temperature of about -80° which occurs very rarely a reduction of about 21% is noted.

[redacted]

[redacted]

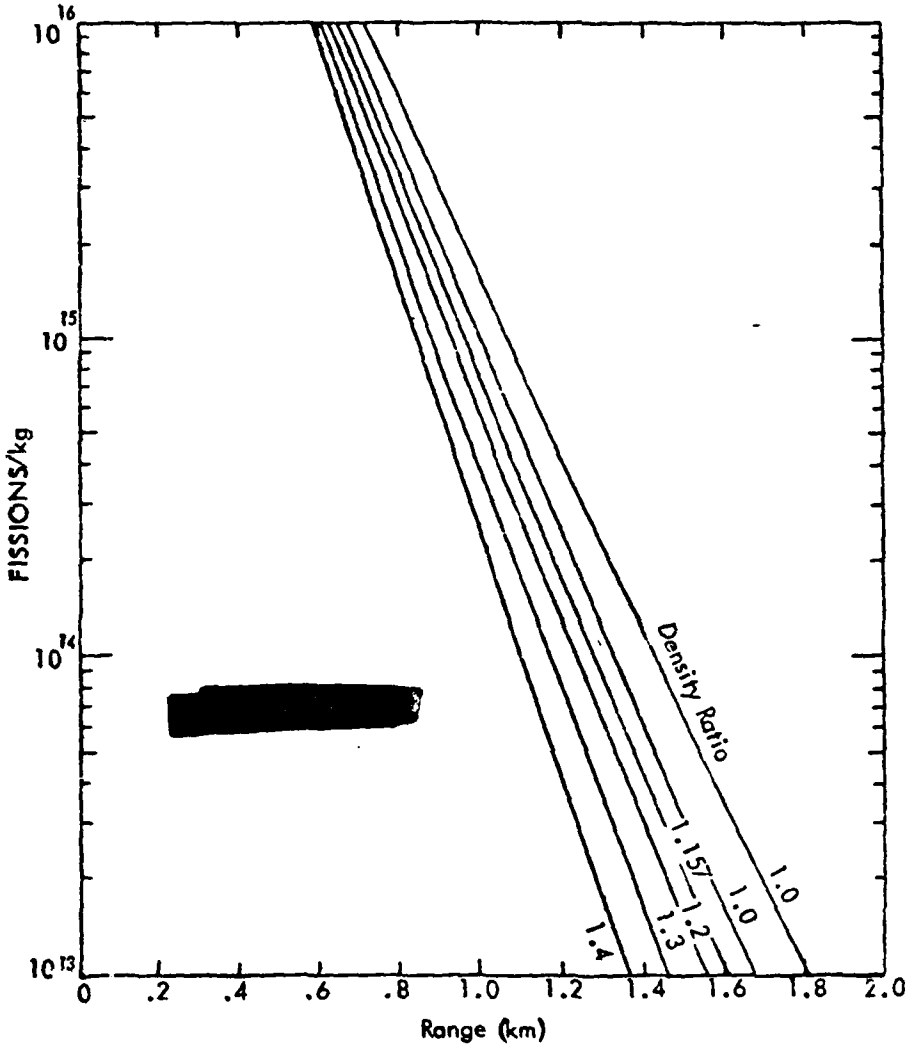

[redacted]

FIGURE 5-1 FISSION HEATING AS A FUNCTION OF RANGE

[redacted]

[redacted]

[redacted] The neutron fluence expressed as the 1 MeV Silicon Equivalent fluence is more commonly used to assess the vulnerability of systems. Figure 5-2 shows the 1 MeV Si Eq fluence versus range for the density ratios considered. For a level of 10^{12} the nominal arctic reduction is about 12%. The extreme difference at 10^{12} is about 25%. At higher levels corresponding to vulnerability criteria for harder systems, the difference is slightly less. At 10^{14} the reductions in range are 10% and 22% respectively.

[redacted] The prompt gamma ray dose rate is a common damage mechanism for TREE. In Figure 5-3 gamma dose rates are shown for the range of densities considered previously and for yields of 10 KT and 1 MT. For the 1 MT case and for a level of 10^{10} rad (Si)/sec the reduction for the arctic winter case is 11% and fo· the extreme case the reduction is 23%. For the 10KT burst, the corresponding reductions are 10% and 20%.

[redacted] In Figure 5-4 the total dose from the prompt gamma rays is shown for a 1 MT source for the density ratios chosen. For the 10^{5} level a reduction in range of about 9% is noted for the arctic winter case and a reduction of about 19% is noted for the extreme case.

[redacted] Note that all reductions found for the arctic winter case are about 10% and the reductions for the extreme case are between 20% and 25%. These correspond to area coverage reductions of 20% and 38% to 44% respectively, which might not be insignificant for specific system considerations. Note also that if one enters the curves at a certain range, for instance 1.2 km on Figure 5-2. the 1 MeV Si Equivalent fluence decreases from about $3.5\text{x}10^{13}$ for temperate climates to $1.5\text{x}10^{13}$ for normal arctic winter to $3.5\text{x}10^{12}$ for arctic extreme weather. These are very significant changes in the fluence levels and could easily span the range from sure kill to sure safe for a system.

[redacted]

[redacted]

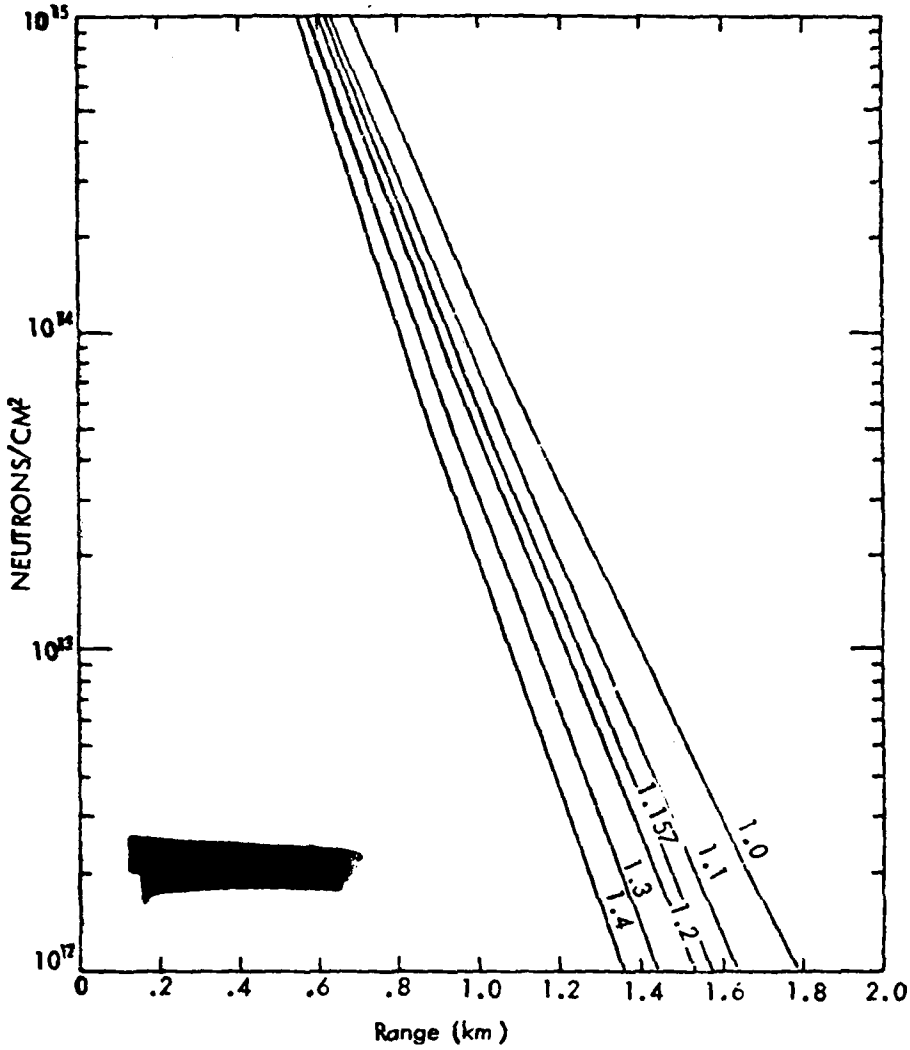

[redacted] FIGURE 5-2 SILICON EQUIVALENT NEUTRON FLUENCE AS A FUNCTION OF RANGE

[redacted]

[redacted]

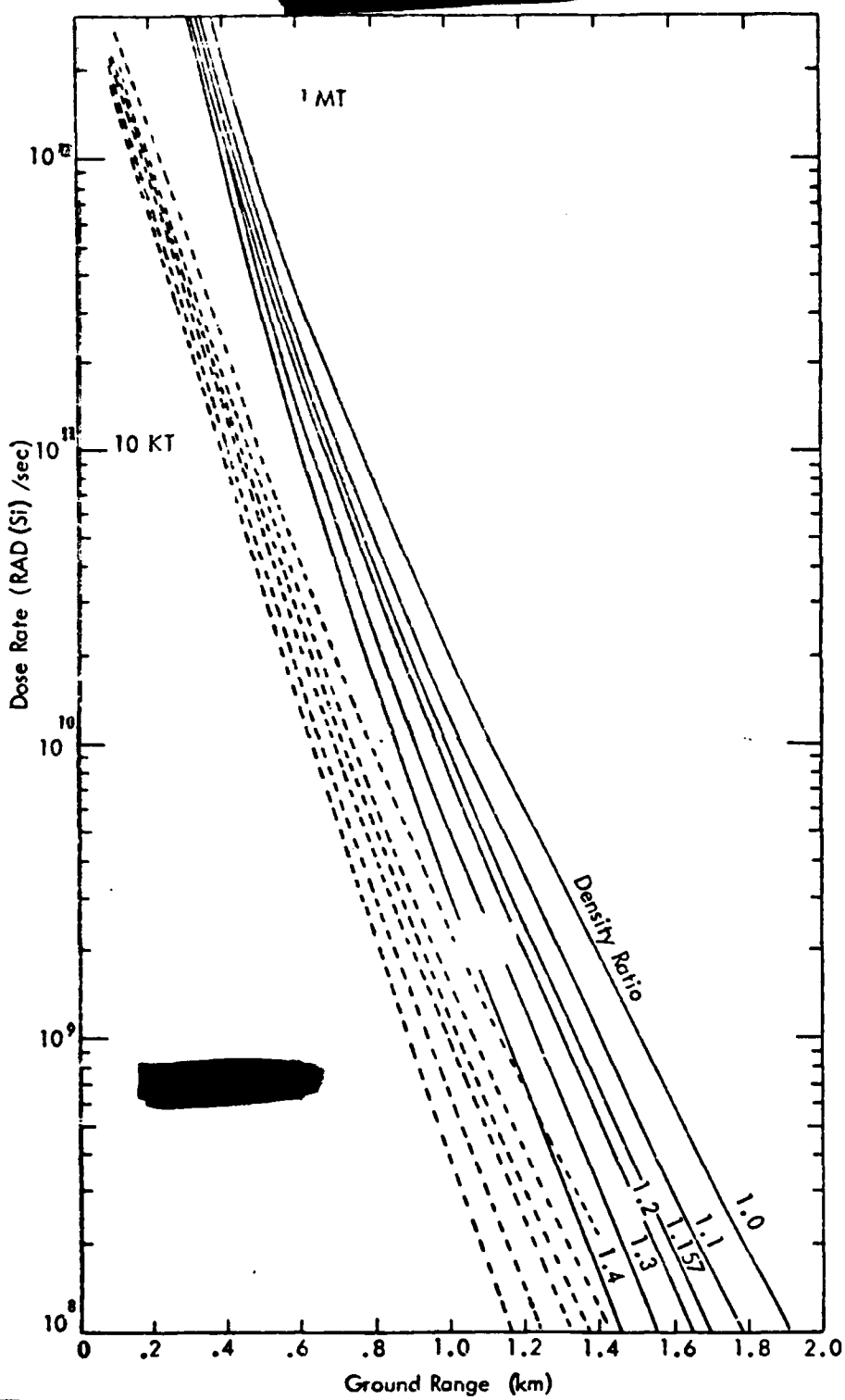

[redacted] FIGURE 5-3 PROMPT γ DOSE RATE AS A FUNCTION OF RANGE

[redacted]

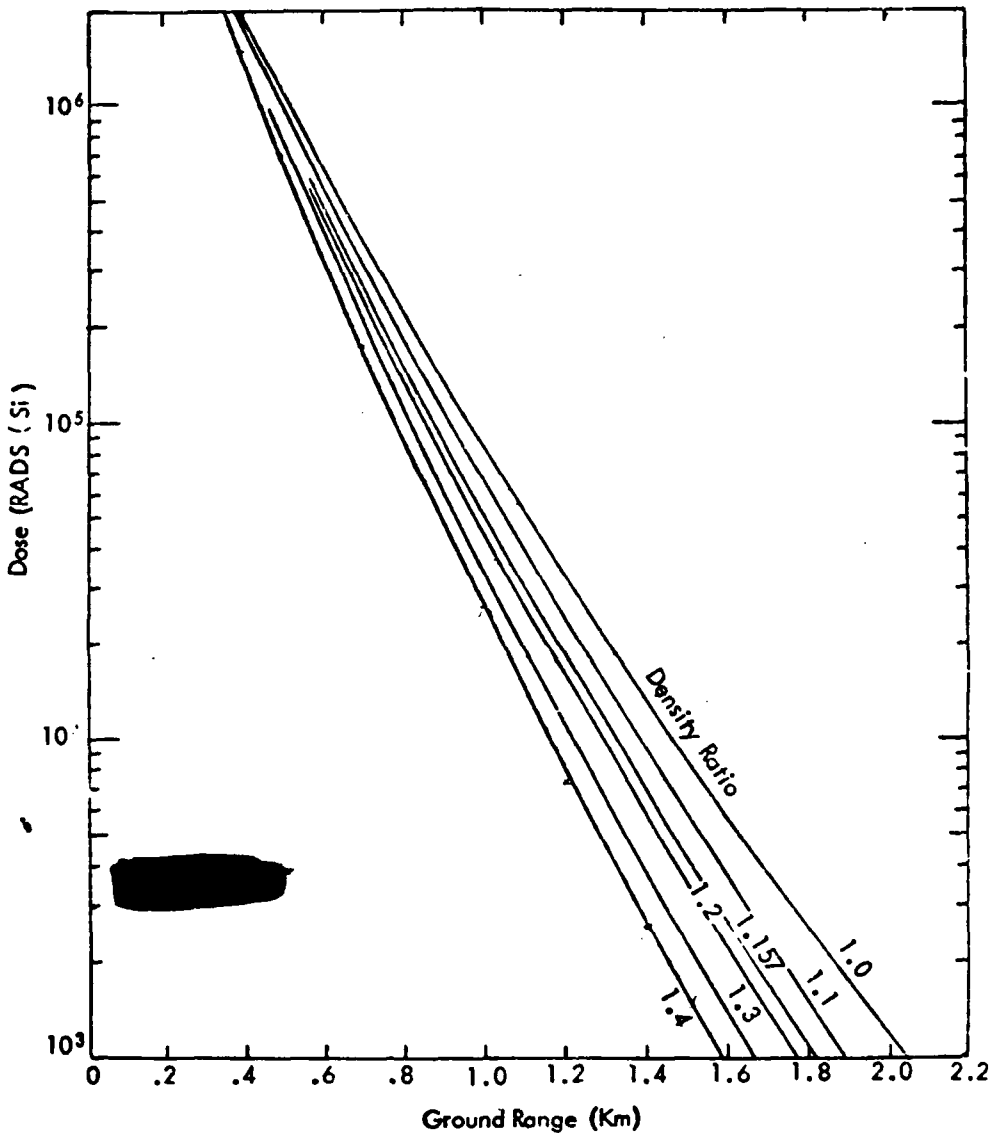

FIGURE 5-4 PROMPT GAMMA DOSE AS A FUNCTION OF RANGE

[redacted]

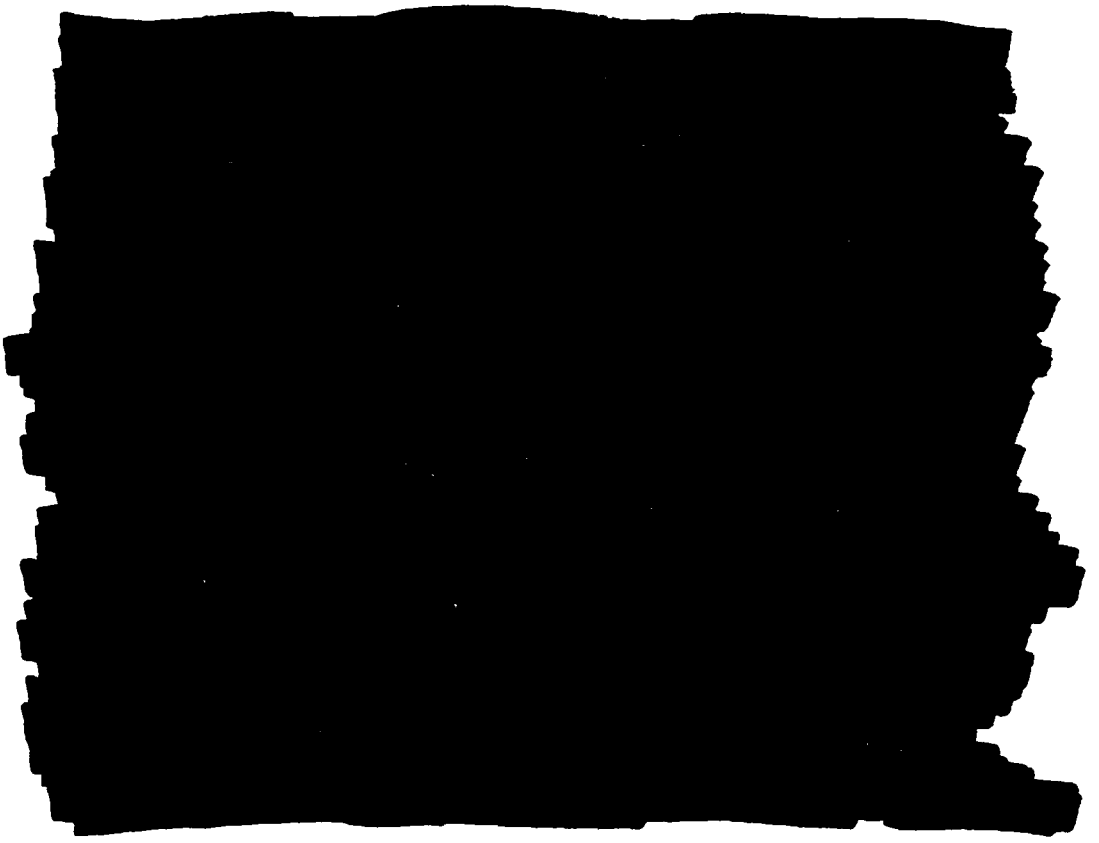

[redacted] The initial fission product radiation depends upon the density in a more complicated fashion than does the prompt radiation. The time scale is such that the atmosphere is significantly perturbed by the weapon. The fireball within which the debris is contained is growing and rising. The shock wave is moving outwards through the air altering the integrated density. Several techniques have been derived to handle this component of the radiation dose as described in EM-1 and computed in ATR. Essentially, infinite air results are scaled to account for the fact that there is a hydrodynamic enhancement because of the low density

[redacted] Page 5-10 was deleted

[redacted]

[redacted] fireball region. If the initial dose is desired, scaling is a difficult task since the time dependence of the various effects must be considered and integrated. The above two techniques use a scaling method due to Mooney and French (1965) to include the ground effects on the dose.

[redacted] Another method developed (KSC, 1974) uses the density profile defined by the HULL code as a function of time and transports the gamma rays through the highly perturbed air by Monte Carlo methods. The HEAT code has been exercised several times to compute specific cases of interest for Ballistic Missile Defense systems. A sample calculation is shown in Figure 5-6 showing the tissue dose as a function of ground range for a 5 MT burst at an altitude of 3.4 ft. The HEAT results are seen to be considerably less than the RRA results which were thought to be compatible with EM-1. However, note that there is significant difference between the RRA model and EM-1. The 500-rad tissue dose level is a very severe personnel dose. At this level and below the difference between the HEAT and EM-1 results are less than 10% while the RRA results are much larger.

[redacted] In comparing HEAT cases run, it was found that the density scaling results using the integrated density from the fireball to field point agreed with HEAT results especially for scaling between comparable cases. For the higher density arctic cases, the fireball will be slightly smaller. Cube root scaling is used to define the fireball radii with increasing altitude (decreasing density). If we use the scaling for higher densities also then reductions of the fireball size of about 4% and 10% would be seen for the arctic and severe density cases. These are within the uncertainties of the fireball modeling itself.

[redacted]

[redacted]

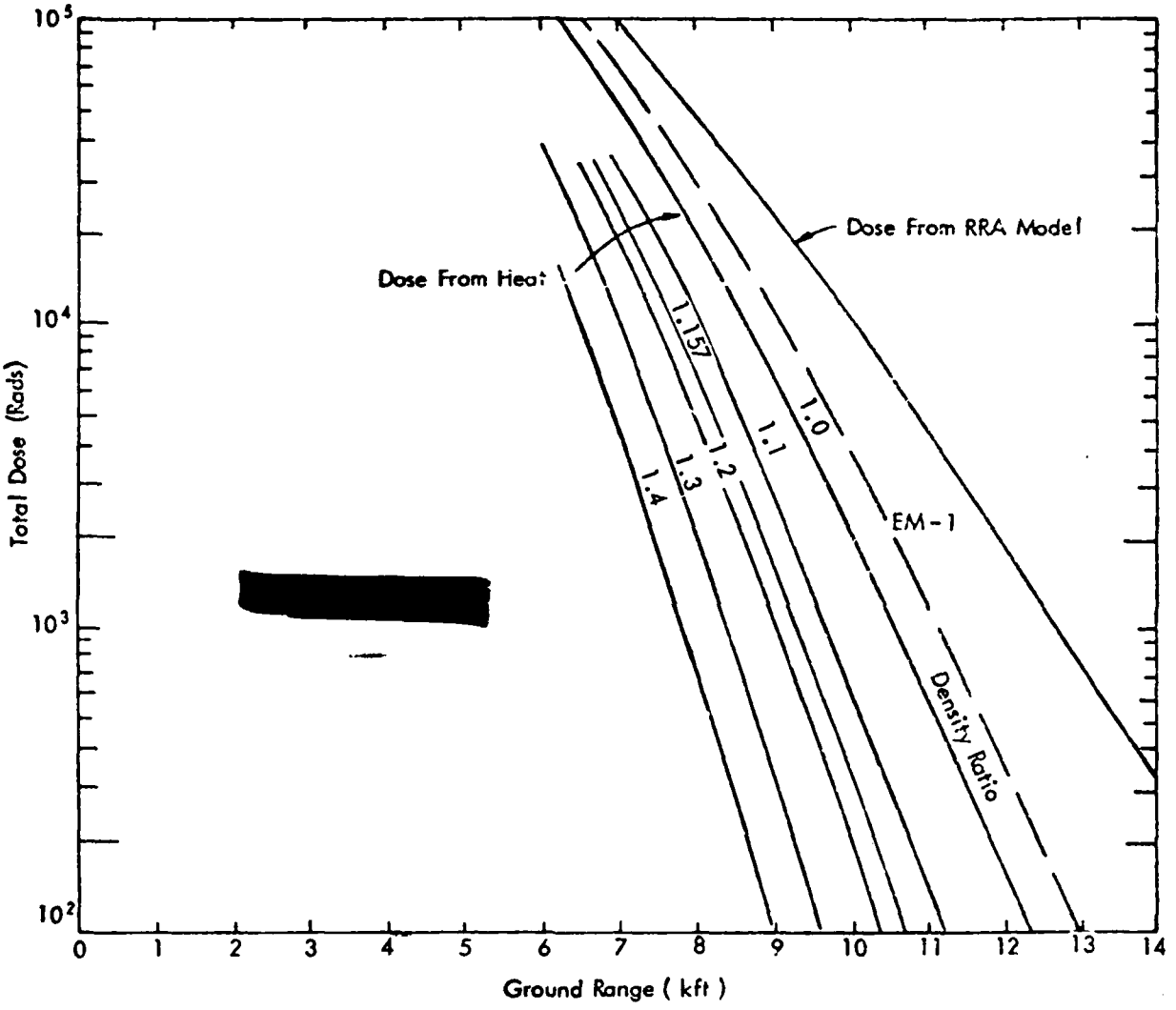

[redacted] FIGURE 5-6 TISSUE DOSE VS GROUND RANGE, 5 MT, 3.4 KFT HOB

[redacted]

[redacted]

[redacted] Therefore, the HEAT results have been scaled by the same scheme as before to show possible dose reductions in Figure 5-6. At the 500 rad tissue level, the reduction is about 13% for the arctic winter case and about 25% for the severe case. Again, these represent significant reductions in area coverage for the arctic cases.

5.2.2 [redacted] Effects of Ground Composition

[redacted] For sources and/or detectors near the ground surface, the radiation fluences are depressed below the infinite air results because there is absorption in the ground and loss of radiation from the atmosphere. The ground composition can affect the production of secondary gamma rays. A set of such calculations (Campbell and Sandmeier, 1973) has been made for several sources and several detector and receiver altitudes above the surface. Surface compositions of dry ground, wet ground and sea water were used to determine the effects of composition. Figure 5-7 shows the results as a function of slant range for a source at 5 m and a detector at 2.5 m above the surface. The results are presented as tissue dose, and the neutron and secondary gamma contributions are shown separately. The neutron dose is seen to be much less than in the free air case and to be essentially independent of surface composition. The secondary gamma doses for the surface cases are larger than for the free air case at the smaller ranges and drop lower at longer ranges. Note that there is some variation in the secondary gamma ray dose for the three compositions and that the difference becomes less with increasing range. The dry ground gives the highest secondary gamma dose and the larger the fraction of water in the ground the smaller the secondary gamma dose.

[redacted]

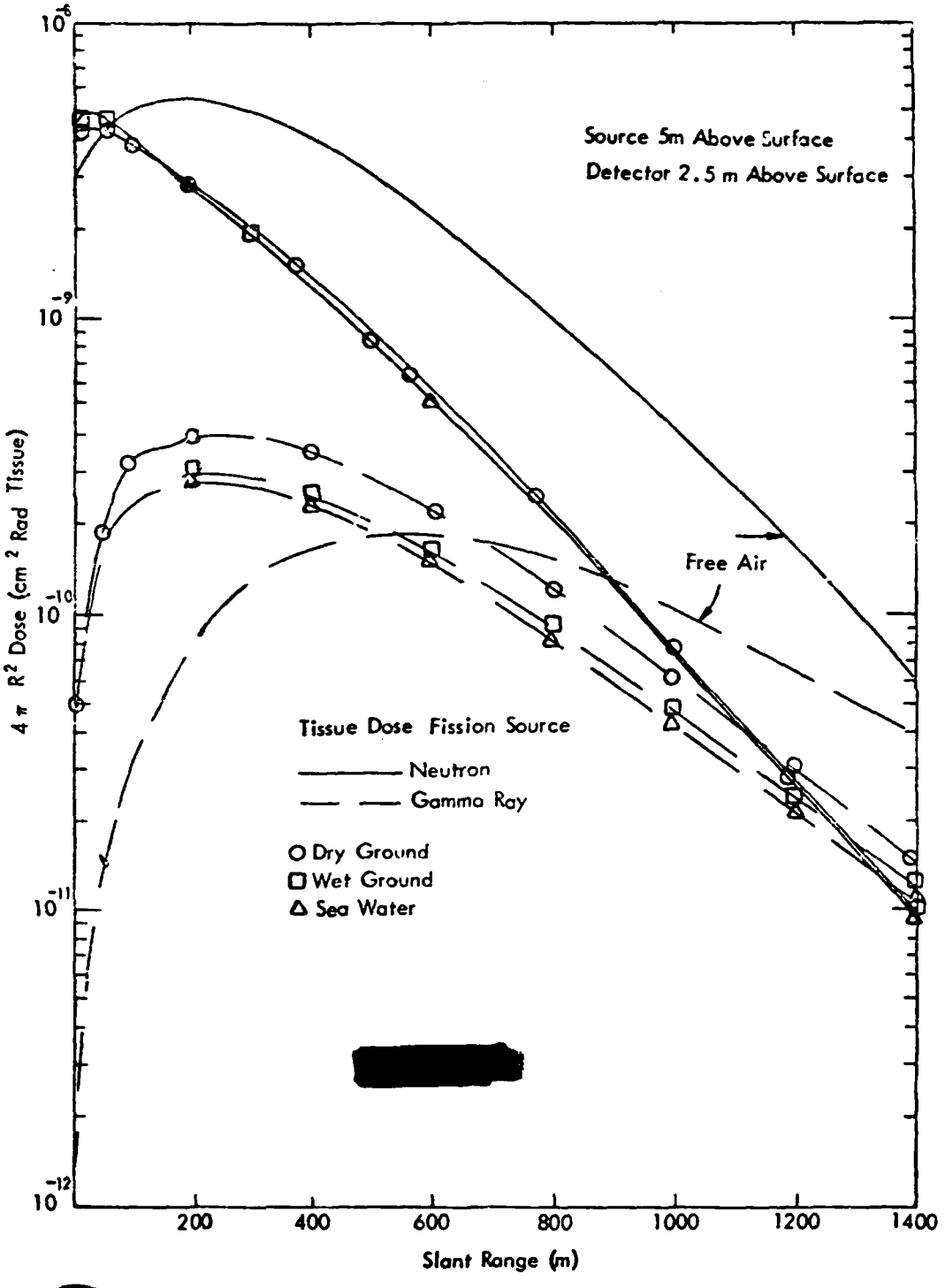

FIGURE 5-7 EFFECT OF SURFACE COMPOSITION ON NEUTRON AND SECONDARY GAMMA DOSES

[redacted]

[redacted]

[redacted]

Arctic soils are said to represent the same general classes that are observed in temperate climates; so no marked departure in the radiation doses would be expected. In the tundra and muskeg areas, the water content is higher than in the temperate climates; so the wet ground curves would be more representative. In those areas with heavy snow or ice cover or over the open sea the sea water curve should be used. It is probable that the curves over fresh water would show some slight decrease below that shown for sea water because of the absence of the salt contribution to the secondary gamma rays.

[redacted]

[redacted]

[redacted] In conclusion, the effect of the ice or snow cover on the prompt radiation would not be expected to be large and would generally be represented by the values that were computed for sea water. The wet ground results should be used for prediction purposes rather than the dry ground as being more representative of arctic conditons.

5.2.3 [redacted] Depth of Burst Effects

[redacted] If the burst occurs below the surface of ground or water, the prompt radiation from the device is strongly affected by the surface material. Only a few feet of material is necessary to markedly reduce the amount of radiation reaching the atmosphere and being transported in the manner described above. No particular differences in this effect would be expected in the arctic as compared with other underground and underwater bursts. In the case of a burst beneath snow, the depth should be measured as the equivalent water depth since the density can be much less than water.

[redacted] The initial radiation from the early time fission products can be an important contributor to the radiation dose even for bursts under the surface. The fission products and activated materials are ejected above the surface and form a radiation source which may be highly anisotropic because of the surrounding surface material ejected into the atmosphere. Calculations of this effect have been made for shallow-buried munitions in the ground, and no major changes would be expected for arctic ground conditions. For those cases involving bursts in ice or snow, no comparable calculations have been made. An estimate of the effect could be made by measuring the snow/ice depth as equivalent soil mass. There is some evidence, however, that for equivalent conditions a larger amount of snow or ice could be ejected into the air resulting in a reduction in the radiation.

[redacted]

[redacted]

5.3 [redacted] Residual Radiation Effects

[redacted] Residual radiation is that radiation that is emitted later than one minute after the explosion. The sources and characteristics of this radiation vary depending on the extent to which fission and fusion reactions contribute to the energy of the weapon. Residual radiation from a fission weapon arises mainly from fission products and, to a lesser extent, from radioactive isotopes formed by neutron reactions in weapon materials and from uranium and plutonium that have escaped fission. Other sources of residual radiation hazard are the activity induced by neutrons that interact with various elements present in the earth, sea, air, or other substances in the explosion environment. The most important of these sources is the neutron-induced activity in soils. The radioactivity from a thermonuclear weapon will not contain the same quantity of fission products that are associated with a pure fission weapon of the same yield; however, the large number of high energy neutrons will produce larger quantities of neutron-induced activity in weapon components and the surroundings. The total radioactivity from such a weapon will, however, generally be less than from a pure fission weapon of the same yield.

[redacted] The residual radioactive contamination (fallout) that results from fission products that are distributed subsequently to a contact surface or subsurface burst is much greater than the radioactive contamination that results from the induced neutron activity. Thus, the neutron-induced activity may be neglected for contact, surface, and subsurface bursts.

[redacted] If a weapon is burst in the transition zone (burst height $<100W^{.135}$ feet) as far as fallout is concerned, the neutron-induced activity generally can also be neglected if the burst height is in the lower three-quarters of the fallout transition zone, i.e., if the burst is below about $75W^{0.35}$ feet. If the height of burst is in the upper quarter of the transition zone (between about $75W^{0.35}$ feet and $100W^{0.35}$ feet), the neutron-induced activity may not be negligible compared to fallout.

[redacted]

[redacted]

5.3.1 [redacted] Induced Activity

[redacted] The type, intensity, and energy distribution of the induced activity produced by the neutrons will depend on which isotopes are produced and in what quantity. These factors depend on the number and energy distribution of the incident neutrons and the chemical composition of the soil. Induced contamination contours are independent of wind, except for some wind redistribution of the surface contaminant. The contours can be expected to be roughly circular.

[redacted] Examination of several thousand analyses of the chemical composition of soils and the relative probabilities of neutron capture by the various elements present in the various samples has indicated that sodium, manganese, and aluminum generally will contribute most of the induced radioactivity. Small changes in the quantities of these materials can change the activity significantly. Other elements can also influence the radioactivity. Some elements have a relatively high probability for capturing neutrons (cross section), but the isotope that is formed after the capture either is not radioactive, does not emit gamma rays, or has such a long half life that the low activity does not produce a hazardous dose rate. The presence of such elements in the soil will tend to lower the hazard from neutron-induced activity.

[redacted] Calculations (Pugh and Galiano, 1959) have shown that the induced activity in sea water is about a factor of 1000 less than in Nevada Test Site soil for times after burst of 1 hour or greater. At early times the contribution of the very short half life ^{28}Al in the soil makes the ratio even larger. From the fact that sea ice has slightly less salt content of sea water and ice over land has a low salt or mineral content, one can assume that induced activity in an snow/ice layer will be less than in sea water.

[redacted]

[redacted]

[redacted] Less induced activation should occur in ice/snow/soil configurations compared to bare soil due to the shielding effect of the ice or snow layer. The magnitude of the effect depends upon the depth of ice or snow. In areas such as the Greenland ice cap, where ice is over 1000-feet thick, little or no neutron induced radiation should occur. The same result should prevail where snow packs of 30-50 feet may occur. Data to support quantitative conclusions with respect to ice and snow have not been discovered.

5.3.2 [redacted] Radioactive Fallout

[redacted] A yet unpublished report (Spencer, Chilton and Eisenhauer) contains an excellent discussion of fallout gamma rays from nuclear detonations with exhaustive literature references in all phases of the fallout problem. In these lists, there are no references to work involving the effects of the arctic environment on fallout.

[redacted] The source of fallout is a combination of the fission products, weapon activation products and activation products from surrounding materials such as soil. For low altitude or surface bursts much of the activated materials will be vaporized or fragmented by the strong shock interactions and swept up into the rising cloud and will contribute to the total fallout dose.

[redacted] At very early times, the fireball is nearly spherical or hemispherical for a surface burst and is beginning to rise as the blast wave begins to move outwards but there has been no significant movement of material. The mixing and entraining of the swept up soil materials is occurring. Calculational models of this development have been described (Huebsch and Olken, 1976) using the HULL hydrodynamics code to describe the flow field from the low altitude burst. Routines are added which describe the growth of water, ice, soluble salts or insoluble particles in the rising expanding cloud. It is possible to include the effect of different meteorological conditions in this model. No cases have been run for conditions approximating the Arctic.

[redacted]

[redacted]

[redacted] A toroidal circulation builds up with very large upward velocities and the gamma source is strongly radiating and moving upwards rapidly. While the movement is occurring the vaporized materials will be cooling and will condense into very small particles. If solid or liquid particles are present, the material will partly diffuse into the surfaces of the particles.

[redacted] For altitudes above which significant solid materials are drawn into the cloud only very small particles will be produced and there will be little localized fallout. In this case, the residual dose near the burst will be primarily due to the induced activity, if any. For lower altitudes of burst, large quantities of material will be entrained and there will be a wide range of particle sizes in the cloud. The larger sizes will precipitate out to form the local intense fallout field and the smaller sizes will remain in the cloud for a long time and may be dispersed over a wide region.

[redacted] The spectrum of debris particles tends to be representative of the soil composition and type. Thus, for bursts in the arctic over land no significant differences would be expected in the cloud loading except possibly a slightly smaller fraction of soil material as compared with water since the water content of the soils in the arctic is typically larger.

[redacted] A burst over snow or ice in the arctic would not contain any of these large solid particles and the average size of the cloud particles would be very small. This would lead to less intense local fallout patterns and a large amount of the radioactive material would be swept to high altitudes and widely dispersed. This case may be nearly the same as occurs with a burst over sea water where the cloud material consists of weapon debris, salt and water. The particles are extremely small but highly hygroscopic.

[redacted]

[redacted]

[redacted] Thus, their size buildup can be very sensitive to local meteorolcgical conditions. The fallout from water bursts is described in EM-1. A much less intense local fallout is expected unless rainout occurs.

[redacted] The salt swept into the atmosphere may have a seeding effect and result in a weapon induced rainout of local material. Because of the lower temperatures and the very high humidity in the arctic, these seeding effects may be enhanced. The moisture capacity of the atmosphere is much less and precipitation may be much more likely than in temperate climates. The particle growth in the cloud may also be affected by the atmospheric parameters. No work in this area was found in the literature.

[redacted] For low yield weapons, most of the moisture comes from air entrained by the developing cloud. In the arctic, the absolute humidity is very low because of the low temperatures so that the water available for producing the larger sized particles may be less. Thus, under these conditions there may be fewer large particles produced and a less intense local fallout.

[redacted] Models have been developed which describe the rising debris cloud and its dispersal by winds. The diffusion of the radioactive material and the influences of precipitation, converging and settling of the particles by gravitation and diffusion are considered. The meteorologic parameters including precipitation, wind patterns, and humidity have a strong effect on the late time fallout.

[redacted] Much of the Arctic region is quite arid. Annual precipitation over the Polar basin, i.e., the Arctic Sea, is less than six inches of water equivalent per year. Most of the precipitation

[redacted]

falls as snow. There are local areas such as north of Hudson Bay and eastern Canada with moderately high snowfall (50-100 in.). Lowest snowfall is in the northern Canadian islands and in north Greenland, where total annual precipitation is frequently less than four inches of water.

Contrary to some popular opinion, surface winds in the Arctic are on the average very light. Observations from Soviet drifting stations in the central Polar Ocean indicate that monthly mean speed at the surface is about 8-10 knots. However, in well developed storms wind observations show speeds on the order of 50 knots. The mean wind speed increases rapidly with altitude and just below the tropopause (7-8km) the highest monthly mean wind speed may reach 40-50 knots. Maximum wind speeds may be much higher. Wind variability is larger in the Arctic.

The fallout prediction models range in complexity from empirical fits to fallout measurements made on the U.S. nuclear test series to very sophisticated numerical models which attempt to describe the development and dispersal of the cloud from first principles. WSEG is an example of the first type of code which has seen wide usage in system codes because of its fast running time and realistic results. The yield of the burst and the wind speed description are the major input parameters. There is no provision for adjusting to other meteorological parameters.

NUCROM (Baum et al, 1974) is an example of a code with intermediate complexity. It is a simplified rainout model which allows some freedom in introducing meteorological parameters. A stabilized debris cloud model is used which is then separated into segments as a function of altitude. Diffusion and migration under the influence of wind are considered and scavenging by precipitation events is allowed. The scavenging efficiencies are handled in a gross manner and detailed particle distributions are not considered.

[redacted]

[redacted] DELFIC (Maloney and Klemm, 1975) is an example of a code which attempts to calculate nuclear fallout from basic physical principles without recourse to empirical modeling of the test results. Detailed calculations are made of the debris cloud rise and loading by particulate matter. Particle size distributions and their evolution with time are computed. A detailed atmospheric definition is used. The distribution of activity with particle size is considered. Precipitation clouds are defined and detailed descriptions of the in-cloud and below-cloud scavenging as a function of debris particle size are given. This code is a long running, expensive code to use but is capable of including the full range of Arctic meteorological parameters.

[redacted] Representative calculations were made (Normant, 1974) of the scavenging by rain and snow clouds for tactical nuclear conditions in Germany. In these cases the burst altitude is high enough to minimize the local strong fallout and the activity is contained in micron-sized particles which would disperse over a very wide area with a low intensity. Scavenging by precipitation can, however, under the right conditions produce a very intense local fallout field. The effect is most important for low yields because the stabilization altitude for large yields is higher than normal cloud altitudes.

[redacted] In Figure 5-8 the rain and snow washout coefficients are compared. The precipitation events were picked to fit European conditions with the rain precipitation rate being 20 mm/hr and the snow being 10 mm/hr. For the larger particle sizes the rain coefficient is seen to be almost an order of magnitude larger than the snow but may be comparable in the micron region.

[redacted]

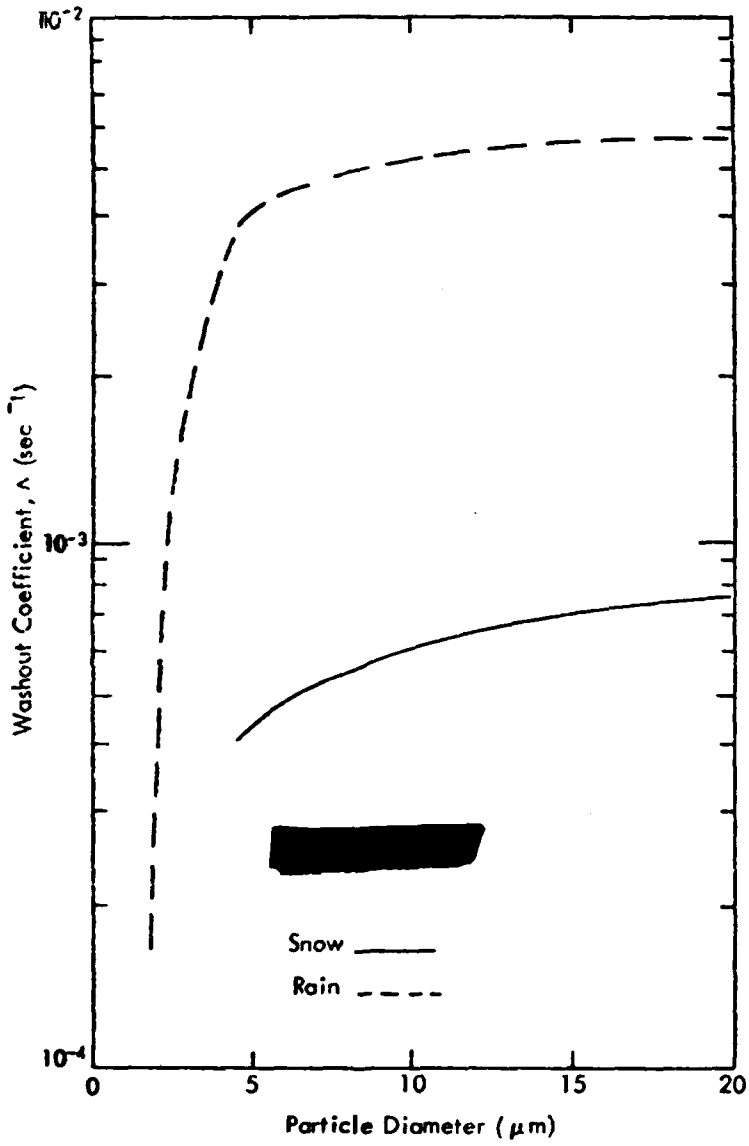

FIGURE 5-8 COMPARISON OF RAIN AND SNOW WASHOUT COEFFICIENTS

[redacted]

[redacted] In Figure 5-9 the fraction of particles scavenged is noted for interactions of 10 minutes and 1 hour with rain and snow clouds. Note that for particle sizes above about .3 micron all of the particles are scavenged even in a 10 minute interaction with a rain cloud. The critical diameter is about .03 micron for snow, and a large proportion of the particles with sizes above this diameter are scavenged for a 10 minute interaction. Normant's calculations of the snow scavenging efficiencies do not agree with other calculations and experiments as will be described in Figure 5-11.

[redacted] The main point of these results is that a fairly short interaction of the debris cloud with a precipitation event can result in essentially complete removal of activity from the cloud and deposition on the ground with the precipitation. Calculations made with typical Arctic precipitation rates would be of interest. Considerations of induced precipitation events and the interaction with the debris cloud would be of great interest and may represent the major difference expected in the Arctic.

[redacted] In the previous figures the submicron particle size is seen to be a region where the scavenging efficiency shows a large dependence upon particle size. This is due to the detailed physical interactions that are occurring and their relative importance. For very small particles Brownian diffusion is very important, and for large particles inertial accretion of particles dominates. The interactions are very complex for micron size particles, and electrical forces may play a major role.

[redacted] An extensive study of scavenging was performed at Illinois Institute of Technology Research Institute (Knutson, 1974) with theoretical and experimental studies of the relative rain and snow scavenging efficiencies being considered. Representative results are shown in Figure 5-10 where the snow

[redacted]

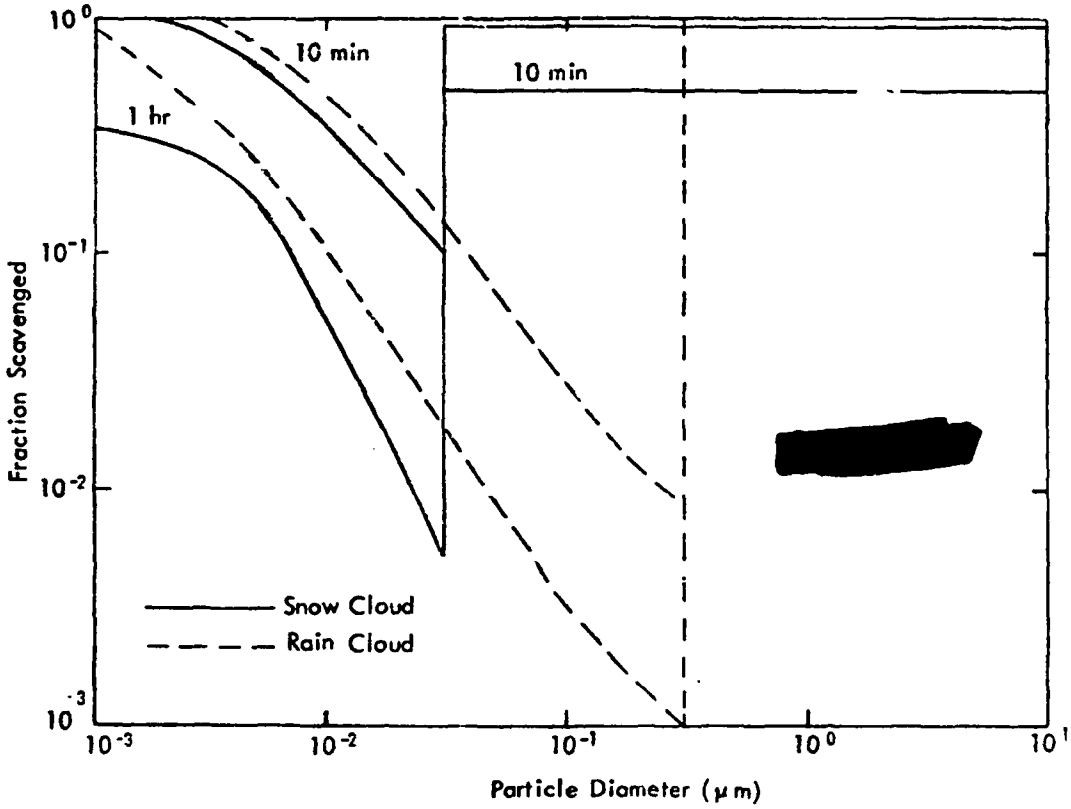

FIGURE 5-9 COMPARISON OF CLOUD SCAVENGING FRACTION

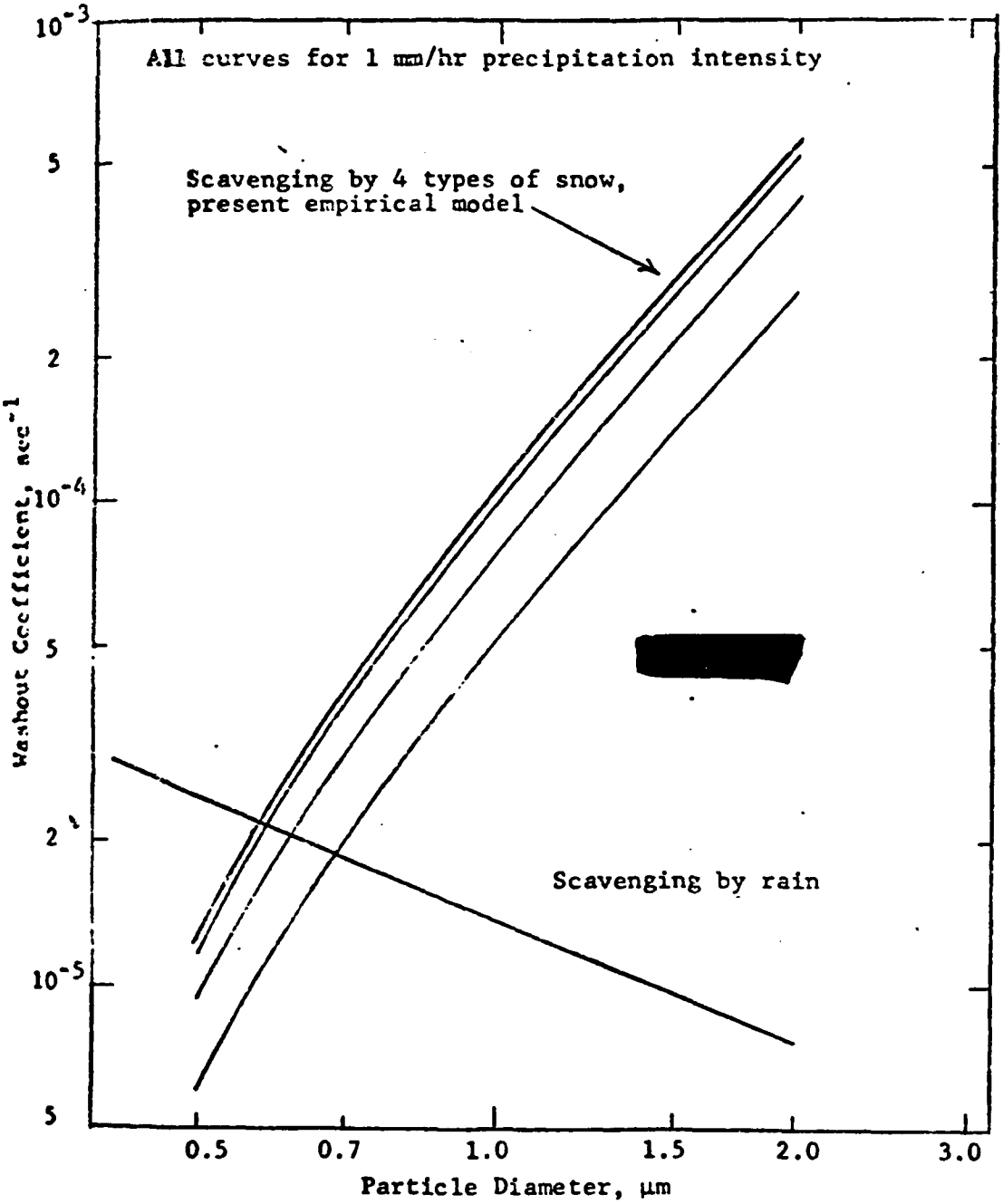

FIGURE 5-10. EMPIRICAL MODELS FOR PARTICLE SCAVENGING BY SNOW AND RAIN (KNUTSON, 1974).

[redacted]

[redacted] scavenging is predicted to be much larger than rain for particle sizes above .5 micron. This contradicts the results given in Figures 5-8 and 5-9 and represents the current uncertainties in these types of data.

[redacted] A recent extensive review (Pitter, 1976) considers snow and ice scavenging and the detailed physical interactions that occur. In Figure 5-11 results from various investigations are compared for ice crystal scavenging. Very wide variations are noted for the submicron to micron size range. The left hand portion of Figure 5-11 summarizes theoretical and laboratory results for the snow scavenging coefficient. The Pitter (labeled present results), Starr and Mason, and Sood and Jackson results all show general agreement with the minimum in the scavenging efficiency occuring at about .5 micron. The Knutson results are considerably larger at the .5 to 2 micron size range but are decreasing rapidly at .2 micron with no indication of an increase at smaller sizes. The DELFIC-PSM results equivalent to the results given in Figure 5-9 are also shown and are seen to be drastically different above .05. An abrupt increase in the efficiency at .05 micron is noted then no variation with increase in particle size. The differences in the results are due to different ways of handling the physical processes between the particles and the snow flakes. Also noted on the right hand portion of the figure are the results of various field measurements of aerosol scavenging coefficients.

[redacted] The main point emphasized by this figure is the current extreme variation in values of the scavenging efficiency for snow. The micron particle size is interesting for airbursts and surface bursts over water, snow and ice. This is precisely where a large uncertainty exists, and the differences noted would cause a large difference in the local fallout from a burst when natural or induced precipitation was occurring.

[redacted]

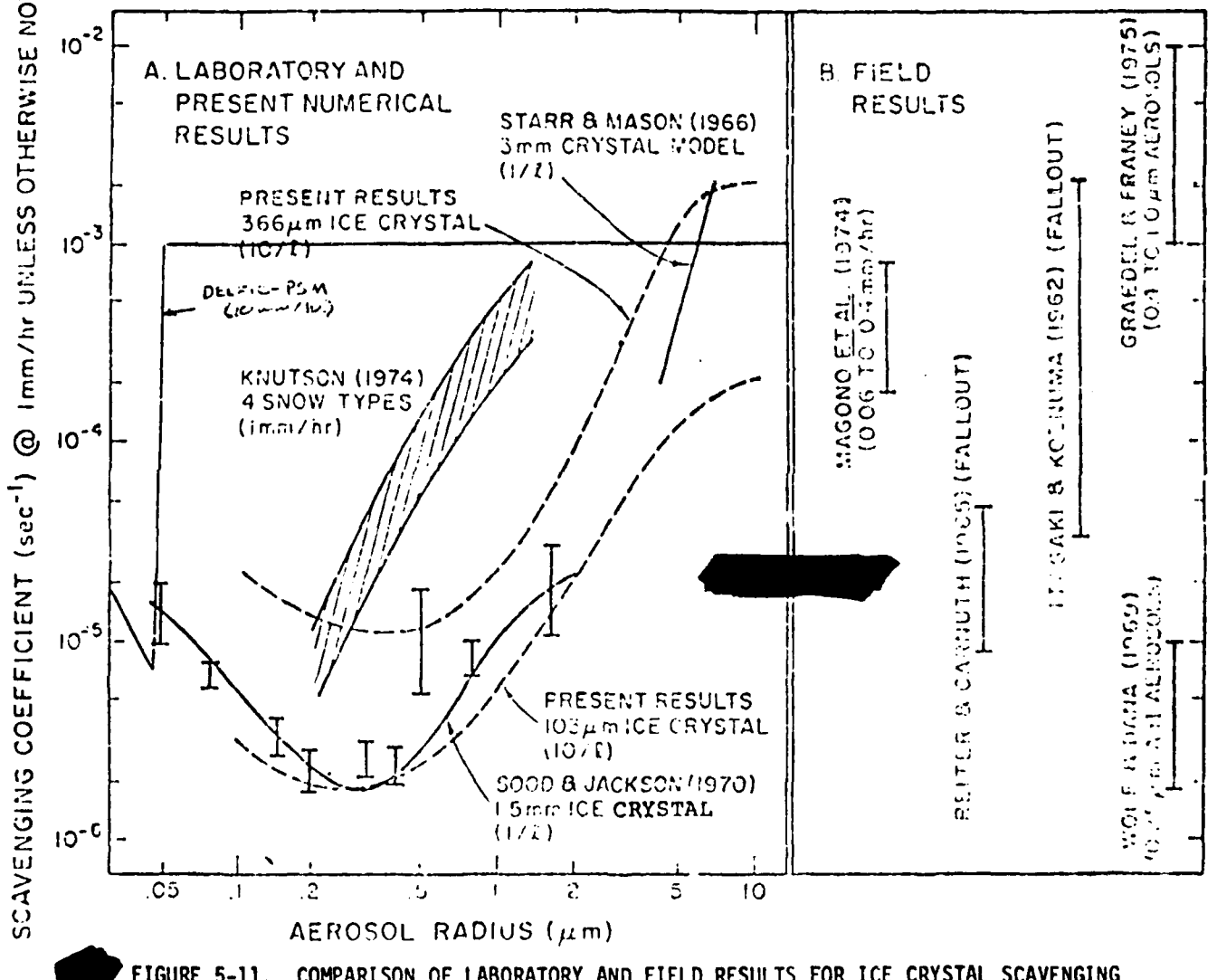

FIGURE 5-11. COMPARISON OF LABORATORY AND FIELD RESULTS FOR ICE CRYSTAL SCAVENGING COEFFICIENTS (Pitter, 1976).

[redacted]

5.3.3 [redacted] Underwater Bursts

5.3.3.1 [redacted] General

[redacted] The sources of radioactivity from an underwater nuclear explosion are (1) the fission product activity in the column and crown, or plumes, (2) the base surge, and (3) the residual radioactivity deposited in the ocean, or radioactive pool. These phenomena are described for a burst in temperate regions in Chapter 5 of DNA EM-1 and in Chapters 7, 9, and 10 of the Underwater Handbook, and methods for predicting the magnitude and duration of the effects are presented. Existing manuals, however, do not address the modifications to these effects that might result from an underwater detonation in Arctic regions.

[redacted] The Arctic environment can affect the sources of radioactivity from underwater nuclear explosions in several ways:

[redacted] • Ice cover may modify the characteristics of the surface phenomena and attendant radiation fields. These phenomena are variable at best, depending as they do on the state of the bubble as it reaches the surface. Part of the energy remaining in the bubble is expended in breaking through solid ice or imparting upward motion to blocks of ice.

[redacted] • Depending upon the depth of burst, an underwater explosion that vents may form a radioactive column, plumes, or base surge. The cold Arctic temperatures will cause freezing of some of these products, producing a local fallout field on the ice and the formation of radioactive ice on the weather decks of ships close to the detonation.

[redacted] • The presence of ice and the typical Arctic water density profile may affect the formation and migration of the radioactive pool, which normally rises to the surface and diffuses fairly rapidly. Heavy ice cover may contain the pool

[redacted]

[redacted]

from a venting explosion to the area cleared by the explosion. In the case of a very deep, non-venting explosion, a solid ice cover may contain the pool below the ice so there is no above-surface evidence of its existence.

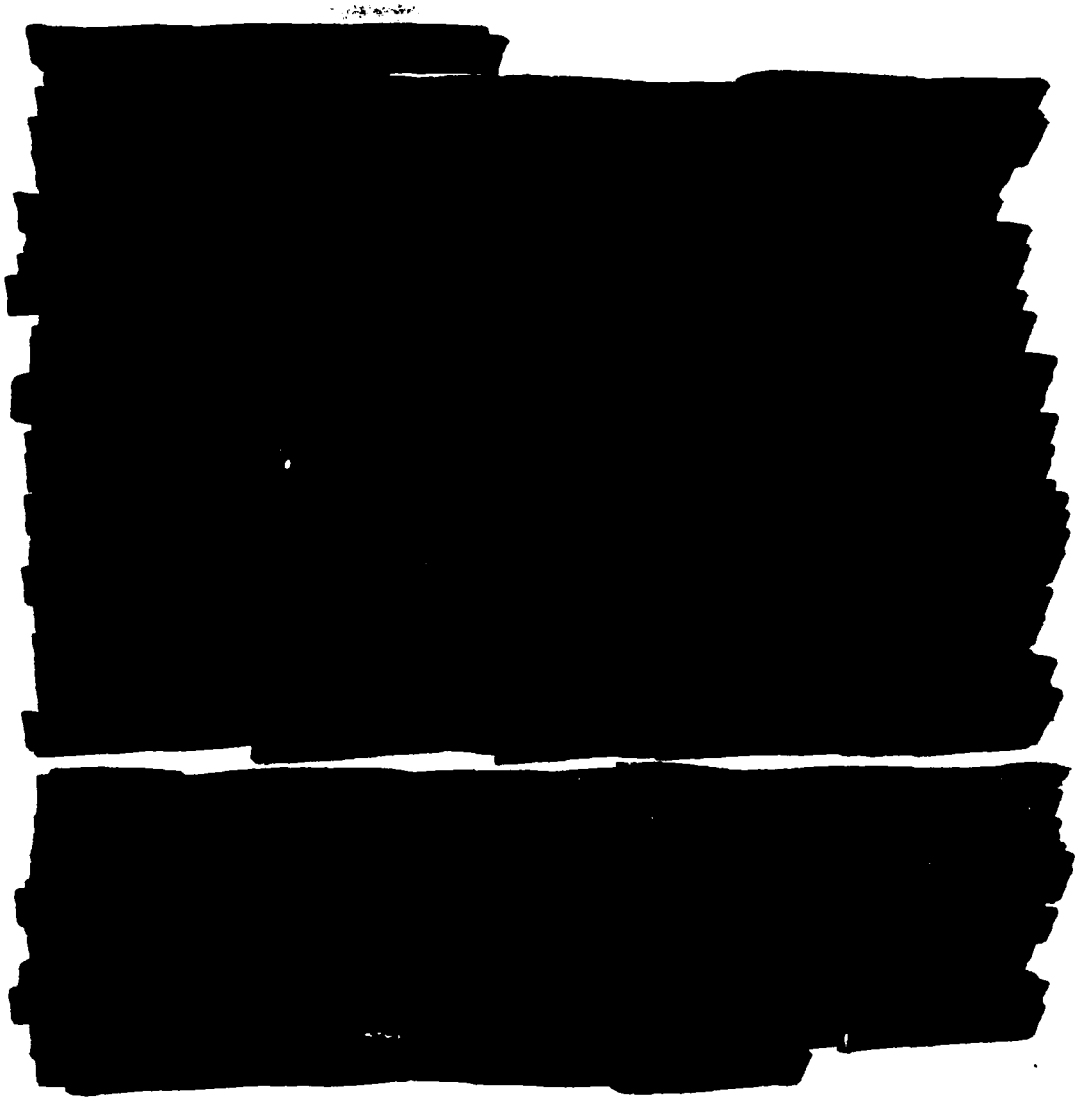

[redacted]

[redacted]

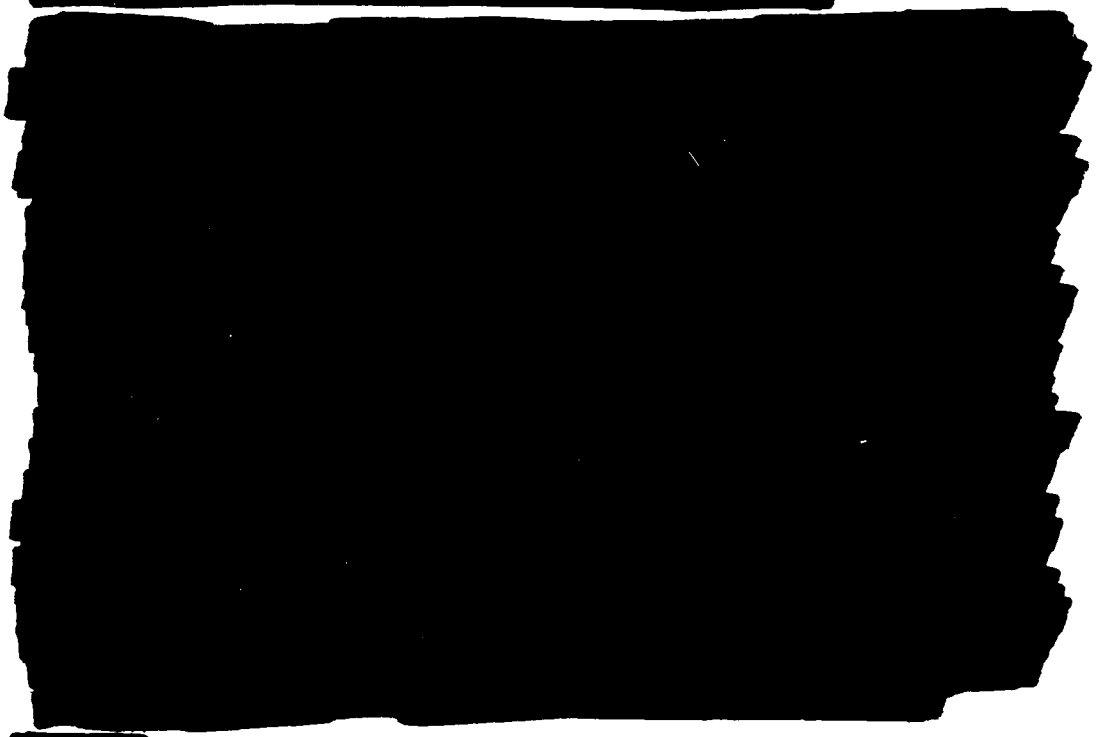

[redacted] Where the extent of the ice permits operations by surface ships, those operating in the vicinity of an underwater burst may encounter a buildup of radioactive material on the superstructure and weather decks due to the freezing of the base surge and spray from the radioactive pool. Shirasawa and Bjerke, 1968 studied this problem in some detail, using the same computer model (DAEDALUS) used to compute dose rates and total dose for the various conditions presented in the examples of Figures 5-46 through 5-75 of DNA EM-1. The report of Shirasawa and Bjerke is the source of the material in the remainder of this section, including the figures.

[redacted] The factors considered in the study include the transit radiation exposure due to radiation emitted directly from the base surge or the contaminated pool, and the deposit

[redacted]

[redacted]

radiation exposure due to emission from fission products after they have settled on ship surfaces. The transit exposure estimates were based on the DAEDALUS model output (exposure rate) with the assumption that the Arctic environment does not alter the radiation characteristics of the base surge and radioactive pool. The deposit exposure estimates were based on the rate and extent of shipboard icing and the concentration of fission products. A number of previous studies were consulted to determine the rate of formation and distribution of ice and its associated fission products from the base surge and pool. A typical destroyer was selected as the representative ship for the calculations, a nominal 10 kt ASW weapon was chosen, four explosion depths were selected (65, 150, 500, 1000 ft in 5000 ft of water), three post-detonation entry times (10, 20, 30 min), and three ship transit speeds (10, 20, 30 kt).

[redacted] The rate of ice increase is a function of temperature and wind speed. Figure 5-12 is a semi-quantitative presentation of the relation of these parameters. The various regions surrounding the conditions for icing shown in Figure 5-1 indicate the following:

Region I	Wind force is not sufficient to blow spray over ship.
Region II	Temperature is not low enough to cause spray to freeze on surfaces.
Region III	Wind force is so high that green water covers decks and keeps melting ice (ice is possible on higher superstructure).
Region IV	Temperature is so low that spray freezes before striking ship.

[redacted] The central area of the diagram where a "heavy" icing rate is indicated corresponds to 2 tons per hour or greater. The "light" area denotes rates of 1 ton per hour or less. In

[redacted]

1

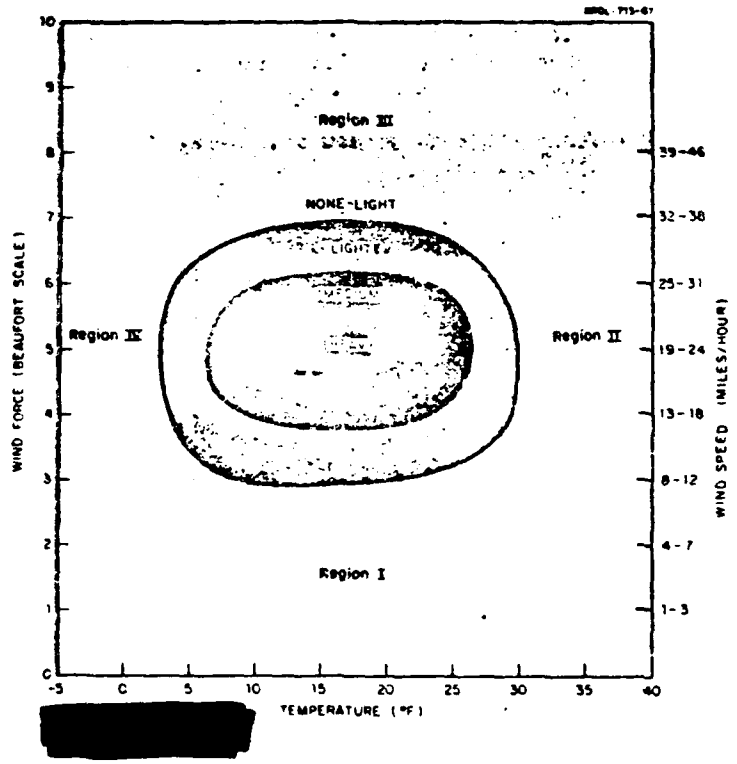

Figure 5-12. Icing Rate as Related to Wind Force and Temperature

(Shirasawa and Bjerke, 1968)

[redacted]

this presentation, the situation described for Region I is the least clear. However, in the studies cited no icing was observed when the wind force was less than Beaufort Force 3 in spite of the low temperatures.

[redacted] Serious icing occurs where temperatures below 29°F (-1.5°C) are combined with flying spray, which forms only with winds of 17 kt or more (U.S. Navy Hydrographic Office Pub. No. 705). The areas within which these conditions occur are more restricted in latitude than is generally realized, owing to the modifying influence of water temperatures on surface air temperatures; however, a significant proportion of ocean operating areas may be subject to serious icing conditions. Figure 5-13 shows areas of probable superstructure icing for January-March, May, and November, based on a southern limit of 10% frequency of temperatures below 32°F (0°C).

[redacted] Shirasawa and Bjerke present the results of the computer calculations for a number of combinations of parameters, but in view of the conclusions of the study these will not be given in detail here. To provide for maximum ionizing radiation exposure, they assumed an early (10 min) entry time into the base surge followed by a traversal of the pool, under a no-wind no-drift condition and with concentric base surge and pool still undergoing dynamic expansion during the traversal. Figures 5-14 and 5-15 summarize the calculations and present a comparison between the deposited and transit contributions to the total exposure, for a 65 ft and a 500 ft depth of burst respectively. It is immediately apparent from the figures that the activity entrapped by ice accretions, regardless of source, is not a major contributor to the total radiological hazard. In each case, the exposure contribution made by base-surge deposit is only 8% or less, while the pool spray deposit is negligible.

[redacted]

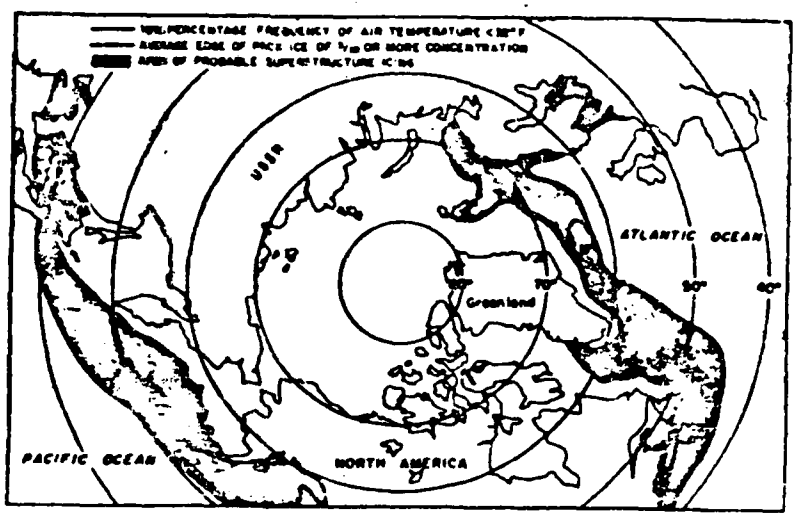

January-March

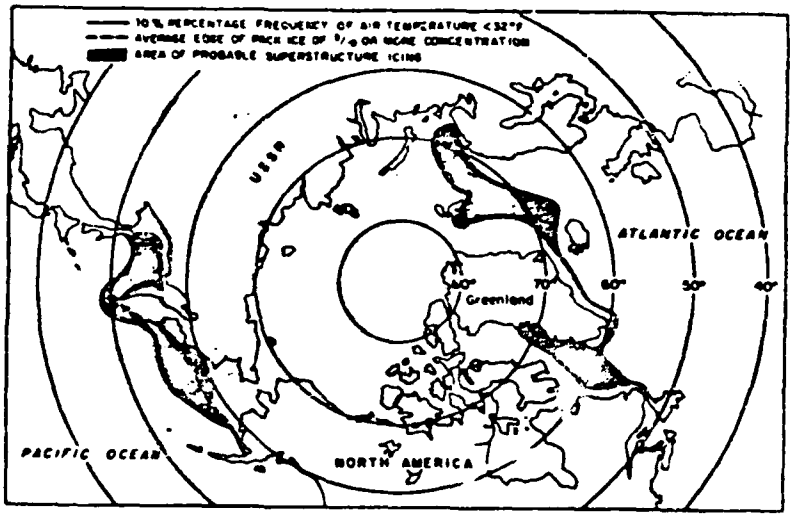

May

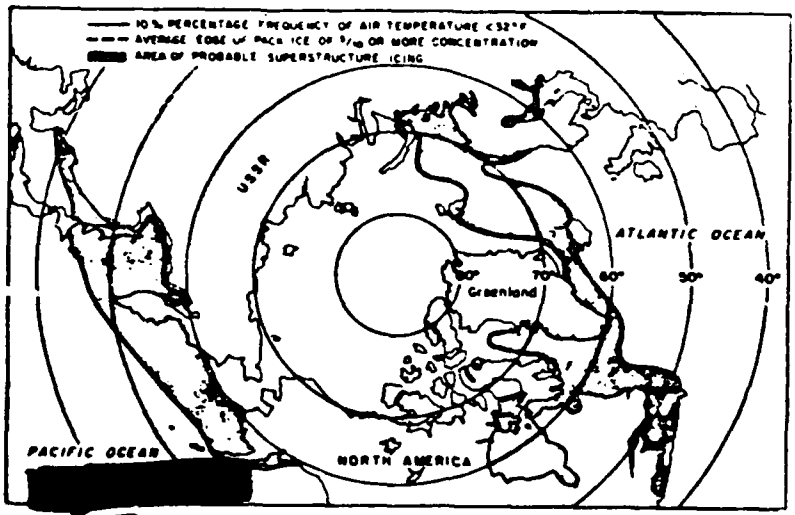

November

Figure 5-13. Areas of Probable Superstructure Icing (Shirasawa and Bjerke, 1968)

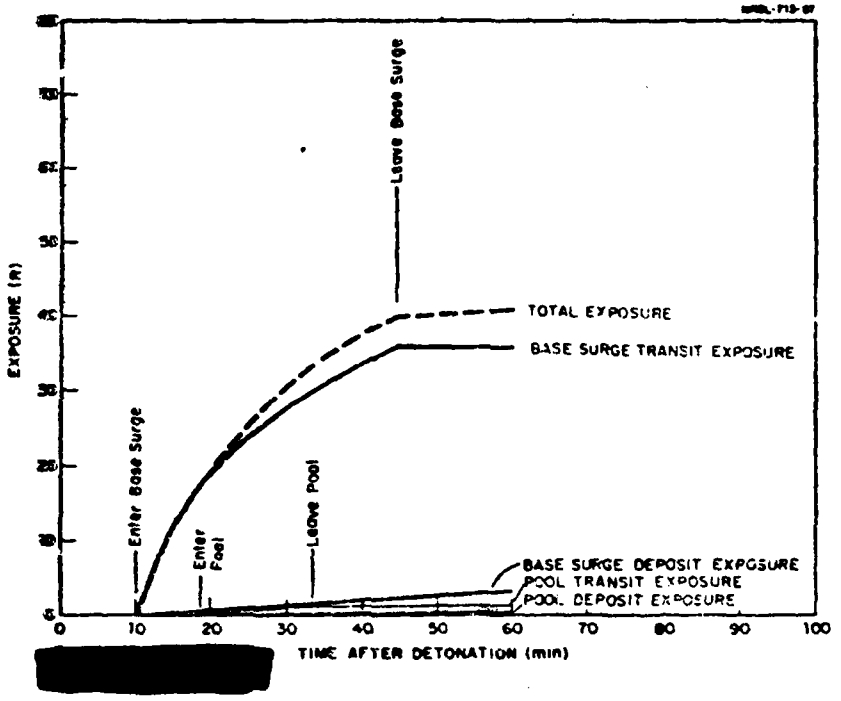

Figure 5-14. Total Exposure From Transit and Deposit Radiation for 65 ft Depth of Burst and 10 min Post-Detonation Entry (10 knot ship speed)

(Shirasawa and Bjerke, 1968)

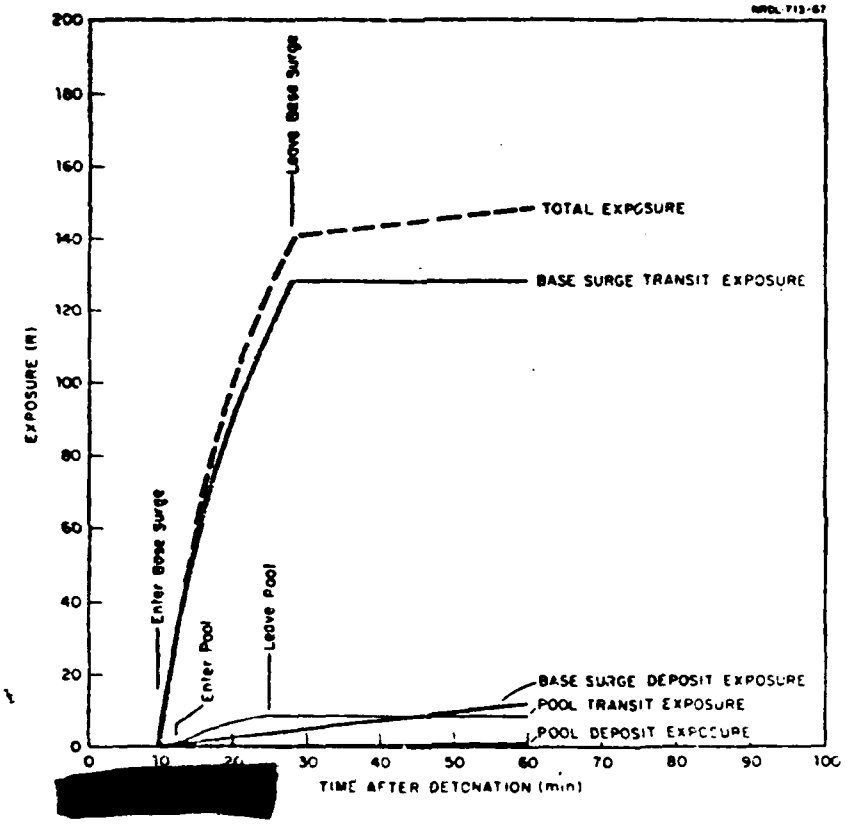

Figure 5-15. Total Exposure From Transit and Deposit Radiation for 500 ft Depth of Burst and 10 min Post-Detonation Entry (10 knot ship speed)

(Shirasawa and Bjerke, 1968)

[redacted]

[redacted] The discussion and conclusions of the Shirasawa and Bjerke report are quoted:

[redacted] "In our preceding consideration of contamination by ice-entrapped fission products, the possibility of countermeasures has been wholly ignored. This was purposely done to permit a maximum hazard evaluation. However, it is obvious that several immediate possibilities exist for reducing degradation of personnel and ship capability following contamination of weather surfaces. Three immediate countermeasures which might be considered are:

1. Reduction of number of personnel in high exposure areas and rotation of personnel.
2. Use of ship washdown system.
3. Initiation of ice removal procedures.

The importance of countermeasures is borne out by consideration of the exposure rates existing on shipboard after traversal maneuvers, because of continued exposure from deposited activity, however small. Implementation of countermeasures will also prevent or minimize contamination ingress as well.

[redacted] "Operation of the washdown system aboard a destroyer was shown to be feasible in freezing weather.* Initiation of this countermeasure upon leaving the radioactive pool would contribute to a significant reduction in the ice deposited by pool spray and/or base surge contact. Though icing may continue during the use of the washdown system, the relatively warmer water from the sea would serve to melt and rinse away the contaminated ice accumulated during the pool and/or base surge traversal. It was estimated * that use of the system for 80 minutes or more under conditions of an air temperature of 10°F and a wind velocity of 21 knots would produce a maximum of 1-inch of ice. This of course would be "clean" ice. It has been estimated that 6 inches of ice, or an ice accumulation of 200 tons, on horizontal and vertical surfaces would interfere with the operation of a destroyer in an 80-knot beam wind.

[redacted] "Removal of slush ice after washdown cessation can, if ship mission and stability permits, be accomplished quite successfully by personnel with shovels, brooms, boards and buckets. These procedures would effect the most direct and efficient removal of

---

* Editor's Note: The reference is to a report by Perkins, W. W. and Railey, R. M., Operation of Shipboard Washdown in Freezing Weather, U.S. Naval Radiological Defense Laboratory USNRDL-TR-972, 31 December 1965, Unclassified

[redacted]

contaminated ice. However, these procedures may create the attendant problem of personnel exposure and the potential hazard of tracking activity inside the ship with subsequent danger of ingestion.

"The following conclusions would appear to be justified within the general limits of this study.

1. The radiological consequences to naval ships of coming in contact with the post-detonation formations typical of underwater nuclear explosions are not significantly changed by an arctic environment.
2. Radiation exposure resulting from freezing spray of radioactive-pool derivation does not present itself as a problem insofar as interference with the tactical missions of ships is concerned.
3. Radiation exposure from the freezing spray of base surge aerosol exceeds that of pool spray deposit, but it is well below levels which would threaten degradation of ship's effort.
4. Initiation of ship washdown operation and/or manual removal of slush ice can reduce the amounts of deposited fission products to levels comparable to those existing in more moderate environments.
5. The limiting radiation hazard for involvement in post-detonation ship maneuvers will be the transit exposure as a result of encountering the base surge and the pool. There is no reason to believe that this exposure will be significantly changed by an arctic environment."

It may be concluded, on the basis of the foregoing, that the estimates of Figures 5-46 through 5-75 of DNA EM-1, prepared for use in temperate climates, may also be used for Arctic environments.

5.3.3.4 [redacted]Radioactive Pool

[redacted] Chapter 10 of the Underwater Handbook contains a detailed technical review of the literature as of December 1966 on the distribution of the radioactive debris and associated

[redacted]

nuclear radiation from underwater nuclear explosions. It was concluded at that time that no adequate comprehensive radiological prediction system existed in the literature. With respect to the radioactive pool, a review of the literature since that time reveals little reason to alter that conclusion significantly. Rinnert, 1967 and 1968 has developed FORTRAN IV computer programs to estimate the exposure rate history and total exposure for surface and subsurface traversals of a radioactive pool, but these are based on the pool model of Ksanda, 1963 and the work of Pritchett, 1966, both of which were available when Chapter 10 was written and were referenced.

[redacted] The Rinnert reports are concerned mostly with the documentation of the programs and do not present results of calculations for ranges of input parameters. They each have an example, however, of information that can be derived from the programs. These examples are presented here, since neither DNA EM-1 nor the Underwater Handbook contains estimates of exposure for a submarine traversal of a radioactive pool. Figure 5-16 shows the calculated exposure rate history for a single set of parameters, and Table 5-1 shows the total exposure for traverses as calculated by the modified Ksanda model (Rinnert, 1967) and by the modified Pritchett model (Rinnert, 1968), for several sets of parameters. Both examples are for unshielded detectors. The submarine's hull and internal piping systems would reduce these exposures by varying amounts, which may be calculated from standard references (e.g., DASA 1892).

[redacted]

[redacted]

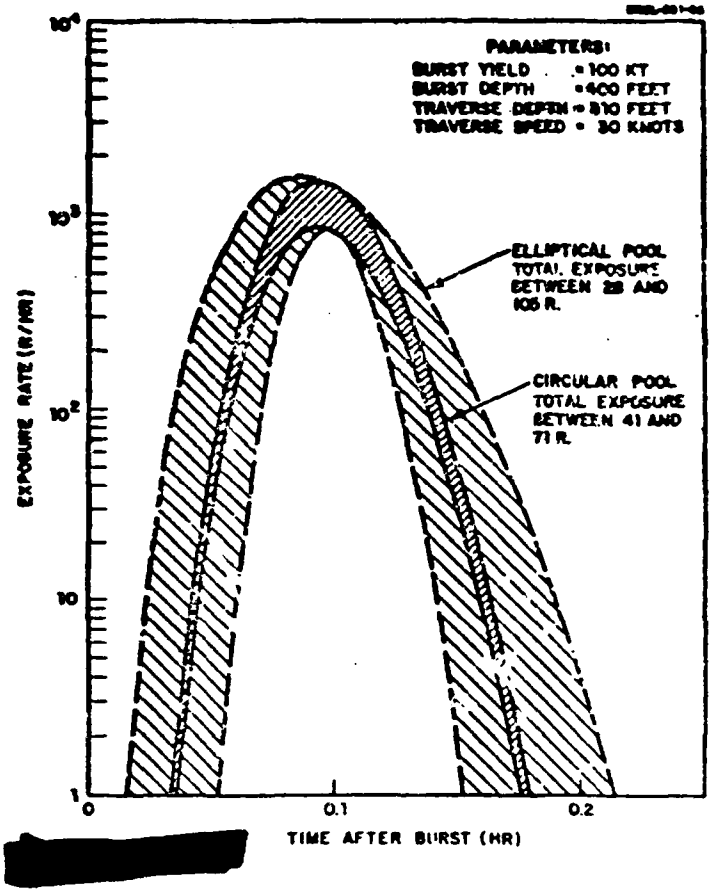

Figure 5-16. Examples of Exposure Rate History of Unshielded Detector Traversing Radioactive Pool

Bands indicate range of estimates for circular pool and for elliptical pool whose minor axis is half the major axis.

[redacted]

TABLE 5-1. TOTAL EXPOSURE FOR SUBMARINE TRAVERSE OF A RADIOACTIVE POOL

(Rinnert, 1968)

Speed of Traverse (Knots)	Total Exposure for Traverse (Rcentgens)		Parameters*
	Modified Pritchett Model	Modified Ksanda Model	
5	4.19	5.09 - 7.30	W = 1
10	5.30	6.29 - 9.03	DOB = 300
15	6.22	7.13 - 10.2	SO = 4000
20	6.89	7.79 - 11.2	ZD = 50
30	8.28	8.82 - 12.7	
40	9.27	9.64 - 13.8	
5	0.48	0.89 - 1.26	W = 1
10	0.52	1.10 - 1.55	DOB = 300
15	0.59	1.20 - 1.70	SO = 4000
20	0.677	1.27 - 1.79	ZD = 300
30	0.12	1.37 - 1.92	
40	1.7×10^{-27}	1.43 - 2.01	
5	14.4	15.7 - 22.9	W = 100
10	17.7	19.3 - 28.3	DOB = 949
15	20.3	21.9 - 32.0	SO = 10,000
20	22.2	23.9 - 34.9	ZD = 50
30	26.2	27.0 - 39.5	
40	30.8	29.5 - 43.1	
5	1.68	2.81 - 4.07	W = 100
10	1.89	3.58 - 5.19	DOB = 949
15	1.97	3.89 - 5.63	SO = 10,000
20	2.11	4.09 - 5.92	ZD = 300
30	2.58	4.35 - 6.30	
40	3.12	4.53 - 6.56	

[redacted]

W Yield, kilotons
DOB Depth of burst, feet
SO Stand-off distance, yards (traverse begins at stand-off distance at time of burst and proceeds across pool, passing through surface zero)
ZD Depth of traverse, feet

[redacted]

[redacted]

[redacted]

It should also be noted that the DAEDALUS calculations referred to in the previous section, presented by Shirasawa and Bjerke, 1968 and in Chapter 5 of DNA EM-1, provide predictions of the free field radiation 15 ft above the ocean surface, and therefore consider radiation coming from only a thin surface layer of the pool. There is little experimental evidence to confirm model predictions of the rate of growth and migration of a radioactive pool, of the fraction of its radioactive content left at various depths as the bubble oscillates and migrates toward the surface, of subsequent history of deep pools left behind, or the conditions under which a substantial amount of radioactivity may never appear at the surface.

[redacted] In view of the uncertainties surrounding radioactive pool formation and behavior under non-Arctic conditions, and the total lack of experimental data of this nature under Arctic conditions, an assessment of the possible effects of the Arctic environment must be regarded as conjectural. Two characteristics of Arctic regions that might alter the behavior of the radioactive pool from what might be expected elsewhere are the presence of ice cover and the strong density gradient in the water column.

[redacted] An underwater explosion at a depth that vents will normally cause the development of a radioactive surface pool initially centered at surface zero. In the case of scattered or broken ice, which is usually only a few meters thick, it is expected that the pool would undergo its normal expansion and diffusion, and there would be little effect of the ice except to

[redacted]

[redacted]

provide a certain amount of shielding against that portion of the radioactivity that is below it. In the case of consolidated pack ice, with extensive pressure ridges and ice keels, the venting explosion will blast a hole in the ice and the radioactive pool will initially be centered in the ice-free water of the hole. Since a 10 m pressure ridge will be accompanied by about a 50 m ice keel, and in extreme cases ice keels may extend to 150 m (Bowditch, 1977, Chapter 36), the horizontal migration and diffusion of the pool may be impeded. If such should occur, the radioactivity in the exposed pool would be smaller in extent and more concentrated than might be expected from the DNA EM-1 examples in Chapter 5. However, since it appears that solid pack ice is necessary for this condition to arise, the effect would be apparent only to aerial observation, and of significance only to the determination of the location of an underwater burst sometime after the fact.

[redacted] As is discussed in Section 7, it is not known how much of the explosion energy is required to break through solid ice cover and vent However, for very small yields or very deep explosions, it may be that the bubble will have insufficient energy when it reaches the surface to fracture whatever thickness of ice is present. In this case a radioactive surface pool will not be formed and the pool will be trapped below the ice layer. This would prevent the detection of the explosion by aerial survey methods, although the radioactive pool would remain a hazard to submarine operations.

[redacted] In Section 1.2.7 it was noted that, in general, strong positive density gradients exist in the upper few hundred meters of the Arctic water column. This region (pycnocline) severely impedes the upward migration of heat and salt and effectively insulates the surface from the water masses below. This characteristic of the region leads to the speculation that much radioactive debris may often be trapped below the surface, whether or not an ice layer is present.

[redacted]

[redacted]

[redacted] Quoting from Chapter 10 of the Underwater Handbook:

> "For deep and very deep explosions, where the bubble experiences several oscillations as it migrates toward the surface, radioactivity may be ejected from the bubble at minima .... Measurements at Operation Wigwam ... indicate that there are both a radioactive surface pool and random lens-like pools of debris in the thermocline layer. These deep pools were measured some days after detonation and were found to be small and quite stable. Whether these deep deposits represent radioactivity that was left behind by the migrating bubble or material carried to the surface by hydrodynamic flow and returned to its original stability level, is not known."

[redacted] Except for the shallowest explosions that vent most of their fission products to the atmosphere with a water column or plumes, and then fall back to form a radioactive pool with surface waters, underwater nuclear detonations in the Arctic will cause a substantial amount of the highly saline, deeper water to mix with the radioactive material. It is conceivable that this water mass with its trapped fission products will sink to and remain in the pycnocline. In addition, any radioactive pools left at depth by the pulsating bubble would have their ascent stopped at the pycnocline. Thus the radioactive effects of the surface pool could be substantially less than those predicted by existing models. The pools would remain a submarine hazard, however.

[redacted]

Pages 5-47 and 5-48 were deleted

[redacted]

[redacted]

[redacted]

[redacted] On the basis of the work of Kaulum and Bennett, 1971, it may be concluded that there are combinations of yield and depth that give a high probability that the radioactive debris from an underwater nuclear explosion may be contained beneath the surface for periods of time long enough for the radioactivity to decay to undetectable levels. Figure 5-17, based on calculations for a wide range of density gradients, including typical Arctic gradients, provides a reasonable basis for estimating the conditions under which a radioactive surface pool would not be formed for yields of 100 kt or less, whether or not ice cover were present. Ice cover would prevent such formation for any detonation deep enough not to rupture the ice. The subsurface pools would, however, be a hazard to submarines.

5.4 [redacted] Radiation Damage Effectiveness

[redacted] There is no reason to expect any changes in the radiation damage vulnerability levels in Arctic conditions. The possible exception is some slight enhancement of effects on personnel. The severe winter Arctic environment imposes a heavy strain on personnel at best so that radiation effects might have a more deleterious reaction at lower levels.

[redacted] Bunkers or personnel shelters buried under snow or ice would provide slightly better protection than concrete on an overburden weight basis. Information on the protection factors is widely available such as given in EM-1.

[redacted]

[redacted]

5.5 [redacted] Conclusions and Recommendations

5.5.1 [redacted] Conclusions

[redacted] No studies considering the effect of arctic environment on prompt radiation environments were found except the Ft. Bliss study (OSWD, 1960). However, the techniques that have been developed to compute radiation environments in temperate environments can be used with no basic changes except using the proper model atmosphere. The density is the only important parameter of interest.

[redacted] Scaling the available infinite air transport results to the arctic winter ground level density indicates that the environment levels corresponding to typical damage criteria for hardened electronics occur at about a 15% smaller radius under arctic conditions than under temperate conditions. At a particular range the fluence or dose level can be 1/2 to 1/3 as large for arctic winter conditions as in temperate conditions. Thus, prompt radiation effects tend to be depressed in the arctic which is an advantage for considering damage to U.S. installations from Soviet bursts. However, the reduction in prompt radiation effects should be considered when considering the effectiveness of U.S. bursts against Soviet systems.

[redacted] The presence of the surface layer under the atmosphere tends to reduce the radiation environment in the air as compared with the free air values. No calculations of this effect have been made for arctic surfaces and conditions. Inspection of the available calculations indicates that there is essentially no difference in the neutron dose as measured close to the surface for wet or dry ground or sea water. The dose from the secondary gamma rays for wet ground is about 20% lower and for sea water is about 30% lower than for dry ground. The dose over fresh water or ice might be somewhat lower still. Since most of the

[redacted]

[redacted]

[redacted] Arctic is covered by wet tundra, fresh water ice or sea and sea ice, one would expect a small reduction in the dose resulting from neutrons from this effect.

[redacted] The dose from the early time fission products can be important in contributing to the total dose received by reentry vehicles, airplanes and ground installations as well as an important contributor to personnel casualties. In addition to the reduction due to the increased density there would be some effect due to the smaller fireball. No calculations of this effect have been made. Scaling estimates indicate that a reduction of about 15% in the range corresponding to a tissue dose of 500 rad can be expected in arctic conditions. This is about the same uncertainty that exists in current modeling of this radiation component.

[redacted] Differences in the fallout in arctic conditions could arise in several ways: differences in the induced activity, differences in the size of the particles the active particles are attached to, differences in the debris cloud development and dispersal due to the meteorological conditions, and for underwater bursts differences in the radioactive material ejection into the air due to the ice cover.

[redacted] The induced activity in bursts over arctic soils will probably be essentially the same as in temperate climates since there is in general the same range of soil types there. For bursts over sea water or sea ice the induced activity is much less than over ground and for bursts over fresh water, snow, or ice the induced activity is zero. Thus, in many situations in the arctic the residual radiation source is due only to the fission yield of the weapon and no induced activity from the thermonuclear component will exist.

[redacted]

[redacted]

[redacted] For bursts over arctic soil the particle sizes which result in the rising debris cloud would not be expected to be different than existing in more temperate climates since the basic soil types are comparable. For bursts on snow, ice or sea water, however, one would expect considerably different debris cloud characteristics. One probably would not expect the arctic case to be much different from a sea burst in temperate areas.

[redacted] Debris cloud development and dispersal has not been considered for arctic conditions. One might expect somewhat different development because of the different density and temperature profiles. Winds are not significantly different in the Arctic except perhaps being more variable; so no significant differences in fallout predictions would be expected except an increase in the uncertainties of such already uncertain predictions.

[redacted] Relative scavenging efficiencies of snow and water have been measured and analyzed with conflicting results. Some studies indicate a much larger scavenging efficiency for snow than water while other studies indicate no difference. The Arctic has a much lower precipitation rate than most temperate areas so that one might expect less of the activity to be scavenged and might expect therefore a more wide ranging and less intense fallout pattern that might occur in temporate areas if precipitation occurs. No studies have been made of induced precipitation by nuclear bursts in the Arctic.

[redacted] The major uncertainties in predicting the effects of nuclear radiation from an underwater burst result from a lack of knowledge of the amount of explosive energy that is required to break through an ice layer and that is therefore lost as far as the development of surface and above-surface phenomena are

[redacted]

[redacted]

[redacted]

concerned. This in turn leads to uncertainty concerning the amount of radioactive material ejected to the atmosphere, the extent of its initial dispersion, and, in the cases of very small yields or great depths of burst, whether the ice will contain the effects of the detonation so that there will be no atmospheric phenomena. It is considered that available studies, though unverified experimentally, are adequate to the understanding of the effects of radioactive products freezing on exposed surfaces and the probable effects of the arctic environment on evolution of the radioactive pool.

[redacted] Studies have been made of the accumulation of activity on ships in icing conditions. This does not seem to be a very important mechanism of damage.

5.5.2 [redacted] Recommendations

[redacted] The effects noted in the prompt radiation environments were not very large but could be of significance for specific systems. It is recommended that currently available air transport results be scaled to provide isofluence and isodose profiles for neutrons, gamma rays and x-rays from selected weapon classes as a function of burst altitude. This could be done for the standard arctic conditions as well as for other extreme conditions which can exist as indicated in Section 1.2.

[redacted] These predictions should be incorporated into the appropriate chapters of EM-1 and perhaps could be a part of a more general section relating to the effects of atmospheric departures from standard on radiation transport.

[redacted] The effects on the early fission product dose should be determined for a few selected cases including possible fireball and cloud development changes. These calculations should be used to indicate scaling procedures so that inexpensive predictions can be prepared for a range of practical cases.

[redacted]

[redacted]

[redacted] Fallout prediction is at best very uncertain. The additional complications introduced by arctic conditions for which the U.S. will never have empirical data make the predictions even more untrustworthy. Since fallout is usually treated as a collateral damage mechanism in military situations, there may be no need to have accurate prediction techniques in the Arctic.

[redacted] Basic studies are required to specify the size distribution of the debris particles in the Arctic. Resolution of the discrepancies that exist in the analyses of the relative scavenging efficiencies of snow and water is necessary before predictions of the fallout under arctic conditions can be made.

[redacted] Computer models exist that could be used to compare the fallout from arctic and temperate climates. These models require as inputs such information as the debris cloud development, loading and particle size distributions, wind patterns as a function of altitude, precipitation patterns and rates, scavenging efficiencies, and particle diffusion characteristics. It is recommended that preliminary studies in these various areas be performed to identify the maximum differences that might exist in these parameters between the arctic and temperate climates. Predictions of the fallout using the minimum parameter differences should be made. If militarily significant differences occur between the arctic and temperate conditions, then additional research may be required in specific areas.

[redacted] Fallout predictions from underwater bursts are very uncertain. The ultimate destiny of the radioactive materials for various DOB is very uncertain and specifically the fraction that appears above the surface to contribute to fallout is unknown. It has been conjectured that the forces associated with the range of yields and depths of burst that are likely

[redacted]

[redacted]

[redacted] to be of interest for underwater bursts are so great that the energy loss in breaking through ice would have minimal effect on the development of surface and above-surface phenomena. Since the fallout is in general less than that expected over land, there may be some question about its importance except in very specific cases involving nearby surface ships. If hydrodynamic calculations are made of the bubble development and shock interactions with the water and ice layers, tracer particles should be introduced in an attempt to determine the distribution of the radioactive particles for various DOB conditions.

5.6 BIBLIOGRAPHY

Baum, Sanford, Wong, Paul W., and Dolan, Phillip J., NUCROM: A Model of Rainout from Nuclear Clouds, DNA 3389F, EGU 72-204, Stanford Research Institute, Menlo Park, California, 27 August 1974, UNCLASSIFIED.

Bowditch, Nathaniel, American Practical Navigator, Defense Mapping Agency Hydrographic Center, Pub. No. 9, 1977 Edition.

Campbell, J. E., and Sandmeier, H. A., Radiation Transport in Air Over Seawater for Application to Low-Altitude, Low-Yield Tactical Nuclear Detonations, NWEF Report 1102, Naval Weapons Evaluation Facility, Albuquerque, New Mexico, 10 April 1973, UNCLASSIFIED.

Caudle, K. F. and Farley, T. E., Nuclear Weapons Effects in Arctic ASW (U), NOLTR 68-86, Naval Ordnance Laboratory, White Oak, MD, 22 May 1968, CONFIDENTIAL, AD-391458L.

DASA, Department of Defense Land Fallout Prediction System, Multi-Volume Series, DASA-1800, now Defense Nuclear Agency, Washington D. C., various dates, Secret RD.

[redacted]

Defense Nuclear Agency, Capabilities of Nuclear Weapons, Part I - Phenomenology. Part II - Damage Criteria, (U), DNA EM-1 (Change 1), Dolan, P. J., Ed., Defense Nuclear Agency, Washington, DC, July 1976, Secret RD.

Defense Nuclear Agency, Handbook of Underwater Nuclear Explosions (U), Three Volumes, each consisting of Parts 1 and 2, DNA 1240H, Defense Nuclear Agency, Washington, DC, Secret RD.

Greede, T. E. and Franey, J. P., Field Measurements of Submicron Aerosol Washout by Snow, Geophysics Research Letters, 2, pp 325-328, 1975, UNCLASSIFIED.

Harris, P. J., et al, Models of Radiation in Air - The ATR Code, DNA 2803I, Science Applications, Inc., LaJolla, CA, May 1972, UNCLASSIFIED.

Huebsch, J. O. and Olken, F., An Analytical Model of the Formation of Multimaterial Particles in Nuclear Explosion Clouds, DNA 3988F, Euclid Research Group, Berkeley, CA, March 1976, CONFIDENTIAL, ADC 009993.

Itagoki, K. and Koenuma, S., Altitude Distribution of Fallout Contained in Rain and Snow, Journal of Geophysical Research, 68, pp. 3927-3933, 1962, UNCLASSIFIED.

Jordano, R. J., et al, Sensitivity of HF Blackout Predictions to Atmospheric Parameters (U), ARBRL-CR-00357, General Electric Company - TEMPO, 816 State Street, Santa Barbara, CA, January 1978, CONFIDENTIAL.

Kaman Sciences, Summary of Ballistic Missile Defense System Vulnerability, Lethality, and Threat Analysis (U), Annual Report, K-74-444(R), Kaman Sciences Corporation, Colo. Springs, CO, 4 December 1974, SECRET RD CNWDI.

Kaulum, Keith W., The Location of Clandestine Underwater Nuclear Explosions, Phase II, Radioactive Plume Detection (U), ESA-TR-70-04, Environmental Science Associates, Burlingame, CA, Octcber 1970, CONFIDENTIAL, AD-512526L.

Kaulum, K. W. and Bennett, C. B., The Location of Clandestine Underwater Nuclear Explosions, Phase I, The Contained Pool Search (U), ESA-TR-71-02, Environmental Science Associates, Burlingame, CA, August 1971, CONFILENTIAL, AD-516872L.

Knutson, E. O., Scavenging Study of Snow and Ice Crystals, IITRI Report No. C6105-28, IIT Research Institute, Chicago, Il, August 1974, UNCLASSIFIED.

Ksanda, C. F., Analysis and Prediction of the Properties of Diffusing Radioactive Pools from Nuclear Explosions in the Ocean (U), USNRDL-TR-725, U. S. Naval Radiological Defense Laboratory, San Francisco, CA, 19 December 1963, CONFIDENTIAL, AD-350547.

Magono, C., et al, A Measurement of Scavenging Effect of Falling Snow Crystals on the Aerosol Concentration, Journal of Meteorological Society of Japan, 52, pp. 407-416, 1974, UNCLASSIFIED.

Maloney, J. C. and Klemm, W. J., Department of Defense Land Fallout Prediction System - An Updated User-Oriented Documentation for DELFIC Mark V, BRL-1783, Ballistic Research Laboratories, Aberdeen Proving Ground, MD, May 1975, UNCLASSIFIED.

Mooney, L. G. and French P. L., Improved Models for Predicting Nuclear Weapon Initial Radiation Environments (U), RRA-T93, DASA 2615, Radiation Research Associates, Fort Worth, Texas, 31 December 1969, SECRET RD CNWDI.

Normant, H. G., A Precipitation Scavenging Model for Studies of Tactical Nuclear Operations, DNA 3661P, Mt. Auburn Research Associates, Inc., Newton, Mass, 18 June 1975, UNCLASSIFIED.

Office of Special Weapons Development, Nuclear Weapons Effects in an Arctic Environment, OSWD 59-2, United States Continental Army Command, Office of Special Weapons Development, Fort Bliss, TX, June 1960, UNCLASSIFIED, AD-344936.

Pitter, R. L., Snow and Ice Scavenging, UCRL 13759, Lawrence Livermore Laboratory, Livermore, CA, August 1977, UNCLASSIFIED.

Pritchett, J. W., Explosion Product Redistribution Mechanisms for Scaled Migrating Underwater Explosion Bubbles, USNRDL-TR-1044, U. S. Naval Radiological Defense Laboratory, San Francisco, CA 94135, 23 May 1966, Unclassified, AD-657 939.

Pritchett, John W., The Containment of Underwater Nuclear Explosions - Theoretical Calculations of Deep Burst Hydrodynamics (U), IRA-TR-1-71, Information Research Associates, Inc., Berkeley, California 94704, 15 February 1971, CONFIDENTIAL, AD-514 861.

Pugh, G. E. and Galiano, R. J., An Analytical Model of Close-In Deposition of Fallout for Use in Operational-Type Studies, Research Memo No. 10, Weapons System Evaluation Group, 1959, UNCLASSIFIED.

Recter, R. and Carnuth, W., Washout Balance Between 700 and 300 Above Sea Level, Proceedings of Conference on Cloud Physics, Tokyo and Sapporo, Japan, pp 390-394, 1965, UNCLASSIFIED.

Rinnert, H. R., Exposure Rate History and Total Exposure for a Surface or Subsurface Traversal of a Radioactive Pool, USNRDL-TR-67-51, U.S. Naval Radiological Defense Laboratory, San Francisco, California 94135, 12 May 1967, UNCLASSIFIED, AD-817 959L.

Rinnert, H. R., Maximum Exposure Rate and Total Exposure for an Early-Time Subsurface Traversal of a Radioactive Pool, USNRDL-TR-68-31, U.S. Naval Radiological Defense Laboratory, San Francisco, CA 94135, 12 February 1968, UNCLASSIFIED, AD-831 244L.

Shirasawa, T. H. and Bjerke, R. A., Nuclear ASW in Arctic Waters: Influence of the Environment on the Radiological Hazard During a Ship Maneuver Following an Underwater Nuclear Explosion, USNDPL-TR-68-46, U.S. Naval Radiological Defense Laboratory, San Francisco, California 94135, 12 March 1968, UNCLASSIFIED, AD-834 435L.

Sood, S. K. and Jackson, M. P., Scavenging by Snow and Ice Crystals, from "Precipitation Scavenging (1970)", 121-136, conf-700601 from NTIS, 1970, UNCLASSIFIED.

Spencer, L. V., Chilton, A. B., and Eisenhaur, C. M., Structure Shielding Against Fallout Gamma Rays From Nuclear Detonations, National Bureau of Standards, in press.

Starr, J. R. and Mason, B. J., The Capture of Airborne Particles by Water Drops and Simulated Snow Crystals, Quarterly Journal of the Royal Meteorological Society, 92, pp 490-499, 1966, UNCLASSIFIED.

U. S. Navy Hydrographic Office, Oceanographic Atlas of the North Atlantic Ocean; Part II - Arctic, H.O. Publication No. 705, U. S. Navy Hydrographic Office, Washington, DC, 1958 (Reprinted 1968), UNCLASSIFIED.

Wolf, M. A. and Dana, M. T., Experimental Studies in Precipitation Scavenging, BNWL-1051, Battelle-Northwest, 1969 UNCLASSIFIED.

THIS PAGE IS INTENTIONALLY LEFT BLANK

[redacted]

SECTION 6
COMMUNICATIONS AND EMP

[redacted] This study was nominally limited to low altitude bursts and effects, and no large effort was to be expended on high altitude effects. During the literature searches one study (Jordano, et al, 1976) was found which specifically addressed the latitude dependence on HF absorption and the effects of model atmosphere differences on debris cloud development. This report was reviewed and a summary of the results is included.

[redacted] Some changes are expected in the EMP on the surface due to the differences in the magnetic field intensities and direction. The variation in EMP SMILE diagrams for various latitudes and various longitudes in the polar region are given.

6.1 [redacted] Arctic Environmental Differences

[redacted] The different profiles for the atmospheric parameters (density, pressure and temperature) for the arctic region can effect the debris cloud development and stabilization altitude. The delayed gamma-ray source function may then be different, which can cause differences in the ionization levels and attenuation properties of the atmosphere for electromagnetic wave propagation. The reaction rate constant. that determine the sustained ionization levels are a function of the temperature and particle concentrations. The concentration of minor species can be important in determining deionization rates and may be altered at high latitudes due to the differences in energetic particle effects noted in this region at high altitudes.

[redacted]

[redacted]

[redacted] The greater intensity of the magnetic field in the polar areas will increase the magnitude of EMP in the region. The direction is more vertical than at lower latitudes which will affect the relative magnitudes of the horizontal and vertical components of the EMP and may affect the coupling of the EMP into targets.

[redacted] The coupling of energy into structures and cables buried under the ice and snow may be affected because of the differences between the conductivity, capacitivity and permeability of ice and snow and of more typical soil materials.

6.2 [redacted] Attenuation of HF Communication

[redacted] The changes in HF absorption from a near surface burst due to the different profiles of density, pressure and temperatures has been considered by Jordano et al (1978). The calculations were done by defining high latitude atmospheric models, incorporating the models in existing communication codes, and comparing the effect on HF communication links passing through the D region. The effect of the atmospheric differences on the debris dynamics was also considered. The influence of the atmospheric parameters on the deionization kinetics was considered, but the effect of differing concentrations of the minor species was not included.

[redacted]

[redacted]

[redacted]

[redacted]

for the July and January 60° N models are shown in Figure 6-1. The July and January extreme profiles were defined by adding to or subtracting from the 60°N profiles a component representing the diurnal variation plus a two-sigma random variation in such a manner as to increase the variation from the mean standard profile. The circles plotted for altitudes below 30 km represent the 75°N January temperature profile described in Section 1.2 and are seen to agree with the defined January extreme model. The WEPH VI/ROSCOE system defines the pressure and density profiles from the temperature profile using hydrostatic equilibrium and the perfect gas law. Above 80 km atomic oxygen is included to match measured mean molecular weights.

[redacted]

[redacted]

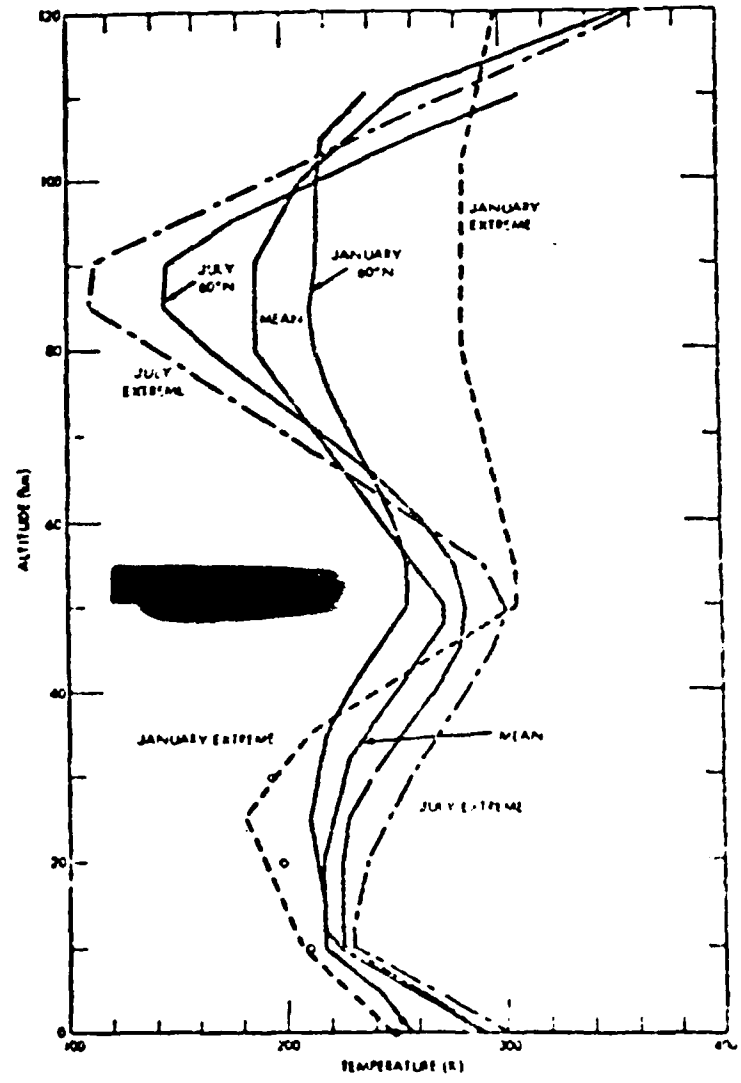

Figure 6-1 Temperature profiles for alternate atmospheres. (Jordano, et al. 1979)

[redacted]

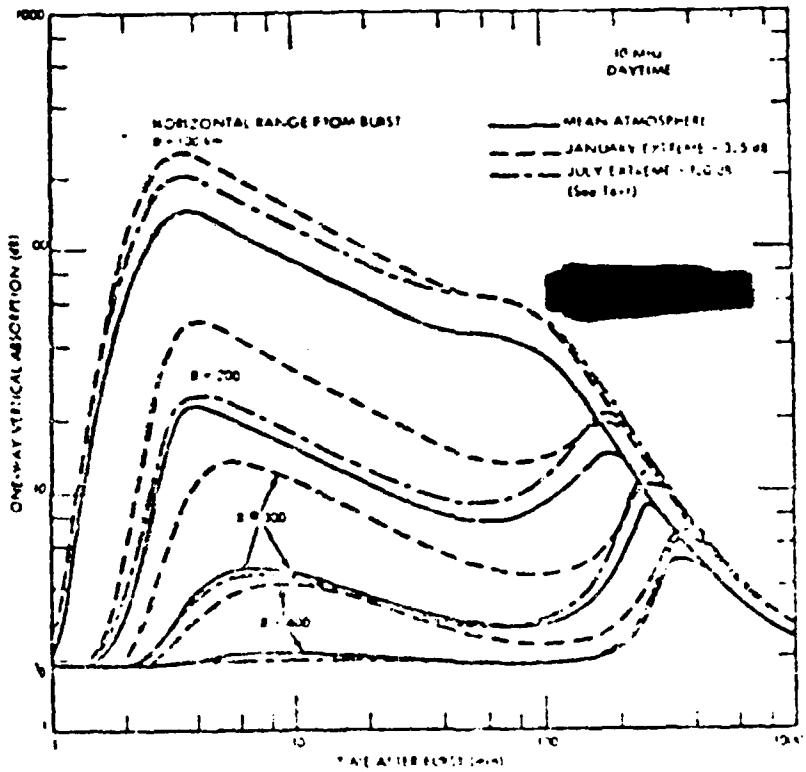

[redacted] Figure 6-2 Absorption caused by nuclear burst in alternate atmospheres in the daytime (fixed debris dynamics).

(Jordano, et al, 1978)

[redacted]

[redacted]

[redacted]

[redacted]

[redacted]

[redacted] The fireball model is discussed in detail by Jordano, et al, and the trends observed are explained by consideration of the starting conditions which determine the initial fireball volume and density, the mass entrainment and mixing phase with dominates the cooling phase until low temperatures are reached. The expansion against the ambient pressure which dominates the

[redacted] Page 6-7 was deleted

[redacted]

final temperature decrease and the ambient temperature in the stabilization region which determines the final temperature the fireball must reach for equilibrium and stabilization.

[redacted]

[redacted] Page 6-9 was deleted

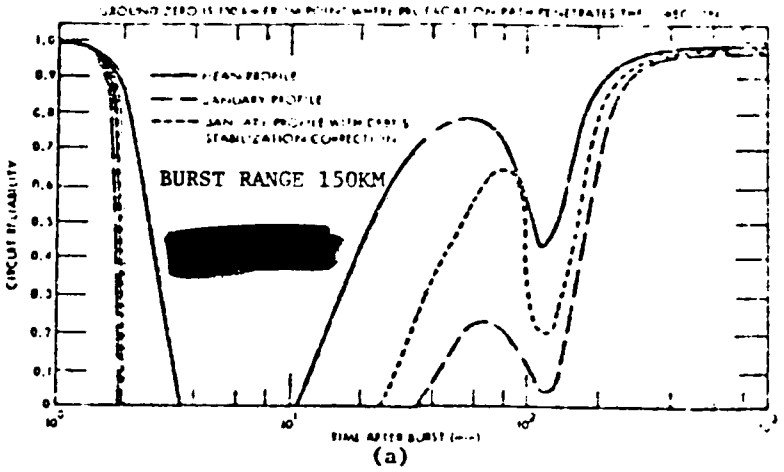

(a)

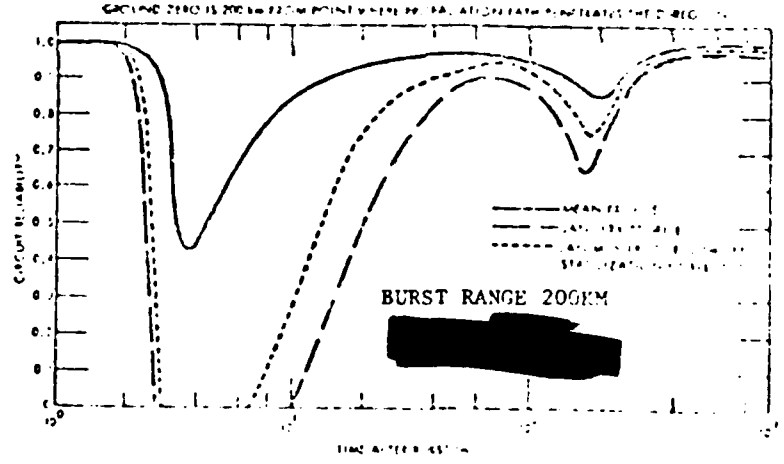

(b)

FIGURE 6-5. CIRCUIT RELIABILITY, OLNEY, MARYLAND TO MAYNARD, MASSACHUSETTS (Jordano, et al, 1978).

[redacted]

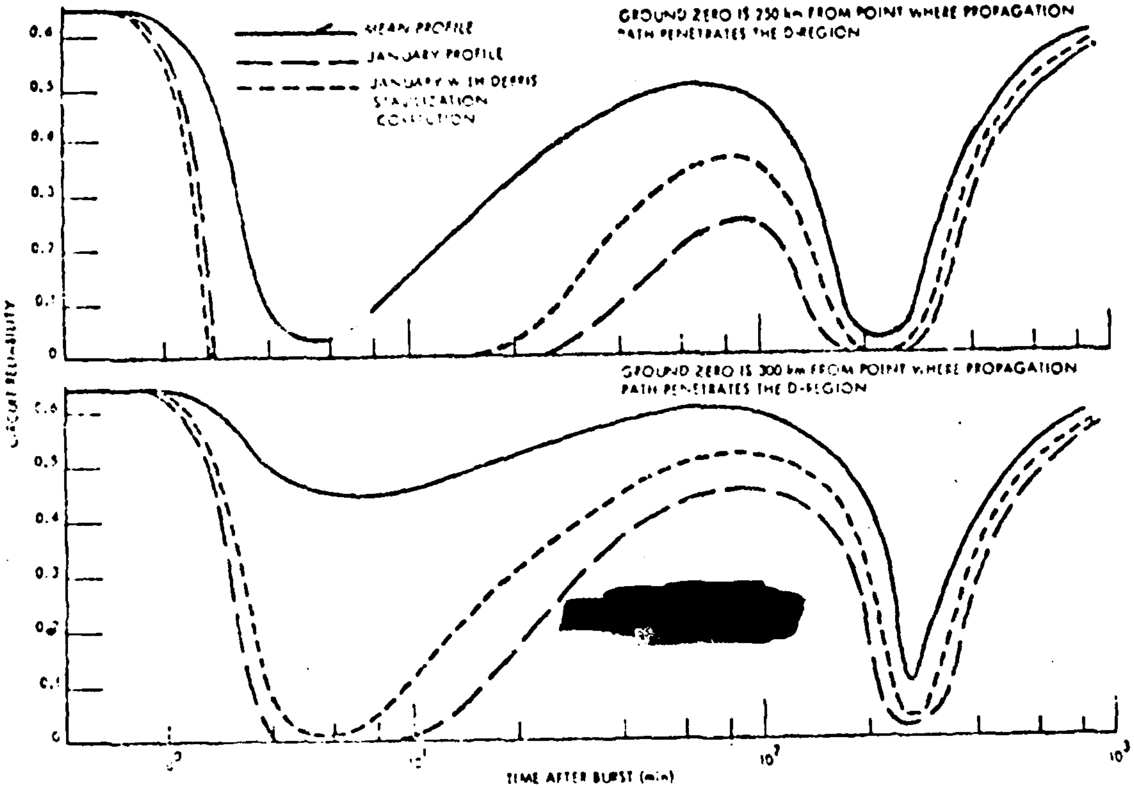

[redacted] FIGURE 6-6. CIRCUIT RELIABILITY, FORT HUACHUCA, ARIZONA TO WESTERN EUROPE; BURST RANGES = 250 km, 300 km (Jordano et al, 1978).

[redacted] Pages 6-12 through 6-19 were deleted

[redacted]

[redacted] It is recommended that additional studies be made on the debris dynamics for Arctic atmospheres. The results of these studies have implications in the determination of fallout under Arctic conditions as well as in the effect on communication blackout.

[redacted] The concentration of minor species in the high altitudes should be considered and their effect on the deionization kinetics should be determined. Prediction of the communication blackout expected by bursts in the Arctic including all of these effects should be made for a wide range of frequencies.

[redacted]

[redacted]

[redacted] The horizontal and vertical components of EMP should be determined for the polar region. Changes in coupling to surface based systems should be considered. Predictions should be made of the coupling of the EMP to cables and facilities buried in frozen ground or covered with snow.

[redacted] 6.5 Bibliography

Ammer, H., et al, The Electromagnetic Pulse from High Altitude Nuclear Bursts (U), K-78-103(R), Kaman Sciences Corporation, Colorado Springs, CO, 1978, SECRET RESTRICTED DATA.

COSPAR, COSPAR International Reference Atmosphere, 1965, North Holland Publishing Company, Amsterdam, 1965, UNCLASSIFIED.

COSPAR, COSPAR International Reference Atmosphere, 1972, Compiled by COSPAR Working Group A, Akademie-Verlag, Berlin, 1972, UNCLASSIFIED

Defense Nuclear Agency, Capabilities of Nuclear Weapons (U), DNA EM-1, Defense Nuclear Agency Effects Manual Number 1, Headquarters, Defense Nuclear Agency, Washington, D. C., 1 July 1972 (Change 1, 1 July 1978), SECRET RESTRICTED DATA. Two volumes, Part I - Phenomenology, Part II - Damage Criteria.

ESSA, U. S. Standard Atmosphere Supplements, 1966, U. S. Government Printing Office, Washington, D. C., 1966, UNCLASSIFIED.

General Research Company, Physical Custodian for Development of ROSCOE: A Radar and Optical Systems Code for Nuclear Effects DNA 3385, General Research Company, Santa Barbara, CA, March 1974, UNCLASSIFIED.

Jordano, R. J. et al, Sensitivity of HF Blackout Predictions to Atmospheric Parameters (U), ARBRL-CR-00357, General Electric Company - TEMPO, 816 State Street, Santa Barbara, CA, 1978, CONFIDENTIAL.

[redacted]

Knapp, W. S., WEPH VI, A Fortran Code for the Calculation of Ionization and Electromagnetic Propagation Effects Due to Nuclear Detonations (U), DNA 3766T-2, GE75TMP-53, General Electric Company - TEMPO, Santa Barbara, CA, October 1976 CONFIDENTIAL.

Kumer, J. B., et al, Low Altitude Phenomenology for Optical Systems, Volume II, RADIR Code Documentation (U), DNA 3977-2, LMSC B340290, Lockheed Palo Alto Research Laboratory, CA September 1975, SECRET

NASA, U. S. Standard Atmosphere, 1962, U. S. Government Printing Office, Washington, D. C., 1962, UNCLASSIFIED.